Universidade do Minho
Escola de Engenharia

Célio Bruno Pinto Fernandes

Optimization of the injection moulding process: from polymer plasticating to final part properties

August 2012

Optimization of the injection moulding process:
from polymer plasticating to final part properties

Célio Bruno Pinto Fernandes

UMinho | 2012

Universidade do Minho
Escola de Engenharia

Célio Bruno Pinto Fernandes

Optimization of the injection moulding process: from polymer plasticating to final part properties

Doctoral Dissertation for PhD degree in Science and Polymer Engineering and Composites

Thesis Supervisors:
António Gaspar Lopes da Cunha
António José Vilela Pontes

August 2012

Autor: Célio Bruno Pinto Fernandes

Email: ex1713@dep.uminho.pt / cbpf@portugalmail.pt

Telefone: +351 916 966 064

Título da tese

Otimização do processo de moldação por injeção: da plasticização do polímero até às propriedades finais da peça

Orientadores

António Gaspar Lopes da Cunha
António José Vilela Pontes

Ano de conclusão

2012

Doutoramento em Ciência e Engenharia de Polímeros e Compósitos

_____

Célio Bruno Pinto Fernandes

Universidade do Minho, 29 de Agosto de 2012

Dedicated to the loving memory of Filomena Pinto.

1960 – 1982

Keep away from people who try to belittle your ambitions.
Small people always do that,
but the really great make you feel that you,
too, can become great.

— Mark Twain

ACKNOWLEDGMENTS

I acknowledge the Portuguese Foundation for Science and Technology (FCT) for their financial support in the framework of the scholarship SFRH/BD/28479/2006.

I sincerely express my gratitude to my advisers António Gaspar-Cunha and António Pontes and to professors Júlio Viana and Miguel Nóbrega for the support and knownledge that they provided.

I thank to all my co-workers in Polymer Engineering Department of Minho University, José Carlos, Sidonie, Tânia, Nelson, Ângela, Rui, Carla, Sónia, Cristina, Luís Ferraz, Paulo Teixeira, Pedro, Gabriela (among others).

To all my closest friends I express my gratitude for all the support and friendship that they give to me.

Finally, I would like to express my gratitude to my lovely family. I thank my grand-mother, Ana Maria, my aunt, Fátima, my cousin, Hugo, my father, Albano, my step-mother, Fátima and my sister Marina for their support and love during all these years. I dedicate this work to my mother, Filomena, I know that you will guide me forever wherever you are now.

ABSTRACT

Recently several scientific studies on the injection moulding process have addressed the establishment of relationships between the thermomechanical, the material morphology and the resultant moulding's mechanical behavior. However, the absence of a link between the plasticating and filling phases of the process is evident in several studies. But the final conditions (e.g., thermal, homogenization) gathered in the plasticating phase are the initial conditions for the following ones, which can determine the moulded product properties and quality.

The main objective of this work is to integrate the plasticating and filling and post-filling phases in order to develop computational tools able to optimize automatically the injection moulding process. Therefore, will be possible the optimization of the injection moulding process through the application of multi-objective evolutionary algorithms based methodology. Simultaneously, the establishment of relationships between the processing conditions, the thermomechanical environment, the induced morphology and the mechanical properties allow the optimization of the performance of injection moulded parts.

RESUMO

Recentemente vários trabalhos científicos sobre o processo de injeção têm estabelecido relações entre a termomecânica do material, a sua morfologia e o comportamento mecânico da moldação. No entanto, é evidente em diversos estudos a ausência de uma ligação entre as fases de plasticização e enchimento da moldação. No entanto, as condições finais (por exemplo, térmicas, uniformização do material) obtidas na fase de plasticização são as condições iniciais das fases seguintes, determinando assim as propriedades e a qualidade do produto final.

O objectivo principal deste trabalho é a integração das fases de plasticização, enchimento e pós-enchimento do processo de moldação por injeção com vista ao desenvolvimento de ferramentas computacionais capazes de otimizar o processo automaticamente. Assim, será possível a otimização das condições operatórias através do desenvolvimento de uma metodologia baseada em algoritmos evolutivos multi-objetivo. Simultâneamente, será possível estabelecer relações entre as condições de processamento, o ambiente termomecânico, a morfologia induzida no material e as propriedades mecânicas de forma a otimizar as caraterísticas finais das peças.

PUBLICATIONS

This thesis is based on the following published and in preparation papers:

- C. Fernandes, A.J. Pontes, J.C. Viana and A. Gaspar-Cunha (2010). Using Multi-Objective Evolutionary Algorithms in the Optimization of Operating Conditions of Polymer Injection Moulding, *Polymer Engineering and Science* **50 Issue 8** 1667–1678;
- C. Fernandes, A.J. Pontes, J.C. Viana and A. Gaspar-Cunha (2012). Using Multi-Objective Evolutionary Algorithms for Optimization of the Cooling System in Polymer Injection Moulding, *Journal of International Polymer Processing* **Issue 2012/02** 213–223;
- C. Fernandes, A.J. Pontes, J.C. Viana, J.N. Nóbrega and A. Gaspar-Cunha (2012). Modelling of Plasticating Injection Moulding – Experimental Assessment, in final phase of preparation;
- C. Fernandes, A.J. Pontes, J.C. Viana and A. Gaspar-Cunha (2012). Optimization of Gate Location and Processing Conditions in Injection Moulding using a Multi-Objective Evolutionary Algorithm, in final phase of preparation.

CONTENTS

LIST OF FIGURES

LIST OF TABLES

ACRONYMS

ABS	Acrylonitrile Butadiene Styrene
AFMS	Approximate Feasible Moulding Space
AI	Artificial Intelligence
ANN	Artificial Neural Networks
ANOVA	Analysis of Variance
BEM	Boundary Element Method
BPNN	Back Propagation Neural Network
CAE	Computer Aided Engineering
CPVs	Controllable Process Variables
CVFEM	Control Volume Finite Element Method
DE	Differential Evolution
DEA	Data Envelopment Analysis
DMPGA	Distributed Multi-population Genetic Algorithm
DOE	Design of Experiment
DRM	Dual Reciprocity Method
EA	Evolutionary Algorithm
ES	Evolutionary Strategies
FDM	Finite Difference Method
FE	Finite Element
FEM	Finite Element Method

GA	Genetic Algorithm
GPS	General Polystyrene
GRNN	Generalized Regression Neural Network
HDPE	High Density Polyethylene
IM	Injection Moulding
IR	Infrared
MANOVA	Multivariate Analysis of Variance
MCA	Mould Cooling Analysis
MOEA	Multi Objective Evolutionary Algorithm
NSGA	Non-dominated Sorted Genetic Algorithm
PEEK	Polyether Ether Ketone
PID	Proportional Integral Derivative
PMs	Performance Measures
PMA	Polymer Melt Analysis
PP	Polypropylene
PS	Polystyrene
PTT	Phan-Thien-Tanner
PVT	Pressure-Volume-Temperature
RPSGAe	Reduced Pareto Set Genetic Algorithm with Elitism
RTM	Resin Transfer Moulding
SA	Simulated Annealing
SAE	Self Adaptive Evolution
SOM	Self Organizing Map
SQP	Sequential Quadratic Programming

UCM	Upper-convected Maxwell
VOF	Volume of Fluid

Greek Characters

α_s	Thermal diffusivity of the solid plug [m^2/s]
$\dot{\gamma}$	Shear rate [s^{-1}]
δ_C	Thickness of melt film C [m]
δ_{DE}	Thickness of melt film DE [m]
δ_f	Flight clearance [m]
ΔL	Incremental step in the injection chamber [m]
η	Viscosity [Pa s]
η_0	Zero-shear viscosity [Pa s]
θ	Helix angle [$^\circ$]
$\overline{\theta}$	Average helix angle [$^\circ$]
θ_s	Helix angle at the root of the screw [$^\circ$]
θ_b	Helix angle at the barrel surface [$^\circ$]
λ	Heat of fusion [J/kg]
ρ	Density [kg/m^3]
ρ_s	Solid polymer density [kg/m^3]
ρ_m	Melt polymer density [kg/m^3]
τ	Shear stress [Pa]
τ_{yz}	Shear stress in direction z [Pa]
$\tau_{yx\|C}$	Shear stress of interface A-C in direction x [Pa]
$\tau_{yx\|DE}$	Shear stress of interface A-DE in direction x [Pa]
ϕ	Solids conveying angle [$^\circ$]
Φ	Viscous-dissipation function

Roman Characters

$\mathbf{a}$	Aceleration vector [m/s^2]
a, K_1, n	Empirical constant of the Carreau-Yasuda model
A_1, A_2, B_1, B_2, K	Constants of the solids conveying pressure
$A_1^{'}$, $B_1^{'}$	Constants of the delay zone I pressure
c_{p_s}	Solid polymer specific heat capacity [J/kg]
c_{p_m}	Melt polymer specific heat capacity [J/kg]
d	Distance in the y direction such that $T_{s_1}(y = d) = T_{s_2}(y = d)$ [m]
CT	Cycle time [s]
dT	Temperature difference on the moulding at the end of filling [°C]
dx, dy, dz	Spatial increments [m]
D_b	Internal barrel diameter [m]
D_i	Internal screw diameter [m]
D_{mould}	Dimension in the mould in i direction [m]
D_{part}	Dimension in the part in i direction [m]
D_s	External screw diameter [m]
e	Flight width [m]
e_m	Mechanical power consumption for the melting zone [W]
e_{mbp}	Power required to build up pressure (melting zone) [W]
e_{mcl}	Power dissipated on the flight clearance (melting zone) [W]
e_{mfC}	Power dissipated on the melt film C (melting zone) [W]
e_{mfDE}	Power dissipated on the melt film DE (melting zone) [W]
e_{mp}	Power dissipated on the melt pool (melting zone) [W]
e_p	Mechanical power consumption for the melt conveying zone [W]
e_{pcl}	Power dissipated on the flight clearance (melt conveying zone) [W]
e_{pp}	Power required to build up pressure (melt conveying zone) [W]
e_{psc}	Power dissipated on the screw channel (melt conveying zone) [W]
e_w	Mechanical power consumption in the solids conveying zone [W]
$e_w^{'}$	Mechanical power consumption in the delay zone I [W]

e_{wb}	Mechanical power dissipated on the barrel surface (solids conveying zone) [W]
e'_{wb}	Mechanical power dissipated on the barrel surface (delay zone I) [W]
e_{wf}	Mechanical power dissipated on the flights (solids conveying zone) [W]
e_{wp}	Mechanical power dissipated for compression (solids conveying zone) [W]
e_{ws}	Mechanical power dissipated on the screw root (solids conveying zone) [W]
E/R	Temperature coefficient of viscosity
f	Exponential relation of the Carreau-Yasuda model
f_b	Barrel friction factor of solid polymer
f_s	Screw friction factor of solid polymer
F_1	Friction between the barrel and the solid bed [N]
F_2, F_6	Forces due to the pressure gradient [N]
F_3, F_4	Friction due to the contact of the solids with the screw walls [N]
F_5	Friction due to the contact of the solids with the screw root [N]
F_7, F_8	Normal reactions [N]
F_i	Fitness
$\mathbf{g}$	Vector acceleration of gravity [m/s^2]
H	Channel depth [m]
H_1	Channel depth of feed zone [m]
H_2	Channel depth of metering zone [m]
$H_{s\|z}$	Solid bed height [m]
k_b	Barrel thermal conductivity [W/m°C]
k_m	Melt polymer thermal conductivity [W/m°C]
k_p	Screw thermal conductivity [W/m°C]
k_s	Solid polymer thermal conductivity [W/m°C]
L_0	Screw initial position [m]
L_1	Screw final position [m]
$L_{injchamber}$	Length of the injection chamber [m]

LS	Linear shrinkage [%]
$LWML$	Length weld plus meld line [m]
$\dot{m}_{A\|z}$	Mass flow rate in the solid bed A at z [kg/s]
$\dot{m}_{A\|z+\Delta z}$	Mass flow rate in the solid bed A at $z + \Delta z$ [kg/s]
$\dot{m}_{B\|z}$	Mass flow rate in the melt film B at z [kg/s]
$\dot{m}_{B\|z+\Delta z}$	Mass flow rate in the melt film B at $z + \Delta z$ [kg/s]
$\dot{m}_{By\|z}$	Rate of melt circulation thorough the pool in $x - y$ plane [kg/s]
$\dot{m}_{C\|z}$	Mass flow rate in the melt film C at z [kg/s]
$\dot{m}_{C\|z+\Delta z}$	Mass flow rate in the melt film C at $z + \Delta z$ [kg/s]
$\dot{m}_{Cx\|z}$	Net flow rate out of the film, to melt pool, in the x direction [kg/s]
$\dot{m}_{DE\|z}$	Mass flow rate in the melt film DE at z [kg/s]
$\dot{m}_{DE\|z+\Delta z}$	Mass flow rate in the melt film DE at $z + \Delta z$ [kg/s]
$\dot{m}_{DEx\|z}$	Net flow rate out of the film D/E, to melt film C, in the x direction [kg/s]
$\dot{m}_T$	Total mass flow rate [kg/s]
N	Screw speed [m/s]
$N_{heatbands}$	Number of heating bands
$N_{injchamber}$	Number of intervals in the length of injection chamber
N_{Ranks}	Number of ranks
p	Number of screw flights in parallel
$\mathbf{p}$	Pressure [Pa]
$P1$	Node at 40 mm of the gate on the injection moulding part
$P2$	Node at 110 mm of the gate on the injection moulding part
P_1	Pressure at down-channel distance z_1 [Pa]
P_2	Pressure at down-channel distance z_2 [Pa]
P_{max}	Maximum mould pressure [Pa]
P_{plast}	Back pressure [Pa]
PW	Pressure work [Pa]
Q	Volumetric output [kg/h]

Q_{inj}	Injection flow rate [kg/h]
R_B	Melting rate over the interface A-B [kg/s]
R_C	Melting rate over the interface between melt film C and solid bed A [kg/s]
R_D	Melting rate over the interface A-D [kg/s]
R_E	Melting rate over the interface A-E [kg/s]
S	Screw pitch [m]
$S_{F/P}$	Switch-over point [%]
t	Time coordenate [s]
t_{2P}	Holding time [s]
t_c	Cycle time [s]
t_c	Cooling time [s]
t_f	Fill time [s]
t_{inj}	Injection time [s]
t_o	Mould open time [s]
t_p	Packing time [s]
t_{plast}	Time of dynamic melting [s]
t_{stop}	Time of screw rest in the backwards position [s]
T	Testing temperature [°C]
$\overline{T}$	Average melt temperature [°C]
T_0	Reference temperature [°C]
T_b	Barrel temperature [°C]
T_{inj}	Melt temperature [°C]
T_m	Melting or flow temperature [°C]
T_{max}	Maximum bulk temperature at the end of filling [°C]
T_{min}	Minimum bulk temperature at the end of filling [°C]
T_{nozzle}	Nozzle temperature [°C]
$T_s(z)$	Screw temperature at z [°C]
T_{s1}	Temperature in sub-region 1 [°C]

T_{s2}	Temperature in sub-region 2 [°C]
T_{so}	Solid polymer temperature [°C]
T_w	Mould temperature [°C]
u, v, w	Velocity components [m/s]
$\hat{u}$	Internal energy [J]
$\mathbf{V}$	Velocity vector field [m/s]
V_b	Barrel velocity [m/s]
V_{bx}	Component x of barrel velocity [m/s]
V_{bz}	Component z of barrel velocity [m/s]
V_{sy}	Solid polymer velocity in direction y [m/s]
V_{sy1}	Solid polymer velocity in direction of melt film C [m/s]
V_{sy2}	Solid polymer velocity in direction of melt film E [m/s]
V_{sz}	Solid bed velocity [m/s]
V_x	Velocity in direction x [m/s]
V_z	Velocity in direction z [m/s]
W	Channel width [m]
$WARP$	Warpage [%]
W_b	Channel width at the barrel surface [m]
W_B	Melt pool width [m]
W_C	Melt film C width [m]
W_{press}	Pressure work [Pa]
W_s	Channel width at the root of the screw [m]
x, y, z	Spatial coordenates

Mathematical Operators

∇	Gradient operator
∂	Partial derivative
$\int$	Integral symbol

Part I

INJECTION MOULDING PROCESS

1

INTRODUCTION

The fingers of your thoughts are moulding your face ceaselessly.

— Charles Reznikoff

Injection Moulding (IM) is one of the most important polymer processing methods for producing plastic parts. The main concern in injection moulding is to produce plastic parts of the desired quality, which are related with mechanical characteristics, dimensional conformity and appearance. The major factors affecting part quality are polymer properties, mould design and operating conditions. The injection moulding process is cyclic and can be characterized by the following main stages:

1. FILLING: the melted polymer is injected into the closed mould;
2. PACKING: the pressure is maintained in high values so that the melted polymer can flow to the interior of the mould to prevent shrinkage during solidification;
3. COOLING/PLASTICIZATION: in this phase the moulded part is cooled during the time necessary to that the part be sufficiently rigid to be ejected. In this stage the screw rotates and the solid polymer is heated inside the injection unit until it reach the melted state (plasticization) to be injected in the next cycle.

In the next sections the main features of an injection moulding machine, the description of the injection moulding cycle, the polymer properties, the mould characteristics and the variables of the process will be presented (Cunha, 2003; Douglas, 1996; Kamal et al., 2009; Osswald et al., 2008; Rosato et al., 2000). At the end of this chapter the objectives of the work are presented and the structure of the thesis is described.

1.1 INJECTION MOULDING MACHINE

A typical injection moulding machines have four units (Figure 1.1):

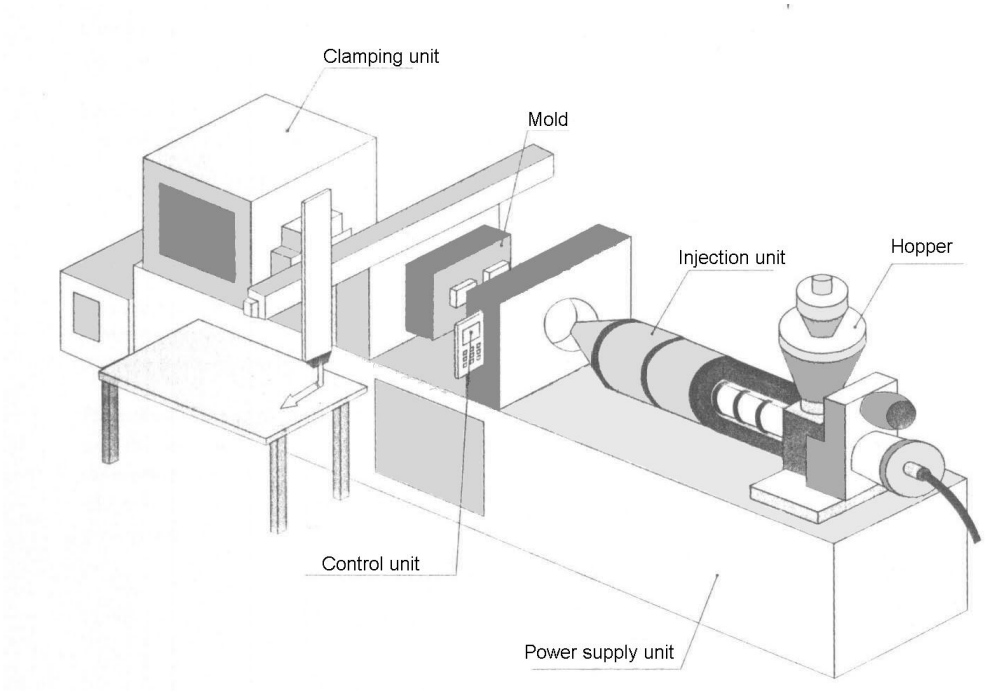

Figure 1.1: Functional units of the injection moulding machine (adapted from Cunha (2003)).

Power supply unit

This unit provides the energy necessary by the actuators existent in the machine. It is based on a system of hydraulic oil pressure and on a pump that is driven by an electric motor.

Injection unit

The injection unit is shown in more detail in Figure 1.2. The major tasks of the injection unit are to melt the polymer, to accumulate the melt in the screw chamber, to inject the melt into the cavity and to maintain the holding pressure during cooling. The main elements of the injection unit are: the hopper, the screw, the heating bands, the barrel and the nozzle.

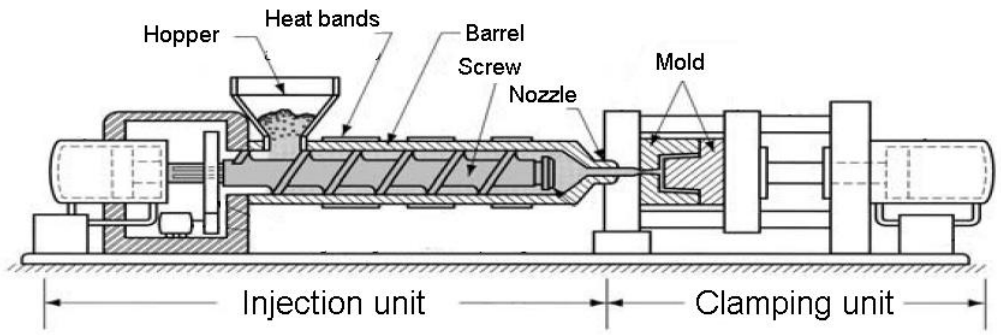

Figure 1.2: Schematic of the injection and clamping unit.

Clamping unit

The clamping unit is shown in Figure 1.2. The main function of a clamping unit is to open and close the mould. The mould must be closed tightly to avoid flash during filling and holding. Modern injection moulding machines can have one of three existent clamping unit types: mechanical, hydraulic and a combination of the two.

Control unit

The operations and the devices necessary to ensure the monitoring and control of the various variables of the process are centralized in this unit. It also provides the interface with the operator and the communications with peripheral or information management systems.

1.2 INJECTION MOULDING CYCLE

Injection moulding is a cyclic process. The sequence of events during the injection moulding of a plastic part, as shown in Figure 1.3, is called the injection moulding cycle.

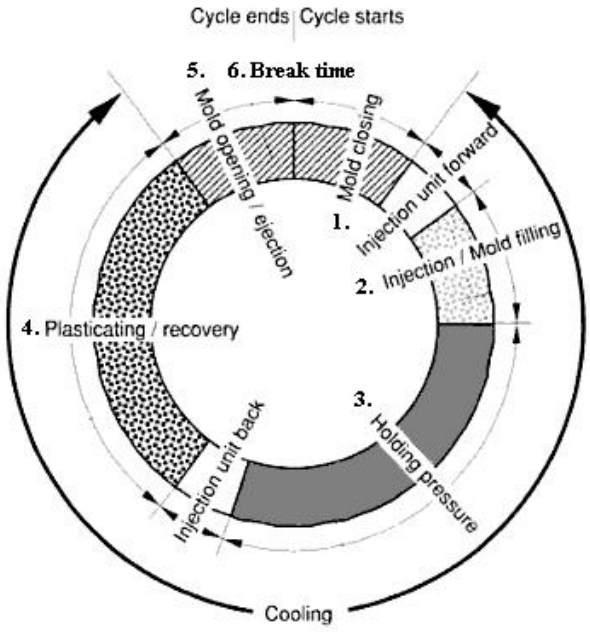

Figure 1.3: Injection moulding cycle (adapted from Osswald et al. (2008)).

The phases of the moulding cycle are practically independent of the type of machine. However, the duration of these stages can be very different, ranging from less than 1 second for very thin pieces, to several minutes for more thick pieces.

Phase 1 - Mould closing

This operation corresponds to the beginning of the cycle and should be as fast as possible. However, this operation depends on the performance of the machine, the characteristics of the mould and the distance to be covered. Its optimization involves the minimization of the opening interval between the halves of the moulds and the judicious adjustment in speed of closure used (see Figure 1.4).

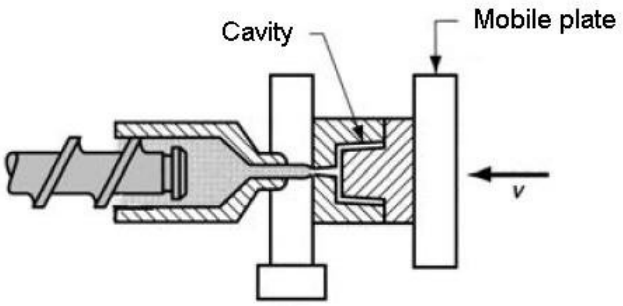

Figure 1.4: Closed mould.

Phase 2 - Injection

The stage of injection is guaranteed by the linear advance of the screw that force the molten material (previously deposited in front of the screw) to enter into the mould and flow within the impression (see Figure 1.5). The injection starts after the cylinder have leaned the nozzle to the mould (in some cases the nozzle can be permanently backboarded) and should be completed when the impression is filled to 95% of its volume. The injection speed selected must correspond to a compromise between time (to ensure the impression global filling) and the quality of the final product.

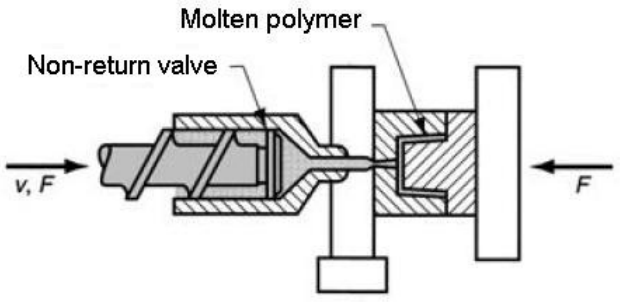

Figure 1.5: Molten injected into the cavity.

Phase 3 - Holding pressure

After the mould fills it is necessary to continue pressurizing the impression, in order to reduce the effect of contraction by cooling and prevent the reflux of the melting. This phase finishes as soon as the entrance of the material in the gate, or the own piece, be sufficiently cooled to inhibit the material flow. This phase is also named as second pressure.

Phase 4 - Plasticating

As soon the consolidation of the gate occurs, the screw can start to rotate in order to begin the plasticization for the next cycle. During this process, the screw is forced to retreat by the effect of pressure created by material that deposits in front of the screw (see Figure 1.6). The moulding continues to cool in the mould. When the pre-defined volume is achieved the screw stops. The cooling finishes as soon the piece reaches a temperature that allows the ejection without distortion.

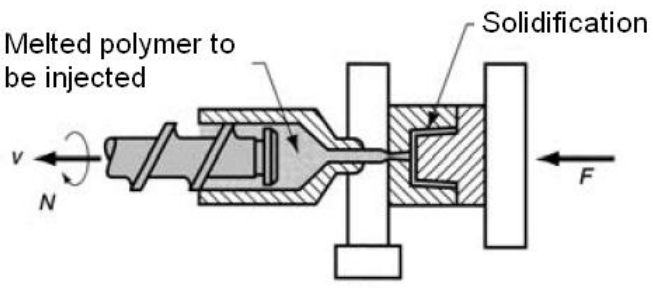

Figure 1.6: Retracted screw.

Phase 5 - Mould opening and ejection

The time for this operation depends on the machine used, the course of mould opening and the movements necessary by the tool to guarantee the extraction of the moulding. Nowadays is more frequent the use of auxiliary manipulation devices to guarantee a high degree of automation of the process (see Figure 1.7).

Phase 6 - Break time

Is the period of time between the end of the extraction and the beginning of the new cycle. Is highly desirable to be zero. High dead times and with variations of cycle to cycle affect drastically the reproducibility of the process.

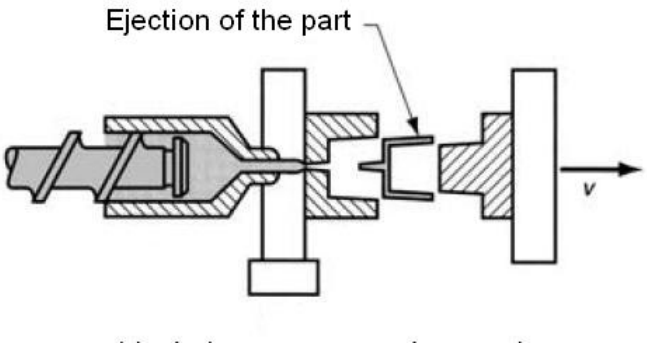

Figure 1.7: Ejection of the part.

1.3 POLYMER PROPERTIES

Plastics have some properties that can affect the repeatability of the moulding process (Douglas, 1996; Thyregod, 2001).

First, plastics are compressible. The packing mechanism of the melt is controlled by the pressure in the mould cavity. Maintaining all other variables constant, higher cavity pressure is achieved with higher hydraulic pressure. Therefore, more plastic will be injected into the mould cavities.

Second, plastics shrink when cooled. After the mould cavity is filled, more melted polymer must be supplied into the cavity to balance the shrinkage caused by the initial cooling. Another variable that influence shrinkage is cooling rate. Lower shrinkage is obtained with a faster cooling rate, i.e. low mould temperature. Higher shrinkage will occur when the cooling rate is small because there is more time for the molecules to align. Shrinkage is also affected by polymer orientation. There are two factors that can modify the polymer orientation, a normal decrease in volume due to temperature change and relaxation of the stretching caused by carbon-carbon linkages.

Finally, the viscosity plays an important role, since it can vary substancially mainly with the temperature and the flow rate. The viscosity decreases with the increase of temperature and flow rate. To manufacture parts with quality it is important to maintain the viscosity unchanged because it affects how much the polymer is compressed in the cavity and consequently how much shrinkage is caused in the part. In conclusion, lower viscosity produces smaller pressure drops and as a result higher cavity pressure, which causes higher compressibility and therefore less shrinkage.

1.4 MOULD

The mould consists of two main components: the cavity and the core. The cavity gives the outer shape of the part. The core forms the inner shape of the part. The empty space formed between the core and the cavity when the mould is closed defines the shape of the part to be moulded. Usually the molten plastic is injected inside the mould from the cavity side.

Due to plastic shrinkage which occurs during cooling the cavity dimensions are equal to the sum of the part dimensions and a shrink factor given by the material manufacturer. Therefore, the determination of the amount of shrinkage is very important in injection moulding but is a complex task because depends of geometries of the part and process conditions of the process.

Runner system

The main features of a mould are: sprue, runner, gate and cavity (Figure 1.8).

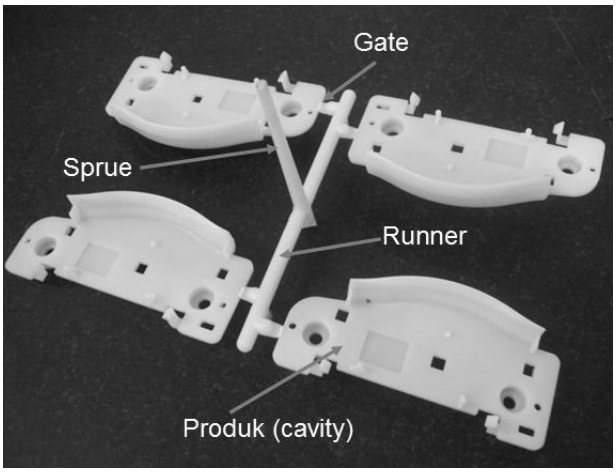

Figure 1.8: Sprue, runner and gates in injection moulding process.

Sprue is the channel where the melt is conveyed from the plasticator nozzle to the runner. Then, the molten plastic is tansported to the cavity through channels that are machined into the two faces of the mould, called runners. Connection between the runner and the cavity is done by the gate. Typically the cross section of the gate is small in order to easily remove the runner from the part and to prevent the appearance of a large gate mark in the part. Finally, the molten plastic pass through one or more gates into the cavity to form the desired part.

The main objective when designing the runner system is to assure that plastic reach all gates at the same time.

Cooling channels

In injection moulding, the exchanges of heat occur during the entire cycle. The heat is generated by two diferent sources, conduction from the barrel and viscous dissipation due to the screw rotation. However, heat removal from the material in the mould is more difficult due to the plastic low thermal conductivity.

The standard method of cooling is to use a coolant (usually water) that is forced to flow through a series of channels machined in the mould plates and connected by hoses to form a continuous pathway. Cooling allows the plastic to solidify and become dimensionally stable before ejection. The coolant receives heat from the mould (which has received heat from the molten plastic) and keeps the mould at a proper temperature to solidify the plastic at the most efficient rate (Douglas, 1996). Coolant temperature and flow rate determine the efficiency of heat removal. The objective is to cool the components as quickly and uniformly as possible to prevent defects in the piece.

Venting

During mould filling air is displaced by the advancing melt front. Therefore, to design a mould is necessary to use some inserts able to remove the air. The accumulation of air in the mould can cause burning of the plastic (burn marks) and incomplete filling of the moulded part.

1.5 PROCESS VARIABLES

Numerous variables affect the injection moulding process. Each process variable can be placed into five basic categories: speed, temperature, pressure, time and distance. All these variables are not independent, changes made in one can affect the others. (Thyregod, 2001; Rosato et al., 2000; Kamal et al., 2009).

Table 1.1 presents typical process variables which need to be monitored and/or controlled in each cycle. The following discussion adresses the description and/or the importance of each one of the referred variables concerning their influence on the process.

TEMPERATURE	TIME	SPEED	PRESSURE	DISTANCE
Melt	Mould close	Mould close	Injection	Melt cushion
Mould	Injection	Mould open	Holding	Screw stroke
Barrel	Hold pressure	Injection	Hydraulic back	Change over position
Ambient	Cooling	Screw rotational		Screw-return
	Screw recovery	Screw return		Mould open
	Mould open	Ejection		Ejection
	Ejection			
	Cycle			

Table 1.1: Process variables.

1.5.1 *Temperature related process variables*

Melt temperature

Melt temperature is the temperature at which the polymer material is maintained throughout the flow path. Melt temperature is affected by cycle time, back pressure, screw speed, barrel temperature settings and the hopper throat temperature. Its value can be modified by simply change one of these process variables.

Mould temperature

The mould temperature must be adjusted in order to regulate the cooling rate of the plastic. Therefore, the excess of heat contained within the molten material has to be removed so that the moulding can be extracted without distortion. The mould temperature is a consequence of process and design variables, for example, the cooling time, the melt temperature, the rate at which the cooling medium is flowing through the mould and the design of the cooling circuit in the mould.

Barrel temperature

The barrel forms the outer boundary of the screw channel. Barrel is equipped with electrical band heaters that supply the most portion of the heat to the plastic during plasticating of injection moulding process.

Ambient temperature

Changes in the temperature of the air surrounding the machine produce fluctuations in the readings provided by the different temperature control units of the machine. These changes in ambient conditions can produce instabilities in the injection process during a longer period of time.

1.5.2 *Time related process variables*

Mould close time

Mould close time is the time it takes for the moving half of the mould to travel the entire distance to meet the stationary half of the mould and lock up with full clamping force.

Injection time

Injection time is the time from which the screw starts its forward movement to the point where the holding pressure is applied. The melted material is forced to enter to the closed mould. The time to force the molten material into the mould is dependent upon some factors such as melt viscosity, the injection speed selected, the dimensions of the gate and the screw stroke used.

Hold pressure time

The hold time is the time in which the screw maintains some pressure in the cavity after the injection phase. The period of time used for the holding pressure to be applied should correspond with the time the gate takes to freeze off or, for the gate to sufficiently solidify.

Cooling time

Cooling time is one of the most important process variables time since it is the longest step of the moulding cycle. It depends on some factors such as, the general shape and the wall thickness of the injected part and the type of material being processed.

Screw recovery time

Screw recovery time is the time required by the screw to return to the injection position. This step must take place before the cooling timer finishes. It depends on the level of back pressure applied (more back pressure implies longer to return the screw) and on the quantity of material needed in each cycle.

Mould open time

Mould open time is the time taken by the mould to open. It depends on the distance required for the mould to fully open and the speed at which it does it.

Ejection time

It is the time necessary to ejection system to come forward and knock the parts out of the mould. The speed at which the system comes forward is what determines the ejection time required.

Cycle time

Is the sum of all time increments of the moulding cycle needed to produce the desired piece. The overall machine cycle time is of great importance because it affects the costs of producing the pieces and is crucial to maintain consistent cycles.

1.5.3 *Speed related process variables*

Mould open and close speeds

It is possible to define different opening and closing mould speeds. Also, speed changes can be done during the opening and closing operations.

Injection speed

The injection speed is the linear speed used to fill the mould with molten material. Injection speed depends on the injection pressure available to maintain a consistent selected filling velocity.

Screw rotation speed

Screw rotation speed is responsible of some of the heat necessary to plasticize the polymer. Higher rotational screw speeds determines higher temperatures in the polymer. Hence, it is important to achieve a correct speed to prevent instabilities on the process.

Screw recovery speed

Screw recovery speed is the speed used to returns the screw.

Ejection speed

Is defined as the speed that the product is extracted. It depends on the design of the mould and the characteristics of the product.

1.5.4 *Pressure related process variables*

Injection pressure

This is the first pressure applied to the molten polymer and is used during the initial filling of the mould. The injection pressure value is very important to maintain a consistent mould filling velocity. The pressure depends on: the polymer being moulded, the viscosity and flow rate of the polymer, the mould filling speed used, the melt and mould temperatures and the distance that the polymer needs to flow in the mould cavity.

Holding pressure

Holding pressure is applied after the mould has been initially filled with melt in order to compact and shape the polymer. Holding pressure is used to finish the filling of the mould and pack the polymer into the cavity image. The magnitude of the holding pressure is controlled by the machine pressure generation system.

Hydraulic back pressure

After the hold pressure phase is finished the screw begins to rotate and the plasticized polymer is pushed forward to the front of the screw. The pressure generated here by the polymer itself begins to push the screw backward. Hydraulic back pressure affects the melt temperature and the homogeneity of the molten polymer. It depends on the type of polymer is being processed, the shot capacity of the barrel, the characteristics of the plasticizing screw, the rotational speed of the screw and the quality of the parts that are produced.

1.5.5 *Distance related process variables*

Melt cushion

The melt cushion is the amount of molten polymer left after injection. The cushion is formed by using a total shot size that is slightly larger than that required to fill the mould. The thickness of the cushion is critical because if it goes to zero the moulded part may warp, crack or don't fill because no pressure exist.

Screw stroke

The screw stroke is the linear distance the screw moves from stationary position (after plasticization) to the selected position of holding pressure application (mould packing).

Changeover position from injection to holding pressure

The switch-over position from injection pressure to holding pressure is initiated at a preselected distance. When the advancing screw reaches this position the machine changes from injection pressure to holding pressure.

Screw return

After the injection phases are finished (filling and packing), the screw begins to rotate to bring fresh polymer forward. This polymer pushes the screw backwards at the set point where it stops turning. In this point the polymer accumulated in front of the screw must be slightly more than required to fill the mould because the extra is to form the cushion.

Mould open distance

First the mould must be opened slowly to break the vacuum that was created in the cavity image during the injection process. After that it may be allowed to open fully at a faster rate. The mould should open a total distance equal to twice the depth of the moulded part.

Ejection distance

The quantity of ejection distance required is only that which will be necessary to push the part free from the mould.

1.6 OBJECTIVES

The main objective of this work is to develop and implement an integrated computational methodology able of optimizing the IM process in order to maximize the final part performance. This methodology must be able of integrating the polymer plasticating and filling and postfilling stages allowing the establishment of relationships between the operative processing conditions and specific equipment design with final parts properties. Thus, the automatic optimization of the global process will be as closed as possible as required in an industrial context. The specific objectives are:

Objective 1

To develop theoretical models able of describing the polymer plasticating phase and implementing them in a computer code.

Objective 2

To optimize the moulding cycle, simultaneously in terms of the process (no defective parts), dimensional and mechanical performance, based in Multi-Objective Evolutionary Algorithms.

Objective 3

To establish relationships between the global processing conditions and the thermomechanical environment.

Objective 4

To customize the thermomechanical environment for a desired dimensional and mechanical response, defining the processing window.

Objective 5

To develop a methodology for the full integration of the process, as need in an industrial context.

In the proposed objective 1 the plasticating phase of the injection moulding process was modelled taking into account its specific features, such as, the backwards movement of the screw, the presence of a non–return valve (flow restrictions) and the heat conduction during the stationary phase (time that the screw is stopped). The implementation of models able of describing the flow of solids, melt and the melting phenomena inside the barrel of the injection unit was made. The process is similar to that of the plasticating phase of the extrusion process. The differences are mainly related with the cyclic character of the injection moulding process. During this task the software available at Department of Polymer Engineering at University of Minho to model extrusion plasticating was adapted to meet these requirements. Then, the modelling routine developed was used to study the influence of some important operative process parameters, such as, barrel temperatures, screw rotation speed, backpressure and length of injection chamber.

In the proposed objective 2 the mould filling routines (C-Mold or Moldflow) were used to optimize the overall processing conditions and the geometries of the injection moulding process. For that purpose, a multi-objective optimization methodology, MOEA, was used. Initially, the MOEA based on Evolutionary Algorithm (EA), was modified in order to take into account the characteristics of the IM process. EA is a technique that mimics the process of natural evolution and uses a population of points as tentative solutions that are improved during the successive generations. The mould filling softwares, C-Mold or Moldflow were used to obtain information concerning the process performance, such as melt temperatures, pressures, warpage and weld lines length and location of the injected part, which will be used in the MOEA. These softwares are easy to couple with the optimization routines since they can be run using a command line. Also, these softwares are able to take into account

crystallisation kinetics and mould deformation. Thus, these softwares take into account real conditions of the injection moulding process as needed for optimization of the process.

The proposed objective 3 involves experimental study of the relationships between operating conditions and final properties. The relationships between the thermomechanical variables and the dimensional and mechanical behavior of the mouldings were assessed. The mechanical behavior of the mouldings was then maximized.

In the proposed objectives 4 and 5 the global optimization approach was implemented for maximization of the mechanical behavior of the mouldings leading to the optimization of the injection moulding process. For a desired mechanical response the injection moulding conditions were optimized considering the global moulding cycle. A complete simulation of all the (real) moulding cycle was then possible. This new tool make possible the optimization of the processing conditions for a given thermomechanical environment. Optimization procedures were implemented in order to identify the processing variables set-up resultant in a given thermomechanical environment by adopting a reverse analysis approach.

1.7 DISSERTATION OUTLINE

The present dissertation is a paperbased dissertation type with a collection of peer-review journal papers published (or under evaluation) in international scientific journals. The list of the included papers can be found in Chapter Publications on page xi. The included papers correspond to specific stages and parts of the above mentioned objectives.

The present dissertation is divided in five main parts:

Part I: Injection Moulding Process;

Part II: Injection Moulding Process - State of the Art;

Part III: Extrusion Plasticating versus Injection Plasticating;

Part IV: Optimization of Injection Moulding Cycle - Case Studies;

Part V: Conclusions and Further Work.

Part I, the present part, presents a description of the injection moulding process concerning the machine characteristics, the injection stages, the polymer properties, the mould and the process variables and finishes with thesis objectives and dissertation outline.

In Part II the description of mathematical modeling research for injection moulding process is presented and some optimization techniques applied by some authors are also referred.

Part III presents the mathematical models for the extrusion process and for the plasticization stage of the injection moulding process.

Part IV describe some case studies optimizing processing conditions, cooling channels design and gate location in injection moulding process using MOEAs.

Finally, in Part V the main conclusions are outlined and suggestions for further work are presented.

Part II

INJECTION MOULDING PROCESS - STATE OF THE ART

INTRODUCTION TO PART II

The beginning of knowledge is the discovery of something we do not understand.

— Frank Herbert

The aim of this part is to present the state-of-the-art related with both the mathematical modelling and the optimization of the injection moulding process. First, the state-of-the-art concerning the mathematical modeling of the injection moulding process is presented. Then, the revision of the literature regarding the optimization of the process will be presented based on various techniques. These techniques includes numerical simulation, process windows, Design of Experiment (DOE), Artificial Neural Networks (ANN), Genetic Algorithm (GA) and Evolutionary Strategies (ES).

2

MATHEMATICAL MODELING

2.1 MODELING OF PLASTICATION STAGE

The injection plastication consists of two main phases. First, a transient phase, in which the screw rotates and retracts a distance predetermined by the required shot size, then a dwell phase, in which the screw is at rest. Melting occurs mainly by heat conduction from the hot barrel and by viscous dissipation.

Few studies have been conducted for the plastication of the injection moulding. The existing studies are based on the models used in the plastication of the single screw extrusion process. For this reason the extrusion models will be described in some detail in a next chapter. A good example is the "cooling experiment" used by Maddock (1959) to study polymer melting in an extruder.

Donovan et al. (1971) studied the nature of the plasticating process in a reciprocating-screw injection moulding machine using the "cooling experiment". Experimental studies were performed with different polymers. As the screw rotates the equilibrium extrusion behavior is gradually achieved.

Donovan (1971) proposed a theoretical model for the transient melting behavior in a reciprocating-screw injection moulding machine. An extension to the transient situation of the steady-state extrusion model (Neumann's melting problem (Becker et al., 1981)) is difficult. Therefore, in combination with the steady-state extrusion model an heuristic approach was used.

Donovan (1974) create a plasticating model serving as an analytical design methodology for the plasticating portion of injection moulding process which combine a transient melting model with other models to calculate the melt temperature and the pressure profile in the plasticating process. A reasonable and consistent predictive accuracy was achieved as shown by the comparisons of the calculations with experimental data obtained under a wide variety of processing conditions.

Lipshitz et al. (1974) proposed a theoretical model for melting in reciprocating screw injection moulding machines. The main features of the model are: a dynamic extrusion melting model for the rotation period, a transient heat conduction model with a phase transition for the screw rest period and a model for the drifting occuring at the beginning of melting during the injection cycle.

Rauwendaal (1992) described quantitatively the solids conveying, melting and melt conveying in a single screw extruder with both axial and rotational motion of the screw. The theoretical description of this extrusion process can be considered as an extension of the theory for non-reciprocating extruders.

Potente et al. (1993) presented a program for the simulation of the plastication process in injection moulding. By examining the operating points of large industrial plants, the validity of the computations for different sizes of plasticating unit was demonstrated.

Yung and Xu (2001) developed a transient melting model for a reciprocating extruder. The model describe the effects of screw rotation speed, barrel thickness and barrel heat capacity on the melting rate.

Yung et al. (2003) studied the transient models for the melting process in the three stages (melting, injection and stop stages) for the reciprocating extruder. Based on the proposed models, the effects of screw rotation speed, barrel thickness, melt viscosity, barrel heat capacity and injection speed on melting rate was studied.

Steller and Iwko (2008) presented the theoretical principles of polymer plasticization in a reciprocating screw injection moulding machine. The model was conceived including three-zones-screw geometry, to-and-from screw motion characterized by controlled stroke and back pressure and existence of static melting phase with controlled dwell times in back and front screw positions. The dynamic melting phase was characterized by a rotating screw with controlled angular velocity and was computed by applying the theory of dynamic extrusion formulated originally by Tadmor (1974), but extended to the three-zones-screw with axial motion. For the static melting was applied the equations that result from the solution of the Neumann problem (Becker et al., 1981).

2.2 MODELING OF FILLING, PACKING-HOLDING AND COOLING STAGES

The complete mathematical model for the injection moulding process involves mass, momentum and energy balance equations, combined with constitutive laws for non-Newtonian fluids and boundary conditions. The location of the advancing fluid front must be determined as a part of the solution. This is hence a free boundary problem. Quite a few mathematical models for describing the physical process of injection moulding were developed.

In particular, Wu et al. (1974), Stevenson (1978) and Stevenson and Chuck (1979) analyzed one-dimensional flow in a center-gated disc. Harry and Parrott (1970) and Lord and Williams (1975) studied the one dimensional filling behavior in rectangular cavity geometry. Kamal and Kenig (1972), Williams and Lord (1975) and Nunn and Fenner (1977) modelled one-dimensional tubular flow of polymer melts.

Wu et al. (1974) solved the transient and non-isothermal problem of filling a disk-shaped cavity using the transport equations for a power law fluid. With the results obtained it was possible to predict gate pressures, fill times and short shots. Also, through the filling process it was possible to obtain the velocity and temperature fields. This information specifies the formation of a frozen surface layer during filling.

Stevenson (1978) presented a graphical method based on dimensional analysis for estimating the injection pressure and clamp force required for injecting amorphous polymers to form disk-shaped parts with a constant wall thickness. The results reported were based on a numerical simulation of a power-law fluid filling a cold mould at a constant injection rate.

Stevenson and Chuck (1979) introduced geometric and semicrystalline - materials approximations for extending the previous analysis to include multigated thin cavities and semicrystalline materials. The geometric approximation, which is based on a simple model for the axial stress distribution in the cavity, was shown to give reasonable predictions when compared with experimental data and a numerical two-directional flow simulation for the filling of an off-center-gated rectangular cavity with Acrylonitrile Butadiene Styrene (ABS) co-polymer. The semicrystalline-materials approximation, in which heat capacity and viscosity changes during crystallization are neglected, was shown to give good agreement with experimental data for the filling of a center-gated disk-shaped cavity with polypropylene.

Harry and Parrott (1970) described a numerical simulation of polymer flow as applied to the injection moulding filling process. The simulation model predict fill lengths and fill

times of thin constant crossection cavities considering heat conduction and viscous heat generation along with the temperature dependence of the flow parameters. The simulation was designed for moulding situations where fill is difficult, such as thin cavity sections, long flow length requirements, or difficult-to-process materials. Experimental moulding trials with two different cavity thicknesses were performed to explore the simulation sensitivity. The thinner cavity illustrated a short shot in all cases with the thick cavity completely filling.

Lord and Williams (1975) described a practically-oriented model computing temperature, pressure and velocity fields in a cavity during the mould filling portion of the injection moulding process. The model can be used for cavities having non-simple shapes and for commonly used moulding compounds with complicated viscosity, shear rate and temperature relationships. Results obtained from exact solutions to special cases and predictions from the model are in good agreement.

Kamal and Kenig (1972) proposed a mathematical model for the quantitative treatment of the injection moulding of thermoplastics as it relates to the behavior of polymer in the cavity. The model was based on setting up the equations of continuity, motion and energy for the system during each of the stages of the injection moulding cycle (filling, packing and cooling) and the coupling of these equations with practical boundary conditions. The model takes into consideration the non-Newtonian behavior of the melt, the effect of temperature on density and viscosity, the latent heat of solidification and the differences in thermal properties between the solid and the melt. Numerical solutions were obtained for the case of spreading radial flow in a semi-circular cavity. The numerical results yield significant data on the progression of the melt front, the flow rate and the velocity profiles at different times and positions in the cavity. They also yield temperature and pressure profiles throughout the packing and cooling stages.

Williams and Lord (1975) developed a finite difference analysis which predicts the temperature, pressure and velocity distributions for the flow of thermoplastic materials in straight and tapered, hot and cold walled circular flow channels. This analysis when combined with the cavity filling analysis described in Part II, gives the moulding engineer the capability of modeling the injection moulding process from the shot to the cavity during injection.

Nunn and Fenner (1977) described a method for the analysis of time dependent heat transfer and flow in a nozzle of an injection moulding machine. Melts are treated as being inelastic but with viscosity's which are non Newtonian and dependent on both temperature and pressure. Using a finite difference method for solving the differential conservation

equations of continuum mechanics it was obtained distributions for velocity, temperature and pressure. Typical results show that the times required to reach steady flow conditions are small compared with total injection times. Heat transfer is predominantly convective and flows leaving injection nozzles and entering moulds are very far from being thermally fully-developed.

The "branching flow" approach has been proposed and implemented for the simulation of polymer flow in typically complex mould cavities using these one-dimensional flow representations. This approach involves laying flat and decomposing the cavity geometry into several conjectured flow paths comprising of a series of one-dimensional segments such as strips, discs, fans and/or tubes. The method requires intelligent judgment from the user because the solution accuracy strongly depends on how the geometry is being branched.

Theoretical studies of two dimensional flow in a thin cavity based on Hele–Shaw flow formulation have been conducted to overcome the deficiency of the branching flow approach. In particular, two approaches have been proposed, namely, network flow, Tadmor et al. (1974), and a two-step "predictor–corrector" method, Hieber and Shen (1980). The former method discretizes the cavity geometry into a network of rectangular elements. The flow domain defined by the melt-front pattern is calculated based on the velocity at the advancing front. The two-step 'predictor–corrector' approach is similar to the network flow approach except that it constantly creates new finite elements at the advancing flow front by taking into account the melt-front velocity and the actual geometry.

Tadmor et al. (1974) proposed a finite element method for solving two dimensional flow problems in complex geometrical configurations commonly encountered in polymer processing. The fluid can be any non-Newtonian fluid which is incompressible, inelastic and time independent. The flow field is divided into an Eulerian mesh of cells. Around each node, located at the center of the cell, a local flow analysis is made. The analysis around all nodes results in a set of linear algebraic equations with the pressures at the nodes as unknowns. The simultaneous solution of these equations results in the required pressure distribution, from which the flow rate distribution is obtained. Solution for the isothermal Newtonian flow problem is obtained by a one-time solution of the equations, whereas solution of a non-Newtonian problem requires iterative solution of the equations.

Hieber and Shen (1980) presented a detailed formulation for simulating the injection-moulding filling of thin cavities of arbitrary planar geometry. The modeling is in terms of generalized Hele-Shaw flow for an inelastic, non-Newtonian fluid under non-isothermal

conditions. A hybrid numerical scheme was employed in which the planar coordinates were described in terms of finite elements and the gapwise and time derivatives were expressed in terms of finite differences. Good agreement was obtained with experimental results in terms of short-shot sequences, weldline formation and pressure traces at prescribed points in the cavity.

Although the branching flow approach is capable of handling complex part (cavity) geometries, it inherently involves intensive user intervention.

Wang et al. (1986) simulate polymer flow in sheet-like cavities with three-dimensional configuration applying a hybrid finite-element/finite-difference/control-volume approach. This approach discretizes the sprue/runner/cavity geometry into a network of one-dimensional tubular elements and two dimensional triangular thin-shell elements. The advancement of the melt front is automatically tracked by computing the filled volume fraction of each control volume associated with the nodes and thus eliminating the user intervention.

This approach became the standard numerical framework for various commercial software packages and research codes and has been extended or incorporated by other researchers to simulate the injection moulding packing phase (Chiang et al., 1991a; Chen and Liu, 1994; Han and Im, 1997; Holm and Langtangen, 1999), mould cooling (Himasekhar et al., 1992), fiber orientation (Chung and Kwon, 1996) and shrinkage and warpage (Chiang et al., 1993).

Chiang et al. (1991a) employed a unified theoretical model to simulate the filling and postfilling stages of the injection-moulding process. The model is based on a hybrid finite-element/finite-difference numerical solution of the generalized Hele-Shaw flow of a compressible viscous fluid under nonisothermal conditions. The shear viscosity of the polymeric material is represented by a Cross model for the shear-rate dependence and a WLF-type functional form for the temperature and pressure dependence, whereas the specific volume is modeled in terms of a double-domain Tait equation. The analysis also handles variable specific heat and thermal conductivity of the polymer as a function of temperature. Automatic melt-front advancement during the cavity-filling stage is calculated using a control-volume scheme.

Chen and Liu (1994) presented a two-phase model for simulating the post-filling stage of injection moulding of amorphous and semicrystalline materials. A finite-element scheme with quadratic shape function for the pressure was proposed. The melt was considered in terms of Hele-Shaw flow for a non-Newtonian fluid using a modified-Cross model with either an Arrhenius-type or WLF-type functional form to describe the viscosity under nonisothermal

conditions; the compressible behavior of the polymer was assumed to obey either a double-domain Tait or single-domain Spencer Gilmore equation of state. To predict the solidified layer and temperature profile the interfacial energy balance equation including the latent-heat effect for semicrystalline materials was coupled with the transient energy equation for the solid and melt phases. Good agreement between the simulation and experimental pressure traces were obtained using two well-characterized materials, namely a commercial-grade Polypropylene (PP) and Polystyrene (PS).

Han and Im (1997) developed a numerical simulation program to predict the flow field in filling and post-filling stages of injection moulding. To simulate the real moulding conditions more accurately, a generalized Hele-Shaw model for a non-Newtonian fluid was assumed considering the effects of phase change and compressibility of the resin. A Finite Element Method (FEM) and Finite Difference Method (FDM) hybrid scheme with control volume approach was employed as the solving technique. For modeling the viscosity of the resin, a modified Cross model was used with a double-domain Tait equation of state being employed in describing the compressibility of the resin during moulding. The energy balance equation, including latent-heat dissipation for semicrystalline materials, was solved in order to predict the solidified layer and temperature profile in detail. Based on a comparison between experiments and simulations, it was found that the currently developed program was useful in unified simulations of filling and post-filling in injection-moulding processes when considering the phase-change effect.

Holm and Langtangen (1999) presented a simulation model for the injection moulding process. For the polymer flow between two flat plates a 2D Hele-Shaw approximation was adopted, whereas the moving polymer-air front was handled by a level-set-like method. The 3D heat equation was solved using finite elements in the flow plane, a spectral method in the perpendicular direction and finite differences in time. A unified simulation framework for the injection moulding process was formulated and evaluated, where it was applied a common 2D mesh for the flow variables as well as for the temperature.

Himasekhar et al. (1992) developed a computer simulation for three-dimensional mould heat transfer during the cooling stage of an injection moulding process. In this simulation, mould heat transfer was considered as cyclic-steady, three-dimensional conduction; heat transfer within the melt region was treated as transient, one-dimensional conduction; heat exchange between the cooling channel surfaces and coolant was treated as steady, as was heat exchange with the ambient air and mould exterior surfaces. A hybrid scheme consisting

of a modified three-dimensional, boundary-element method for the mould region and a finite-difference method with a variable mesh for the melt region were applied as part of the numerical implementation. These two analysis were iteratively coupled so as to match the temperature and heat flux at the mould-melt interface.

Chung and Kwon (1996) shown that on injection moulding of short fiber reinforced plastics, fiber orientation during mould filling is determined by the flow field and the interactions between the fibers. The flow field is, in turn, affected by the orientation of fibers. In the coupled analysis of mould filling flow and fiber orientation the Dinh and Armstrong rheological equation of state for semiconcentrated fiber suspensions was incorporated. The viscous shear stress and extra shear stress due to fibers dominate the momentum balance in the coupled Hele-Shaw flow approximation, but the extra in-plane stretching stress terms could be of the same order as those shear stress terms, for large in-plane stretching of suspensions of large particle number. Thus, for the mould filling pressure a new equation was derived including the stresses due to the in-plane velocity gradients. The moulding simulation was then performed by solving the new pressure equation and the energy equation via a finite element/finite difference method, as well as evolution equations for the second-order orientation tensor via the fourth-order Runge-Kutta method. The effects of stresses due to the in-plane velocity gradient on pressure, velocity and fiber orientation fields were investigated in the center-gated radial diverging flow in the cases of both an isothermal Newtonian fluid matrix and a nonisothermal polymeric matrix.

Chiang et al. (1993) employed a coupled analysis of the fluid flow and heat transfer in the polymer melt during the filling and post-filling stages of the injection-moulding process and of mould cooling/heating which occurs during the entire process. Polymer Melt Analysis (PMA) was carried out through a unified theoretical model implemented using a hybrid finite-element/finite-difference/control-volume numerical solution of the generalized Hele-Shaw flow of a compressible viscous fluid under non-isothermal conditions. Further, Mould Cooling Analysis (MCA) was carried out utilizing a periodic heat conduction model implemented using a modified three-dimensional boundary-element method. To faithfully accommodate the effects of mould cooling on the fluid flow and heat transfer in the polymer melt, PMA and MCA were coupled for appropriate data exchange and iterations carried out until a convergent solution for mould temperatures and for flow, pressure and temperatures within the polymer melt were obtained.

However, the HeleShaw flow formulation has its limitations due to the inherent creeping-flow and thin-wall assumptions. For example, it cannot accurately model the three-dimensional flow behaviors within thick and complex components or at the melt fronts (fountain flows), flow junctions, regions where the part thickness changes abruptly or separate melt fronts meet (weld lines) and regions around special part features such as bosses, corners and/or ribs. Therefore, in order to generate complementary and more detailed information related to the flow characteristics and stress distributions in thin moulded parts a three-dimensional (3D) simulation model should be used (Hétu et al., 1998; Pichelin and Coupez, 1998, 1999; Xue et al., 1999; Chang and Yang, 2001).

Hétu et al. (1998) presented a 3D finite element model capable of predicting the velocity, pressure and temperature fields, as well as the position of the flow fronts. The velocity and pressure fields are governed by the generalized Stokes equations. The fluid behavior was predicted through the Carreau Law and Arrhenius constitutive models. These equations were solved using a Galerkin formulation. A mixed formulation was used to satisfy the continuity equation. The tracking of the flow front was modeled by using a pseudo-concentration method and the model equations were solved using a Petrov-Galerkin formulation. The validity of the method has been tested through the analysis of the flow in simple geometries.

Pichelin and Coupez (1998) described a general solution for the 3D mould filling by incompressible viscous fluid. It is based on the combination of an extended flow solver and the solution of a transport equation governing the flow front position. The flow solver uses tetrahedral elements, a first order stable mixed velocity pressure formulation entering in the family of the MINI-element and a global iterative solution. The characteristic function of the fluid domain was shown to follow a conservative law and the moving fluid description was transformed into a transport equation in the whole domain to be filled. An explicit discontinuous Taylor-Galerkin scheme was introduced to solve this fluid motion equation.

Pichelin and Coupez (1999) introduced a Taylor discontinuous Galerkin method to solve the thermal problem in the context of the 3D mould filling by viscous incompressible fluid. This numerical scheme was designed to deal with the physical phenomena of shear and temperature dependent viscosity, viscous heat generation and heat transfer by conduction and convection. This approach aims to simulate non-isothermal flows of viscous fluid with moving free surfaces and more particularly the injection moulding process involving thermal shocks at the interface between the cold mould wall and the hot polymer.

Xue et al. (1999) presented a fully three-dimensional numerical simulation of viscoelastic flows using an implicit finite volume method. The viscoelastic flow problems involving the stress singularity, including plane stick-slip flow, the flow past a junction in a channel and the 3-D edge flow, were used to test the ability of the method to predict the singularity features with accuracy. The accuracy of the numerical predictions was judged by comparing with the known asymptotic behavior for Newtonian fluids and some viscoelastic fluids and the investigations were extended to the viscoelastic cases with unknown singular behavior. The Phan-Thien-Tanner (PTT) model and in some cases, the Upper-convected Maxwell (UCM) model, were used to describe viscoelastic fluids.

Chang and Yang (2001) developed an implicit finite volume approach to simulate the three-dimensional mould filling problems encountered during the injection moulding. The described numerical model deals with the three-dimensional isothermal flow of incompressible, high-viscous Newtonian fluids with moving interfaces. The collocated finite volume method and the SIMPLE segregated algorithm were used to discretize and solve the Navier–Stokes equation. In addition, a bounded compressive high-resolution differencing scheme was adopted to solve the advection equation to capture the interface on a Eulerian framework. Several two- and three-dimensional examples were presented to validate the presented approach and illustrate its capabilities.

Rajupalem et al. (1997) and Talwar et al. (1998) used an equal-order velocity–pressure formulation to solve the Navier–Stokes equations in their three-dimensional simulation of mould filling/packing phases.

Rajupalem et al. (1997) developed a fully three-dimensional mould filling simulation tool with the objective of eliminating the problems that comes with the use of the Hele-Shaw approximation to simplify the simulation of the injection moulding process. All the relevant conservation equations are solved using 3D finite elements.

Talwar et al. (1998) demonstrated the increasing feasibility of simulating the injection moulding process while obviating the need to reduce the mould into a two-dimensional object of representation. This work continues on an earlier presentation in that the derivation of the relevant equations for packing or holding phase of the process is presented and the computational techniques employed are discussed. They demonstrate the robustness of the method with two practical examples.

Ilinca and Hétu (2000) used a pressure stabilized Petrov–Galerkin method to solve the Navier–Stokes equations in their three-dimensional numerical model for the filling-packing-

cooling stages of injection moulding. The methodology consisted in solving the three-dimensional (3D) equations modeling the momentum, mass and energy conservation. The packing and cooling stages of the injection moulding process were modeled by including the compressibility effects. The performances of the proposed approach were quantified for the injection of a thin plate for which experimental data are available. The procedure was then applied to a thick 3D part and it was obtained accurate solutions.

Khayat et al. (2001) used a Boundary Element Method (BEM) for three-dimensional, free-surface cavity flow of viscous, incompressible fluids. An adaptive (Lagrangian) boundary-element approach for the general three-dimensional simulation of confined free surface flow of viscous incompressible fluids was adopted. The method is stable as it includes re-meshing capabilities of the deforming free surface and thus can handle large deformations. A simple algorithm was developed for mesh refinement of the deforming free surface mesh. Problems like the transient nature of the flow in the extrusion through circular and square dies, the filling of circular and square disks as in conventional injection moulding and the flow during gas-assisted injection moulding inside a duct, with relevance to the important problem of viscous fingering were illustrated in this work.

Finally, Cao et al. (2005) developed a fully three-dimensional mould filling simulation program. The governing equations are in terms of Navier-Stokes problems for the viscous, incompressible, on isothermal and non-Newtonian fluid. To avoid the simultaneous determination of the coupled velocity and pressure, the article introduced an iterative method that at any given time step solves the components independently. In addition, the article also presents a mixed implicit and ''up-wind'' scheme to discrete the energy equation. It can overcome the spatial oscillations of temperature in numerical simulation.

Table 2.1 summarizes the mathematical modeling research for the filling, packing-holding and cooling stages of injection moulding process and includes the main key features of the works developed by the authors. The first author to present 1D models for filling and post-filling phases of injection moulding was Kamal and Kenig (1972). After two decades, Chiang et al. (1993) presented 2D models for the three phases and Ilinca and Hétu (2000) developed the 3D models to describe the injection stages.

	Injection stages			
Authors	*Filling*	*Packing*	*Cooling*	*Mathematical Models*
Wu et al. (1974)	Yes	No	No	1D
Stevenson (1978)	Yes	No	No	1D
Stevenson and Chuck (1979)	Yes	No	No	1D
Harry and Parrott (1970)	Yes	No	No	1D
Lord and Williams (1975)	Yes	No	No	1D
Kamal and Kenig (1972)	Yes	Yes	Yes	1D
Williams and Lord (1975)	Yes	No	No	1D
Nunn and Fenner (1977)	Yes	No	No	1D
Tadmor et al. (1974)	Yes	No	No	2D
Hieber and Shen (1980)	Yes	No	No	2D
Wang et al. (1986)	Yes	No	No	2D
Chiang et al. (1991)	Yes	Yes	No	2D
Chen and Liu (1994)	Yes	Yes	No	2D
Han and Im (1997)	Yes	Yes	No	2D
Holm and Langtangen (1999)	Yes	Yes	Yes	2D
Himasekhar et al. (1992)	No	No	Yes	2D
Chung and Kwon (1996)	Yes	No	No	2D
Chiang et al. (1993)	Yes	Yes	Yes	2D
Hétu et al. (1998)	Yes	No	No	3D
Pichelin and Coupez (1998)	Yes	No	No	3D
Pichelin and Coupez (1999)	Yes	No	No	3D
Xue et al. (1999)	Yes	No	No	3D
Chang and Yang (2001)	Yes	No	No	3D
Rajupalem et al. (1997)	Yes	Yes	No	3D
Talwar et al. (1998)	Yes	Yes	No	3D
Ilinca and Hétu (2000)	Yes	Yes	Yes	3D
Khayat et al. (2001)	Yes	No	No	3D
Cao et al. (2005)	Yes	No	No	3D

Table 2.1: Mathematical modeling research for injection moulding process.

3

OPTIMIZATION

3.1 NUMERICAL SIMULATION APPROACH

Combination of mathematical models, numerical methods and user interface programming were the basis of some typical numerical simulation models. These models were developed to simulate the process behavior of injection moulding in the filling, postfilling and cooling stages. Some of the research that provides numerical simulation results for different aspects of injection moulding process is presented here.

Jong and Wang (1990) described an automatic and optimal design of runner systems in injection moulding based on flow simulation.

Lee and Kim (1995a) investigated optimal gate locations using evaluation criteria of warpage, weld and meld lines and izod impact strength. A local search was conducted on the nodes using the criteria to determine the quality of the node.

Lee and Kim (1995b) used a modified complex method to reduce warpage by optimizing the thicknesses of different surfaces, the warpage being further reduced by obtaining the optimum processing conditions.

Seow and Lam (1997) used a method that focuses on cavity balancing to reduce distortion. By balancing the flow, over-packing and residual stresses are decreased. A straight flow path was assumed. It provided good results in cavity balancing for simple two-dimensional objects. The optimization routine described in the paper has shown its effectiveness in optimizing the thickness distribution to achieve balanced flow. The method was implemented and adapted to commercial software (Moldflow).

Douglas et al. (1998) is the first to design a mould by combining polymer process modelling, design sensitivity analysis and numerical optimization. The gate location and injection pressure profile were optimized through minimizing fill time while satisfying constraints on injection pressure, injection flow rate and mould clamp force. The methodology was demonstrated by using simple geometry.

Tang et al. (1997, 1998) used 2D transient FEM simulations coupled with Powell's optimization method to optimize the cooling channel geometry to get uniform temperature in the polymer part.

Park and Kwon (1998b) developed 2D and 3D stationary BEM simulations in the injection moulds coupled with 1D transient analytical computation in the polymer part (throughout the thickness). The heat transfer integral equation is differentiated to get sensitivities of a cost function to the parameters (Park and Kwon, 1998c). The calculated sensitivities are then used to optimize the position of linear cooling channels for simple shapes (Park and Kwon, 1998a).

Later, Lam and Seow (2000) presented a new method for flow path generation using the hill-climbing algorithm. It overcomes the difficulties of the straight flow path assumption by deriving the flow paths from the fill pattern of the cavity. Combining the flow paths generated with the optimization routine developed, automatic cavity balancing was achieved with excellent results.

Lam and Jin (2001) put forward gate location optimization schemes based on the flow path concept. Standard deviation of flow path length, standard deviation of fill time, or range of fill time was employed as the objective function, respectively.

Huang and Fadel (2001) used 2D transient FEM simulations to optimize the use of moulds materials according to part temperature uniformity or cycle time.

Kumar et al. (2002) presented the optimization of the moulding conditions based on the simulations results for the non-isothermal mould-filling and an empirical relation predicting cooling time. The optimization problem is characterized by an objective function that is the weighted sum of temperature difference of the melt temperature at the end of the filling stage, maximum injection pressure and cycle time, so that we can get process parameters (mould temperature, melt temperature and fill time) which will result in maximum productivity and good quality product. The resulting optimization problem was solved by an exhaustive search in the constrained space obtained by an Approximate Feasible Moulding Space (AFMS).

Courbebaisse and Garcia (2002) presented a new approach towards optimization of polymer injection moulding by doing a shape analysis. Firstly, they present the flow modeling based on Hele–Shaw equations and the Volume of Fluid (VOF) method. Secondly, they present the geometrical characterization of the mould geometry by using mathematical morphology transformations in order to extract shape parameters. Finally, taking in consideration shape parameters such as optimal centering and skeleton transformation, the objective of their work

was to estimate the best location of the injection points to obtain lowest injection pressure and balanced filling of the mould. Subsequently, they developed this methodology further and applied it to single gate location optimization of an L-shape example (Courbebaisse, 2005). It is easy to use and not time-consuming, while it only serves the turning of simple flat parts with uniform thickness.

Shen et al. (2004) developed a general methodology that automatically predicts the optimal gate location of injection moulds based on injection-moulding simulation. They defined a cost function, which measure the performances of polymer injection operation affected by the gate location. This function includes filling pressure, filling time difference between different flow paths, temperature difference and overpack percentage. Finally, a modified hill-climbing algorithm that combines the designer's intuition with a deterministic hill-climbing search was used to search the optimal gate location.

Mathey et al. (2004) developed an optimization procedure to improve cooling of injection moulds. The model uses a mathematical programming method, Sequential Quadratic Programming (SQP), to modify and improve automatically the geometry and the process parameters according to an objective function (e.g., cooling time or temperature uniformity). The SQP method was coupled with the BEM to solve thermal problems of cooling during injection.

Zhai et al. (2005a) presented the two gate location optimization of one moulding cavity by an efficient search method based on pressure gradient and subsequently positioned weld lines to the desired locations by varying runner sizes for multi-gate parts (Zhai et al., 2006). Zhai et al. (2005b) investigated optimal gate location with evaluation criteria of injection pressure at the end of filling.

Pirc et al. (2007) used BEM and Dual Reciprocity Method (DRM) applied to unsteady heat transfer of injection moulds. The BEM software was combined with an adaptive reduced modeling. Then, they presented a practical methodology to optimize both the position and the shape of the cooling channels in injection moulding process. For that they coupled the direct computation with an optimization algorithm such as SQP. In this study they considered a potential problem defined in a 2D unbounded domain.

Later, Pirc et al. (2008) extended that methodology to optimize both the position and the shape of the cooling channels in 3D injection moulding process. The optimization variables used were the position and shape parameters for the cooling channels and the outputs were

the temperature of the plastic-part surface and the variation of the temperature along this surface.

Agazzi et al. (2010) propose a methodology for the optimal design of the cooling system. Based on geometrical analysis, the cooling line was defined by using conformal cooling concept. It defines the locations of the cooling channels. Focus on the distribution and intensity of the fluid temperature along the cooling line which is fixed was studied in the paper. They formulate the determination of this temperature distribution, as the minimization of an objective function composed of two terms. It was shown how this two antagonist terms have to be weighted to make the best compromise. The expected result was an improvement of the part quality in terms of shrinkage and warpage.

Table 3.1 summarizes the numerical simulation optimization research for the injection moulding process identifying the main aspect studied by the authors.

One advantage of the numerical simulation is that it could provide useful information in part design, mould design and process design of injection moulding. A number of process parameters for injection moulding can be obtained through the simulation packages. However, this approach involves cresting a finite element model and running a number of simulations in order to obtain the acceptable moulding parameters.

3.2 TRIAL-AND-ERROR APPROACHES

Setting the process parameters of injection moulding is a highly skilled job based on the operator's "know-how" and intuitive sense acquired through long-term experience rather than through a theoretical and analytical approach. The methods based on that plan to determine the process parameters for injection moulding are called techniques from the trial and error approach. Attempts were made in utilizing the simulation results to determine a set of moulding parameters. Some tend to define a defect free moulding region or working window for injection moulding (Process Window Approach). Some applied DOE techniques to define an acceptable parameter setting. However, these approaches require a certain number of trial runs of the injection moulding programs.

	Numerical results				
Authors	*Runner System*	*Process conditions*	*Gate location*	*Cavity balancing*	*Cooling channel*
Jong and Wang (1990)	Yes	No	No	No	No
Lee and Kim (1995a)	No	Yes	No	No	No
Lee and Kim (1995b)	No	No	Yes	No	No
Seow and Lam (1997)	No	No	No	Yes	No
Douglas et al. (1998)	No	Yes	Yes	No	No
Tang et al. (1997 and 1998)	No	No	No	No	Yes
Park and Kwon (1998a,b,c)	No	No	No	No	Yes
Seow and Lam (2000)	No	No	No	Yes	No
Lam and Jin (2001)	No	No	Yes	No	No
Huang and Fadel (2001)	No	No	No	No	Yes
Kumar et al. (2002)	No	Yes	No	No	No
Courbebaisse and Garcia (2002 and 2005)	No	No	Yes	No	No
Shen et al. (2004)	No	No	Yes	No	No
Mathey et al. (2004)	No	No	No	No	Yes
Zhai et al. (2005a and 2005b)	No	No	Yes	No	No
Zhai et al. (2006)	Yes	No	No	No	No
Pirc et al. (2007)	No	No	No	No	Yes
Pirc et al. (2008)	No	No	No	No	Yes
Agazzi et al. (2010)	No	No	No	No	Yes

Table 3.1: Numerical simulation research for injection moulding process.

3.2.1 *Process Window*

Several attempts that aim to determine a feasible process zone for injection moulding were developed since the quality of moulded parts is greatly affected by the conditions under which they are processed. This process zone is always referred as a process window. In the development of a process window for injection moulding various techniques were introduced. Some researchers developed a process window through a number of simulation trials with different combinations of moulding parameters.

Pandelidis and Zou (1990a) studied the optimal injection gate locations with a quality function consisting of temperature differences, overpack and frictional heating terms. A combination of simulated annealing and the hill-climbing method was then used to find the optimal node. The process variables were also optimized in a later paper Pandelidis and Zou (1990b).

Seaman et al. (1993) implemented an algorithm that runs in real-time and provides immediate feedback to a process operator about the current operating point in a manufacturing process. A method for automatic control of quality was presented and is based on building a quality-based model for the process. In this model, the output measurements are product properties and inputs are process command signals and parameters of process controllers. This model was used within a multiobjective optimization algorithm: the quality controller. The quality controller iteratively adapts the process inputs and controllers on-line, so that quality is continuously optimized. The algorithm was applied to the tuning of process inputs for the plastication and injection phases of an injection moulding process. The optimization took place with respect to three quality characteristics: cycle time, flashing and underfill. Later, Seaman et al. (1994) explored the use of multiobjective optimization for the purpose of extending Proportional Integral Derivative (PID) controllers to applications that require the optimization of multiple objectives. It was applied to the tuning of a PID controller to meet multiple objectives for the plastication phase of an injection moulding process.

Tan and Yuen (1996) developed a computer system for computing an initial setting for an injection moulding machine. First, possible processing conditions are determined by considering only the material type and machine model. Then an initial processing condition is determined from these possible conditions by reasoning using the empirical rules. This reasoning is formalized by fuzzy logic. Finally, the machine setting corresponds to the

determined initial processing condition is calculated by simple formula. The performance of the system was verified by experiments. Results show that the computed setting is acceptable for simple geometry.

Li et al. (2007) used feature warpage to describe the warpage of injection moulded parts and is evaluated based on the numerical simulation software. To optimize the single gate location for plastic injection mould the feature warpage evaluation based on numerical simulation is combined with a simulated annealing algorithm. The method results in an optimal gate location, by which the part is satisfactory for the manufacturer.

Table 3.2 summarizes the process window optimization research that has been done in the injection moulding process identifying the main aspect studied by the authors.

Normally, an acceptable result of injection moulding can be yielded based on the process window approach. However, development of a full set of process windows would be very difficult because of the large number of process parameters involved and the number of possible interactions among the parameters.

	Process Window				
Authors	*Runner System*	*Process conditions*	*Gate location*	*Cavity balancing*	*Cooling channel*
Pandelidis and Zou (1990a)	No	No	Yes	No	No
Pandelidis and Zou (1990b)	No	Yes	No	No	No
Seaman (1993/94)	No	No	No	No	No
Tan and Yuen (1996)	No	No	No	No	No
Li et al. (2007)	No	No	Yes	No	No

Table 3.2: Process window optimization research for injection moulding process.

3.2.2 *Design of Experiment*

DOE techniques are attempted to obtain the understanding of the injection moulding process. Among the various DOE techniques, the Taguchi method was widely used to determine optimal process parameters for injection moulding.

Chang and Faison (2001) applied the Taguchi method to systematically investigate the effects of process conditions on the shrinkage (along and across the flow directions) of three plastics: High Density Polyethylene (HDPE), General Polystyrene (GPS) and ABS. Mould and melt temperatures, along with holding pressure and holding time, are the most significant

influences on the shrinkage behaviors of three materials. The optimal conditions for reducing shrinkage identified by the Taguchi method were experimentally verified and validated by t-statistic tests.

Huang and Tai (2001) analyzed the effective factors of warpage in injection-moulded items applying the Taguchi method. Filling time, mould temperature, gate dimensions, melt temperature, packing pressure and packing time were identified as the effective factors of warpage in the injection-moulded products. Computer simulations of the injection moulding process were carried out to obtain the warpage data. Then, the contribution percentage of each factor was found and the optimum set of parameters driving the effective factors in injection moulding was determined to produce a product with the minimum warpage.

Wu and Liang (2005) discussed the effect of various process parameters on the characteristics of the weld line of an injection-moulded part. The influence of cross-sectional dimension on the weld-line strength was also studied. The mould was designed in such a way that specimens with and without weld lines can be developed separately. The Taguchi method was applied to study the individual contribution of process parameters on the tensile strength. Melt temperature, mould temperature, injection speed and packing pressure were selected as the most influential variables. The microstructure of weld lines was clearly observed from the micrographs.

Feng et al. (2006) examines multiple quality optimization of the injection moulding for Polyether Ether Ketone (PEEK). It also looks into the dimensional deviation and strength of screws that are reduced and improved for the moulding quality, respectively. This study applies the Taguchi method to cut down on the number of experiments and combines grey relational analysis to determine the optimal processing parameters for multiple quality characteristics. The quality characteristics of this experiment were the screw's outer diameter, tensile strength and twisting strength. First the processing parameters that may affect the injection moulding were determined with the L_{18} (21× 37) orthogonal, including mould temperature, pre-plasticity amount, injection pressure, injection speed, screw speed, packing pressure, packing time and cooling time. Then, the grey relational analysis, whose response table and response graph indicated the optimum processing parameters for multiple quality characteristics, was applied. The efficiency of this optimization model had been successfully proved by experiments and can be compliant with the research purpose of taking active actions for waste prevention.

Tang et al. (2007) produced a thin plate with dimension 120mm×50mm and 1mm thickness. It was used for testing on the effective factors to minimize the warpage defect. Firstly, fabricating the plastic injection mould was done. After that, the mould was assembled on the injection moulding machine. When the thin plates have been produced, they were used for testing on the effective factors in warpage problem by applying the experimental design of Taguchi method. The factors used were melt temperature, filling time, packing pressure and packing time. Among these factors, the melt temperature is the most effective factor. However, the filling time is not a significant factor.

Dong et al. (2008) present the parametric sensitivity study of the replication of a cross microchannel by injection moulding with a nickel mould insert. The effects of processing parameters of the injection moulding on the transcription properties of cross-sectional geometry of the microchannel were quantitatively characterized by means of design of experiments based on the Taguchi method by varying mould temperature, melt temperature, injection speed and packing pressure. From the sensitivity analysis of the experimental results based on the relative error, it was identified that mould temperature is the most sensitive processing parameter in this study. The optimal and worst processing conditions were found in the study from the investigations of the injection moulded products via a scanning electron microscope and a noncontact 3D confocal microscope.

Table 3.3 summarizes the design of experiment optimization research that has been done in the injection moulding process identifying the main aspect studied by the authors.

Interactions among process variables with a minimum number of test runs could be found with the Taguchi parameter design. Furthermore, analysis of the experimental results could help to develop a model of injection moulding process, which allows the prediction of part characteristics as a function of process conditions. Such a model can then be used to find the optimal parameters setting. Although, the DOE approach requires a certain measure of expert knowledge of both statistics and process engineering in experiment planning.

	Design of experiment				
Authors	*Runner System*	*Process conditions*	*Gate location*	*Cavity balancing*	*Cooling channel*
Chang and Faison (2001)	No	Yes	No	No	No
Huang and Tai (2001)	No	Yes	No	No	No
Wu and Liang (2005)	No	Yes	No	No	No
Feng et al. (2006)	No	Yes	No	No	No
Tang et al. (2007)	No	Yes	No	No	No
Dong et al. (2008)	No	Yes	No	No	No

Table 3.3: Design of experiment optimization research for injection moulding process.

3.3 ARTIFICIAL INTELLIGENCE APPROACHES

Some Artificial Intelligence (AI) techniques were used in the determination of the parameter setting for injection moulding. ANN and EA are emerging as the new approaches in the determination of the process parameters for injection moulding. A trained neural network system can quickly provide a set of moulding parameters according to the results of the predicted quality of moulded parts. However, the time required in the training and retraining a neural network could be very high. By using EA approach, the system can locally optimize the moulding parameters even without the knowledge about the process. Actually, some studies combine different techniques to improve the optimization of injection moulding process.

3.3.1 *Artificial Neural Network*

ANN is a technique that emulates the neural reasoning behavior of biological neural systems. An input layer accepts scaled input values and passes these values to a series of hidden layers and finally to an output layer. A neural network must be trained by methodically examining sets of input values and their associated outputs. A trained neural network system has the ability to transform nonlinear mathematical modeling into a simplified black-box structure that is capable of generalizing the set of previously learned instances (Krose and Smagt, 1996; Wilde, 2004). Neural network approach was applied in building a process model for quality control in injection moulding. The inputs to the networks are the process parameters

and the outputs are the quality characteristics. Several systems are developed based on the rule-based approach to provide solutions to moulding problems. Some recently developed systems are based on the case-based approach to assist in setting the moulding conditions.

Zhao and Gao (1999) measured and analyzed the melt temperature at an injection nozzle exit. They proposed a systematic method for predicting the melt temperature profile by modeling the three consecutive stages, plastication, dwell and injection. The variables considered were the rotation speed, back pressure, barrel heater temperatures, nozzle heater temperature, dwell time and injection velocity profile. The modeling of the melt temperature during plastication was carried out by a set of ANN. The mathematical model for the dwell period was developed and solved by the FDM. The melt flow during the injection phase was modeled as a free boundary problem and solved by the FEM. Combining the modeling of these three stages they predicted the melt temperature.

Sadeghi (2000) used an ANN method for off-line planning and control of quality, using computer-aided engineering software. The simulation work was implemented in order to develop a neural network model to predict the part quality or soundness in terms of lack or existence of short shot and weld line defect phenomenon in the plastic injection mouldings, based on key process variables as mould temperature, melt temperature, injection pressure and material grade.

Yarlagadda and Khong (2001) developed a neural network to predict plastic injection moulding process parameters. First, the governing equations for mould filling stage were analyzed in order to identify the input parameters for the proposed network. The output parameters of the network developed are injection time and injection pressure. Moulding conditions such as melt temperature, die temperature, injection pressure and injection time dominate the quality of the part produced.

Yarlagadda (2002) presented an integrated neural network system for prediction of process parameters such as injection pressure and injection time in metal injection moulding process. In the developed system the various issues addressed are: establishing a physical model for the analysis, determining the process parameters from analysis results, introducing a neural network system for function mapping and building a knowledge base system for manipulating empirical knowledge.

Huang and Lee (2003) employed two intelligent neural network control strategies to adjust the injection speed of the filling phase and control the nozzle pressure of the post-filling phase. A feed forward neural network with back propagation learning was used to control

the nozzle pressure of the post-filling stage with a certain overshoot. In addition, this control strategy has a self learning ability which takes care of the variation of injection speed, mould change and system time-varying change. The experimental results have verified this approach and have improved the performance of an industrial injection moulding machine.

Chen et al. (2004) proposed an on-line soft-sensor scheme to predict on-line the melt-flow-length via a recurrent neural network model using on-line measurable process variables as inputs. Developed on the basis of experimental data from a set of moulds with certain basic geometric features, the soft-sensor proved to be capable of predicting the melt-flow-length for moulds with different shapes.

Liao et al. (2007) used an approach so that the fluctuation of injected plastic part mass can be predicted using ANN quite accurately when key moulding process variables are changed. The approach of the work intends to contribute towards utilization of an ANN method for on-line planning and auto-adjustment of moulding process variables as melt temperature, injection pressure, injection speed and mould temperature.

Castro et al. (2007) proposed a method utilizing Computer Aided Engineering (CAE), statistical testing, artificial neural networks and data envelopment analysis to find the best compromises between multiple performance measures to prescribe the values for the controllable process variables in IM while considering their variability explicitly. The approach is illustrated with two case studies. The first case study adresses location of the injection gate and the second case study illustrate how this approach applies when purely experimental results are available.

Chen et al. (2008) presented a Self Organizing Map (SOM) plus a Back Propagation Neural Network (BPNN) model for the dynamic quality predictor. Three SOM-based parameters (injection stroke curve, injection velocity curve and pressure curve) and six process parameters (injection time, VP switch position, packing pressure, packing time, injection velocity and injection stroke) were the input parameters of the model, with one output variable of sample weight. The three SOM-based extraction parameters with the six manufacturing process parameters were dedicated to training and testing the BPNN. In addition, another BPNN model was employed for comparison. The numerical results revealed that the proposed dynamic model not only effectively increased the prediction performance of product quality but also obtained more-reliable product quality in advance.

Shie (2008) analyzed contour distortions, wear and tensile properties of PP components applied in the interior coffer of automobiles. A hybrid method integrating a trained Generalized

Regression Neural Network (GRNN) and a SQP method was proposed to determine an optimal parameter setting of the injection-moulding process.

Table 3.4 summarizes the artificial neural network optimization research that has been done in the injection moulding process identifying the main aspect studied by the authors.

Neural networks generate their own rules by learning from a certain training examples. This procedure is quite time consuming. In addition, neural networks cannot communicate how they work to the users so that it may be difficult to see what they are doing wrong. As a consequence, users cannot gain the understanding of the injection moulding process through the neural networks.

	Artificial neural network				
Authors	*Runner System*	*Process conditions*	*Gate location*	*Cavity balancing*	*Cooling channel*
Zhao and Gao (1999)	No	Yes	No	No	No
Sadeghi (2000)	No	Yes	No	No	No
Yarlagadda and Khong (2001)	No	Yes	No	No	No
Yarlagadda (2002)	No	Yes	No	No	No
Huang and Lee (2003)	No	No	No	No	No
Chen et al. (2004)	No	No	No	No	No
Liao et al. (2007)	No	Yes	No	No	No
Castro (2007)	No	No	Yes	No	No
Chen et al. (2008)	No	Yes	No	No	No
Shie (2008)	No	Yes	No	No	No

Table 3.4: Artificial neural network optimization research for injection moulding process.

3.3.2 *Evolutionary Algorithms*

EAs draw inspiration from the natural search and selection processes leading to the survival of the fittest individuals. The evolutionary computation techniques can be classified into four main categories: genetic algorithms (Holland, 1975), evolution strategies (Rechenberg, 1973), evolutionary programming (Fogel et al., 1966) and genetic programming (Koza, 1992). This classification is based in some details and historical development facts rather than in major functioning differences. In fact, their biological basis is essentially the same.

EA based methods are also proposed to address the problem of moulding condition optimization. Also, recent works tend to develop a system for parameter setting of injection moulding that combine and mutually strengthen the different AI technologies.

Young (1994) developed a gate location optimization method for liquid composite moulding (which has similarity to injection moulding) based on minimization of the mould-filling pressure, uneven-filling pattern and temperature difference during mould filling. The resin injection pressure was considered only because of the limit of the capacity of the equipment. The relationship between resin-filling pattern and injection pressure was not discussed.

Kim et al. (1996) applied GA in the development of systems for the optimization of the process parameters, which consist of the mould temperature, the melt temperature and the filling time, for injection moulding based on the results of flow simulation. The performance of the process was quantified using a weighted sum of the temperature difference, "overpack" and frictionally overheating criteria.

Ye (1999) employed a genetic algorithm in the optimization of injection moulding process and verified that the genetic algorithm was more efficient computationally than the simulated annealing algorithm. Application of these algorithms to determine gate location and optimal process condition in injection moulding was demonstrated with examples.

Kim et al. (2000) developed a numerical simulation for isothermal mould filling in the Resin Transfer Moulding (RTM) process by using Control Volume Finite Element Method (CVFEM). This CVFEM coupled interactively with GA, was used as an effective searching technique for determining optimum gate locations in order to minimize fill time in complex geometry.

Lee et al. (2001) developed a genetic algorithm based process planning system to optimize concurrently the operation selections and sequences for the manufacture of mould bases. The system first identifies the machining features automatically. All possible combinations of processes (machine, machining direction and cutting tool) are then generated based on available machining resources. By considering the multi-selection tasks simultaneously, a specially designed genetic algorithm searches through the entire solution space to identify the optimal plan. This planner is expected to assist users in optimizing process plans for the whole mould base.

Mok et al. (2001) described a hybrid neural network and genetic algorithm approach to determine a set of initial process parameters for injection moulding. Implementation of the system has demonstrated that the time required for the determination of initial process

parameters for injection moulding can be greatly reduced. The solutions recommended by the system can contribute to the production of good quality moulded parts.

Turng and Peic (2002) presented a system implementation and experimental verifications of an integrated CAE optimization tool that couples a process simulation program with optimization algorithms to determine intelligently and automatically the optimal design and process variables for injection moulding. Various local and global optimization algorithms were used like SQP, Self Adaptive Evolution (SAE), Differential Evolution (DE) and Simulated Annealing (SA).

Shi et al. (2003) presented a strategy for the optimization of the plastic injection moulding process. The strategy combines a neural network and a genetic algorithm. An approximate analysis model was developed with a BPNN to reduce the expensive computation required by numerical simulation and a nonbinary genetic algorithm was applied to solve the optimization model. Various plastic injection moulding process parameters, such as mould temperature, melt temperature, injection time and injection pressure are considered.

Alam and Kamal (2003) suggested that the maximum difference in shrinkage among the parts is an appropriate measure of product quality in the runner-balancing problem. They proposed a new approach to runner balancing, which accounts for product costs by including runner system volume and cycle time. The optimization problem was solved with a multi-objective genetic algorithm, Non-dominated Sorted Genetic Algorithm (NSGA).

Later, Alam and Kamal (2004) reformulated the runner-balancing problem. The objectives of this problem include the runner-system volume, the cycle time and the maximum difference in shrinkage among the parts. Optimizing the independent variables, which include the runner diameters and lengths and processing conditions, minimizes the objectives. They found that the optimization of the secondary runner lengths and processing conditions greatly reduced costs associated with balanced runner systems.

Finally, Alam and Kamal (2005) presented a general methodology to robust process optimization that incorporated several innovative strategies and applied to the injection moulding runner balancing problem. A multi-objective genetic algorithm was used in conjunction with a small sensitivity matrix to simulate the effects of process variation, which were characterized with a one-sided measure of robustness. The optimal solutions of balanced runner systems exhibited trade-offs between material costs and the percentage of rejected parts. Robust solutions improved the average part quality and in certain cases, reduced its standard deviation, in order to minimize the numbers of rejected parts.

Lam et al. (2004) explored an approach to optimize both cooling channel design and process condition selection simultaneously through an evolutionary algorithm. The design variables used were: co-ordinates of centers of cooling channels, sizes of cooling channels, flow rate and inlet temperature of the coolant in each cooling channel, packing time, cooling time and clamp open time. The prototype system proposed in the paper was an integration of the genetic algorithm and CAE technology. The objective was to achieve the most uniform cavity surface temperature to assure product quality.

Kurtaran et al. (2005) determined the best injection moulding process conditions for a bus ceiling lamp to enable minimum warpage. Mould temperature, melt temperature, packing pressure, packing time and cooling time were considered as process parameters. In finding optimum values, power of Finite Element (FE) software Moldflow, artificial neural network, statistical design of experiments and genetic algorithm were exploited. FE analysis were conducted for combination of process parameters designed using statistical full factorial experimental design. An efficient predictive model for warpage was created using feed forward artificial neural network exploiting FE analysis results. Neural network model was integrated with an effective genetic algorithm to find the optimum process parameter values.

Ozcelik and Erzurumlu (2005) studied the minimization of warpage on thin shell plastic parts by integrating finite element analysis, statistical design of experiment method, response surface methodology and genetic algorithm. First, to achieve the minimum warpage, optimum process condition dimensional parameters were determined. Next, finite element analysis were conducted for combination of dimensional parameters organized using statistical three-level full factorial experimental design method. A predictive model for warpage was created in terms of the dimensional parameters using response surface methodology. Finally, response surface model was interfaced with an effective genetic algorithm to find the optimum process parameter values.

Ozcelik and Erzurumlu (2006) introduced an efficient optimization methodology using ANN and genetic algorithm in minimizing warpage of thin shell plastic parts manufactured by injection moulding. Appropriate process condition parameters were determined to achieve the minimum warpage. Mould temperature, melt temperature, packing pressure, packing time, runner type, gate location and cooling time were considered as process conditions parameters. The most critical process parameters influencing warpage were determined using finite element analysis results based on analysis of variance method. A predictive model for warpage was created in terms of the most important process parameters using

artificial neural network methodology. ANN model was interfaced with an effective genetic algorithm to find the optimum process parameter values.

Lam et al. (2006) proposed a strategy of using a hybrid approach in injection moulding conditions optimization. This hybrid approach employs GA method first to identify candidate local minimum regions by deriving a number of elite solutions from the GA optimization results. These elite solutions are then used as a starting point to initiate the gradient method while searching for the local minimum. The optimal moulding conditions (melt temperature, mould temperature and injection time) are then derived by selecting the best from among the solutions corresponding to these local minimum. The objective is to determine the moulding condition for optimal part quality.

Qiao (2006) implemented a systematic computer-aided methodology for the optimization of cooling system design. Cycle-averaged cooling analysis, perturbation-based sensitivity analysis and the hybrid simulated annealing and Davidon–Fletcher–Powel method optimizer were applied to search for the optimal design. Significant uniformity of the temperature distribution along the cavity surface was obtained as a result of the optimization process.

Changyu et al. (2007) proposed a combining artificial neural network and genetic algorithm method to optimize the injection moulding process. A back-propagation neural network model was developed to map the complex non-linear relationship between process conditions and quality indexes of the injection moulded parts and the GA was used in the process conditions optimization (melt temperature, mould temperature, injection time, packing time and holding pressure). In order to improve the quality index of the volumetric shrinkage variation in the part a combining ANN/GA method was used in the process optimization for an industrial part.

Chen et al. (2007) presented a research that integrates Taguchi's parameter design methods with back-propagation neural networks, genetic algorithms and engineering optimization concepts, to optimize the initial process settings of plastic injection moulding equipment. Product weight and length were used for quality characteristics in the process parameter optimization of plastic injection moulding.

Wu et al. (2011) presented a study to simultaneously consider the combination of different classes of design factors as well as the weld line as a design constraint in which both the length and position are taken into account in injection moulding optimization. The study adopts an enhanced genetic algorithm, called Distributed Multi-population Genetic Algorithm (DMPGA) which combines a pre-existing optimization algorithm with commercial

Moldflow software and a master–slave distributed architecture. The results of this study show that DMPGA can not only effectively decrease maximum part warpage without violating the weld line constraint, but also conquer hurdles attributed to constraint handling and computational demand.

Table 3.5 summarizes the evolutionary algorithms optimization research that has been done in the injection moulding process identifying the main aspect studied by the authors, while Table 3.6 presents specif features concerning these works.

The effectiveness of the GA and evolutionary strategies is much dependent on the choice of the operating range of process parameters and design of a fitness function, which quantifies the quality of moulded parts. Besides, the control parameters of GA and evolutionary strategies such as population size, crossover rate and mutation rate must be properly defined.

The main limitations of the above methodologies are the following. First, most of the approaches proposed either consider one objective or use an aggregation function of the various objectives. This is not the better way to deal with the multi-objective nature of these optimization problems since this implies the aggregation in a single function of very different measures with different meanings. Therefore, the optimization effect is restricted by the determination of some weighting factors. This type of methodology is not able to capture the trade-off between the objectives, which can bias the solution found. Second, the methodologies proposed are not totally integrated, i.e., they do not consider the optimization and modeling processes as a whole process. Third, in some cases the extension of the proposed methodology to more complicated geometries is not obvious. Also, most of the optimizations are either unconstrained or subject to the constraints on the design parameters and manufacturing operations, ignoring important features of injection moulding like weld lines on the part, cooling channels locations and runner sizes.

Gaspar-Cunha and Viana (2005) proposed the use of an automatic optimization methodology based on MOEA for the maximization of the mechanical response of injection mouldings. For that purpose an MOEA was linked to an injection moulding simulator code (C-Mold). This allows the optimization of the processing conditions (injection flow rate, melt temperature and mould temperature) for a desired morphological state or for an enhanced mechanical response. The methodology proposed is general enough to be used with any injection moulding simulator code and is able to optimize multi.objectives producing results with physical meaning when applied to polymer processing techniques.

	Evolutionary algorithms				
Authors	*Runner System*	*Process conditions*	*Gate location*	*Cavity balancing*	*Cooling channel*
Young (1994)	No	No	Yes	No	No
Kim et al. (1996)	No	Yes	No	No	No
Ye and Wang (1999)	No	No	No	No	No
Kim et al. (2000)	No	No	Yes	No	No
Lee et al. (2001)	No	No	No	No	No
Mok et al. (2001)	No	Yes	No	No	No
Turng and Peic (2002)	No	Yes	No	No	No
Shi et al. (2003)	No	No	No	No	No
Alam and Kamal (2003/04/05)	Yes	No	No	No	No
Lam et al. (2004)	No	Yes	No	No	Yes
Kurtaran et al. (2005)	No	Yes	No	No	No
Ozcelik and Erzurumlu (2005)	No	Yes	No	No	No
Ozcelik and Erzurumlu (2006)	No	Yes	No	No	No
Lam et al. (2006)	No	Yes	No	No	No
Qiao (2006)	No	No	No	No	Yes
Changyu et al. (2007)	No	Yes	No	No	No
Chen et al. (2007)	No	Yes	No	No	No
Wu et al. (2011)	Yes	Yes	No	No	No

Table 3.5: Evolutionary algorithms optimization research for injection moulding process.

	Genetic algorithms and evolutionary strategies approach		
Authors	**Fitness evaluation**	**Optimization or decision variable(s)**	**Aim**
Ye and Wang (1999)	Single objective	Gate locations and process conditions	Maximum pressure at the end of filling and maximum curvature among all elements of the part
Kim et al. (2000)	Single objective	Gate locations	Fill time
Lee et al. (2001)	Single objective	Operation selections and sequences for the manufacture of mould bases	Overall machining time
Shi et al. (2003)	Single objective	Mould temperature, melt temperature, injection time, injection pressure	Maximum shear stress
Lam et al. (2004)	Single objective	Co-ordinates of centres of cooling channels, sizes of cooling channels, flow rate, inlet temperature of the coolant in each cooling channel, packing time, cooling time, clamp open time	Standard deviation of cavity surface temperature
Kurtaran et al. (2005)	Single objective	Mould temperature, melt temperature, packing pressure, packing pressure time, cooling time	Warpage
Ozcelik and Erzurumlu (2005)	Single objective	Dimensional parameters	Warpage
Ozcelik and Erzurumlu (2006)	Single objective	Mould temperature, melt temperature, packing pressure, packing pressure time, cooling time	Warpage
Qiao (2006)	Single objective	Locations of cooling channels	Standard deviation of cavity surface temperature
Changyu et al. (2007)	Single objective	Melt temperature, mould temperature, injection time, packing time, holding pressure	Volumetric shrinkage variation
Wu et al. (2011)	Single objective	Runner size, moulding conditions and part geometry	Maximum part warpage
Turng and Peic (2002)	Single objective/Aggregation function	Melt temperature, injection speed, packing pressure, packing time, mould temperature, cooling time	Shrinkage in length, cycle time, volumetric shrinkage

	Genetic algorithms and evolutionary strategies approach		
Authors	**Fitness evaluation**	**Optimization or decision variable(s)**	**Aim**
Young (1994)	Aggregation function	Gate locations	Mould-filling pressure, uneven-filling pattern and temperature difference during mould filling
Kim et al. (1996)	Aggregation function	Mould temperature, melt temperature, filling time	Temperature difference, overpack, frictionally overheating
Mok et al. (2001)	Aggregation function	Part design parameters, mould design parameters, process parameters of injection moulding	Quality measures (maximum wall shear stress, maximum representative shear rate, maximum temperature difference, cycle time)
Lam et al. (2006)	Aggregation function	Melt temperature, mould temperature, injection time	Maximum shear stress, maximum cooling time
Chen et al. (2007)	Aggregation function	Melt temperature, injection velocity, injection pressure, VP switch, packing pressure, packing time	Product's length and weight
Alam and Kamal (2003/04/05)	Multi objective	Runner diameters and lengths, processing conditions	Runner-system volume, cycle time, maximum difference in shrinkage

Table 3.6: Genetic algorithms and evolutionary strategies characterization in injection moulding process.

Part III

EXTRUSION PLASTICATING VERSUS INJECTION PLASTICATING

INTRODUCTION TO PART III

I can calculate the motion of heavenly bodies but not the madness of people.

— Isaac Newton

Fluid mechanics is the study of fluids either in motion (fluid dynamics) or at rest (fluid statics) and the subsequent effects of the fluid upon the boundaries, which may be either solid surfaces or interfaces with other fluids.

The basic equations are considered here to be the three laws of conservation for physical systems:

1. Conservation of mass (continuity)
2. Conservation of momentum (Newton's second law)
3. Conservation of energy (first law of thermodynamics)

The three differential equations of fluid motion can be summarized as follows:

Continuity:

$$\frac{\partial \rho}{\partial t} + \nabla \cdot (\rho V) = 0 \tag{3.1}$$

Momentum:

$$\rho \frac{dV}{dt} = \rho g - \nabla \mathbf{p} + \nabla \cdot \tau_{ij} \tag{3.2}$$

Energy:

$$\rho \frac{d\hat{u}}{dt} + \mathbf{p}\,(\nabla \cdot V) = \nabla \cdot (k \nabla T) + \Phi \tag{3.3}$$

where ρ is the density, V is the velocity, g is the vector acceleration of gravity, $\mathbf{p}$ is the pressure, τ_{ij} is the stress tensor, $\hat{u}$ is the internal energy, k is the coefficient of thermal conductivity, T is the temperature and Φ is the dissipation function.

In general, the density is variable, so that these three equations contain five unknowns, ρ, V, $\mathbf{p}$, $\hat{u}$ and T. To complete the system of equations two state relations of the thermodynamic properties are defined:

$$\rho = \rho\left(\mathbf{p}, T\right) \qquad \hat{u} = \hat{u}\left(\mathbf{p}, T\right) \tag{3.4}$$

The system of equations 3.1 to 3.4 is well posed (White, 1991; Schlichting, 1979) and can be solved analytically or numerically, subject to the proper boundary conditions.

The next two sections presents theoretical models able of describe polymer flow during the plasticating phase of extrusion, Chapter 4 (adapted from Gaspar-Cunha (2000)) and injection moulding, Chapter 5, accordingly to the fluid mechanics basic equations defined above.

EXTRUSION PLASTICATING

The objective of extrusion process is to create a form for a particular material forcing him moving through a channel. The polymers are usually extruded in its molten form. The machine mostly used in the extrusion process have inside an Archimedes type screw which is able to provide quantities of molten material in a continuous manner.

Although there are extruders with two or more screws, the one screw extruders are the most used. Figure 4.1 shows some of the components of an one screw extruder.

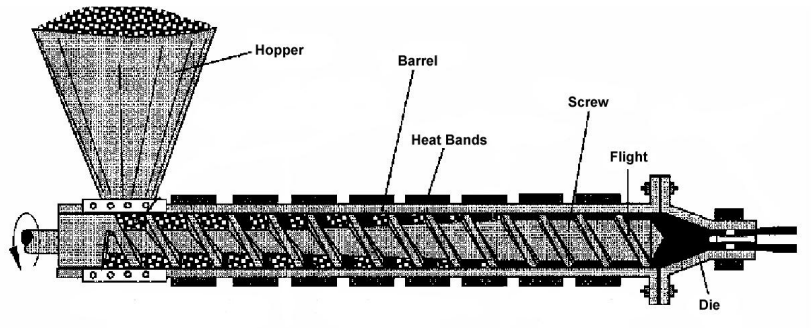

Figure 4.1: Typical single screw extruder.

The screw has (at least) three distinct geometrical sections (Figure 4.2): the feed zone, where the channel depth is constant (H_1); the compression zone, where the channel depth changes along the axis; and the metering zone , where the channel depth is again constant but smaller (H_2) .

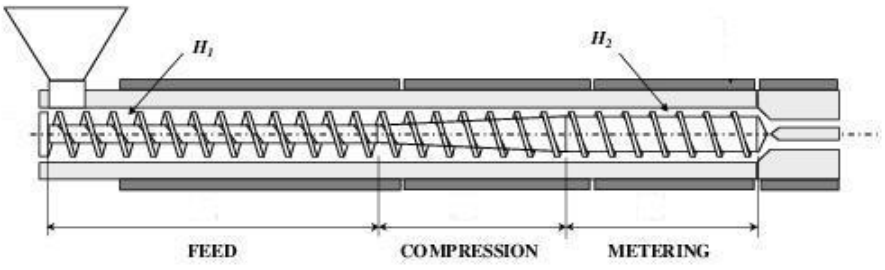

Figure 4.2: Three zone screw.

In the single screw extrusion the solid material is placed in the hopper and is transported to the screw channel by gravity. In the first turns of the screw the solid material is transported to the heated barrel, through the action of the rotating movement of the screw, where it melts.

Finally, in the metering zone is generated the necessary pressure so that polymer cross the die and take the final shape.

4.1 EXTRUDER GEOMETRY AND SIMPLIFICATIONS

Geometry of a single screw extruder is defined by the characteristics of the screw and the barrel as illustrated in Figure 4.3. The internal barrel diameter is D_b, the internal and external screw diameters are D_i and D_s, respectively, and the screw pitch is S.

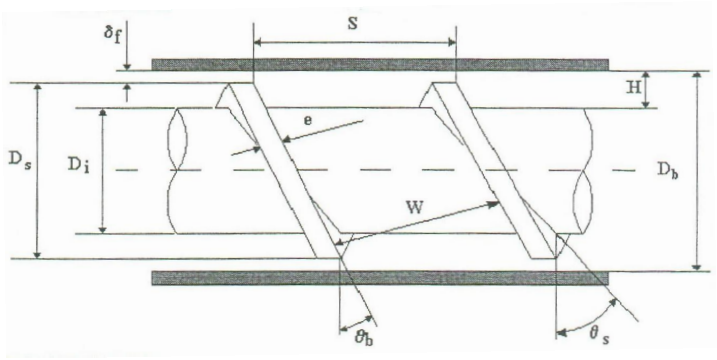

Figure 4.3: Geometry of an extruder screw.

The channel depth H , the flight clearance δ_f, the helix angle θ and the channel width W (at the root of the screw, θ_s and W_s, at the barrel surface, θ_b and W_b) can be calculated by:

$$H = \frac{D_b - D_i}{2} \tag{4.1}$$

$$\delta_f = \frac{D_b - D_s}{2} \tag{4.2}$$

$$\theta_s = \arctan\left(\frac{S}{\pi D_i}\right) \tag{4.3}$$

$$\theta_b = \arctan\left(\frac{S}{\pi D_s}\right) \tag{4.4}$$

$$W_s = S\cos\left(\theta_s\right) - e \tag{4.5}$$

$$W_b = S\cos\left(\theta_b\right) - e \tag{4.6}$$

The flight width, e, and the channel width, W, are measured in a direction normal to the flights. The number of screw flights in parallel, p, is usually equal to one.

Some simplifications are generally used in the studies that describe the modelling of plasticating single screw extrusion. They can be associated with the geometry of the screw channel and to the cinematic conditions:

1. The channel can be unrolled and treated as a rectangular cross section, so that Cartesian coordinates are used. The error introduced by this approximation is negligible, since the channel depth is much smaller than the screw diameter (Tadmor and Klein, 1970; Fenner, 1979; Stevens and Covas, 1995). Using this simplification the channel width and the helix angle become constants and can be calculated by their average values, $\overline{W}$ and $\overline{\theta}$. Figure 4.4 shows the screw of Figure 4.3 unrolled into a plan, through the tips of the screw flights, by cutting along a parallel line to the axis of the screw. Thus, a rectangular channel of variable depth is obtained.

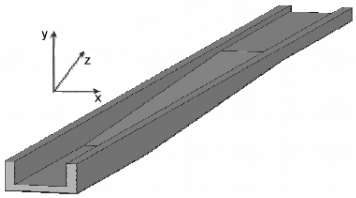

Figure 4.4: Unrolled screw channel.

2. The screw is stationary and the barrel rotates. This simplification is usually adopted since it is easier to visualize and study the extrusion physical phenomena (Tadmor and Klein, 1970; Rauwendaal et al., 1998). Therefore, barrel velocity (V_b) and its components (V_{bx} and V_{bz}) on a Cartesian system can be defined (Figure 4.5).

$$V_b = \pi N D_b \tag{4.7}$$

$$V_{bx} = V_b \sin(\theta_b) \tag{4.8}$$

$$V_{bz} = V_b \cos(\theta_b) \tag{4.9}$$

where N is the screw speed.

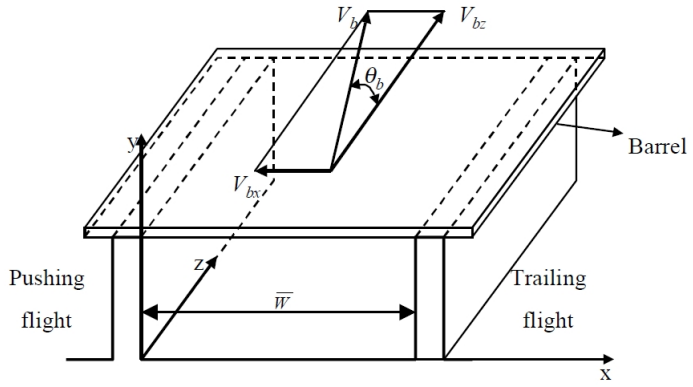

Figure 4.5: Barrel velocity components.

4.2 EXTRUSION FUNCTIONAL ZONES

The extrusion plasticating process starts with the introduction of polymer in the hopper, then polymer is melted and homogenized and finally is forced to pass through the die. The physical phenomena that occur inside the extruder are complex and include the solids conveying, the polymer melting and the melt conveying. The theoretical and experimental work done in recent decades has shown that the extrusion process implied the existence of the functional zones identified in Figure 4.6.

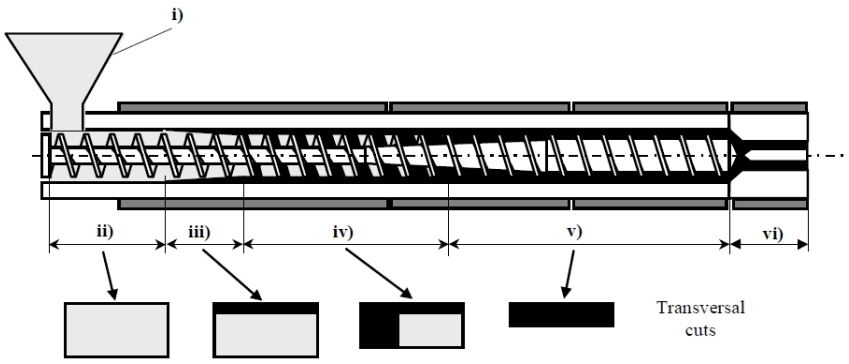

Figure 4.6: Physical phenomena inside the extruder.

The solid polymer is placed in the hopper *i)* and by gravity moves inside the cylinder, where is a Archimedes screw in rotation at a certain speed. This way, the solid polymer is dragged along the screw channel *(ii)* and starts to melt *iii)*. The molten polymer starts to accumulate into a melt pool *iv)*. The melt is homogenized, pressurized *(v)* and forced to pass through the die, which gives the final shape to the product *(vi)*.

The extrusion plasticating modeling consists in the description of heat transfer and mass flow phenomenas (through the balance equations of mass, moment and energy) in each

functional zone, taking into account the correct boundary conditions. For modelling purposes these functional zones are sequentially connected using the appropriate boundary conditions, i.e., the results obtained within one zone are the input conditions for the subsequent one. The system geometry, the polymer properties and the operating conditions are taken into account, in order to obtain some performance measure of the process, such as output, melt temperature, power consumption or degree of mixing.

The aim of the following sections is to present mathematical models that describe each functional zone, taking into account the respective boundary conditions (Gaspar-Cunha, 2000).

4.3 SOLIDS CONVEYING

The extension of the solids conveying zone is measured from the hopper until the location, on the screw, where the first polymer pellets melt. Generally, an initial condition for the calculations on the solids conveying zone on the screw is the pressure at bottom of the hopper.

Pressure generation

Broyer and Tadmor (1972) considered the following simplifications calculating the gradient of pressure:

- The pellets behave as a continuous elastic plug;
- The solid plug contacts perfectly all sides of the screw channel and barrel;
- The flight clearance is neglected;
- The various friction coefficients are constant;
- The polymer density is assumed to be constant;
- Gravitational and inertial forces are neglected.

From geometric considerations, the volumetric output is given by (Tadmor and Klein, 1970; Broyer and Tadmor, 1972):

$$Q = \pi^2 N H D_b (D_b - H) \frac{\tan\phi \tan\theta_b}{\tan\phi + \tan\theta_b} \left[1 - \frac{pe}{\pi (D_b - H) \sin\bar{\theta}}\right] \tag{4.10}$$

where ϕ is the solids conveying angle, measured by the difference between barrel velocity (V_b) and the material along the canal (V_{bz}), see Figure 4.7.

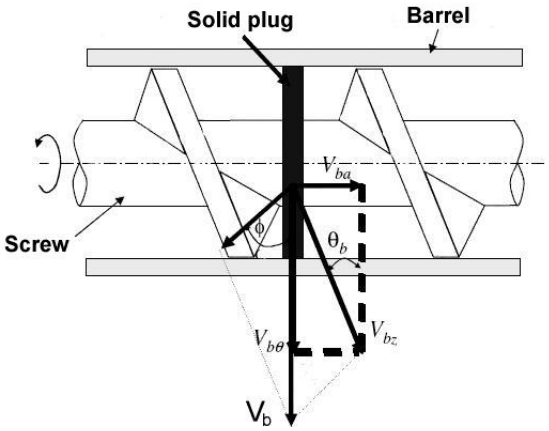

Figure 4.7: Representation of the solids conveying angle.

The pressure profile is obtained from force and torque balances made on a differential downchannel element, as shown in Figure 4.8 (Tadmor and Klein, 1970; Broyer and Tadmor, 1972). The forces include friction (F_1) between the barrel and the solid bed (acting in a direction making an angle $\theta + \phi$ with the down-channel direction), friction due to the contact of the solids with the screw root (F_5) and screw walls (F_3 and F_4), respectively, normal reactions (F_7 and F_8) and forces due to the pressure gradient (F_6 and F_2).

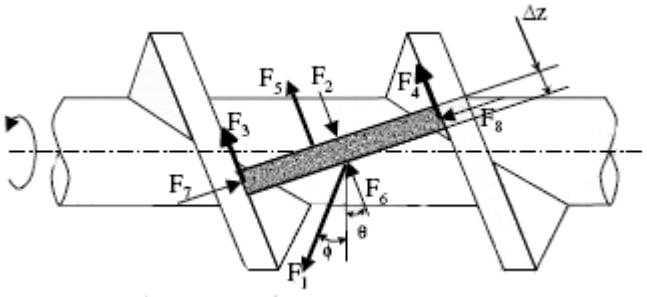

Figure 4.8: Forces acting on a solid bed element.

The pressure rise is given by:

$$P_2 = P_1 \cdot \exp\left[\int_{z_1}^{z_2} \left(\frac{B_1 - A_1 K}{B_2 + A_2 K}\right) dz\right] \tag{4.11}$$

where P_1 and P_2 are the pressures at down-channel distance z_1 and z_2, respectively. A_1, A_2, B_1, B_2 and K are constants.

Power consumption

The mechanical power consumption in the solids conveying zone (e_w) results from:

$$e_w = e_{wb} + e_{ws} + e_{wf} + e_{wp} \tag{4.12}$$

where e_{wb} , e_{ws}, e_{wf} and e_{wp} are the mechanical power dissipated on the barrel surface, on the screw root, on the flights and for compression, respectively.

Temperature profile

Solving the energy equation we can predict the temperature profile in the solid plug, which depends on:

- heat convection along the channel due to the polymer motion;
- heat conduction (in the radial direction) due to the temperature gradients;
- heat conduction in the down-channel direction.

The last assumption can be neglected when compared with the other two. Therefore, the temperature profile along the screw channel can be described by Equation 4.13, where the left term represents heat convection and right term represents the heat conduction in the radial direction:

$$V_{sz} \frac{\partial T}{\partial z} = \alpha_s \frac{\partial^2 T}{\partial y^2} \tag{4.13}$$

where V_{sz} is the solid bed velocity, T is the cross temperature profile (direction y) and α_s is the thermal diffusivity of the solid plug.

4.4 DELAY

The melting mechanism does not start immediately at the end of solids conveying zone. Before he start occurs solids conveying that are partially covered by a film of molten material. This stage is called delay and begins when the material in the interface melts (by heat conduction, or mechanical energy dissipation) and extends to the beginning of the melt pool formation. Therefore, delay zone can be characterized by two stages (Figure 4.9), the first consists in the formation of a melt film in the interface, the second in the formation of a melt film close to all the screw surfaces.

Figure 4.9: Two-stage delay zone.

4.4.1 *Delay zone I*

In this zone the solid bed contacts the screw walls and root, where the local temperature increases due to heat dissipation from friction, as shown in Figure 4.10. When the solid polymer reaches its melting point this mechanism is completed. Simultaneously, the solid polymer continues to melt at the melt film-solid bed interface.

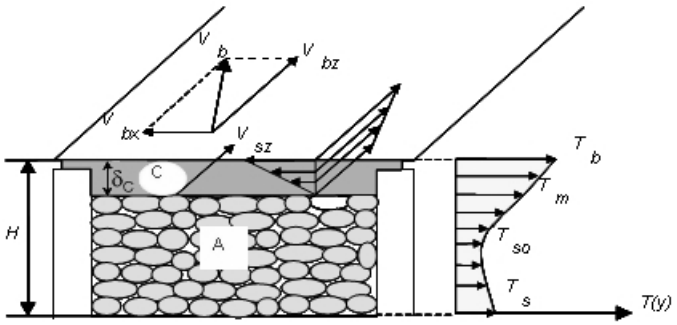

Figure 4.10: Cross-section for delay zone I.

The calculation of the film thickness profile, the temperature profiles in the film and in the solid bed, the pressure generation, the power consumption and the zone length is developed by Kacir and Tadmor (1972). Additionally, the model developed by Gaspar-Cunha (2000) considers:

- heat convection in the down-channel direction;
- heat conduction in the radial direction;
- heat convection in the radial direction.

The following assumptions are established:

- The solid bed is an isotropic and homogeneous continuum;

- Melt leakage over the flight tips is neglected;
- The molten polymer is an inelastic viscous fluid;
- The flow is steady;
- The solid-melt interface is smooth;
- The melt film flow is fully developed in the down and cross channel directions (i.e., $\frac{\partial V_x}{\partial x} = 0$ and $\frac{\partial V_z}{\partial z} = 0$);
- Gravitational and inertial forces are neglected.

Melt film

The momentum and energy equations are the following (Elbirli et al., 1984; Lee and Han, 1990; Huang and Peng, 1993; Han et al., 1996):

$$\frac{\partial P}{\partial x} = \frac{\partial}{\partial y}\left(\eta \frac{\partial V_x}{\partial y}\right) \tag{4.14}$$

$$\frac{\partial P}{\partial y} = 0 \tag{4.15}$$

$$\frac{\partial P}{\partial z} = \frac{\partial}{\partial y}\left(\eta \frac{\partial V_z}{\partial y}\right) \tag{4.16}$$

$$\rho_m c_p V_z \frac{\partial T}{\partial z} = k_m \frac{\partial^2 T}{\partial y^2} + \eta \dot{\gamma}^2 \tag{4.17}$$

where ρ_m is the melt density, c_p is the melt specific heat, k_m is the melt thermal conductivity, η is the melt viscosity (which is calculated using a temperature dependent power law) and $\dot{\gamma}$ is the shear rate.

Since the leakage flow is neglected, the melt must recirculate in the x-direction:

$$\int_0^{\delta_C} V_x dy = 0 \tag{4.18}$$

where δ_C is the melt film thickness.

The relevant boundary conditions are:

$$\begin{cases} V_x(y=0)=0 \\ V_x(y=\delta_C)=-V_{bx} \end{cases} \quad \begin{cases} V_z(y=0)=V_{sz} \\ V_z(y=\delta_C)=V_{bz} \end{cases} \quad \begin{cases} T(y=0)=T_m \\ T(y=\delta_C)=T_b \end{cases} \tag{4.19}$$

where T_m is the melting temperature.

Solid bed

Here, a displacement of the solids towards the melt film must occur, due to melting (Tadmor and Klein, 1970; Elbirli et al., 1984). The heat convection in the radial direction must be included in the energy equation.

$$V_{sy}\frac{\partial T}{\partial y}+V_{sz}\frac{\partial T}{\partial z}=\alpha_s\frac{\partial^2 T}{\partial y^2} \tag{4.20}$$

where V_{sy} is the velocity towards the solid-melt interface.

Mass and heat balances over the solid-melt interface

The melt film and the solid bed behavior can be coupled through mass and heat balances in the interface. The mass flow rate in the melt film $(\dot{m}_{C|z+\Delta z})$ is determined by the rate of melting over the interface (R_C), see Figure 4.11, which represents an elemental portion of the interface between the melt film, C and the solid bed A.

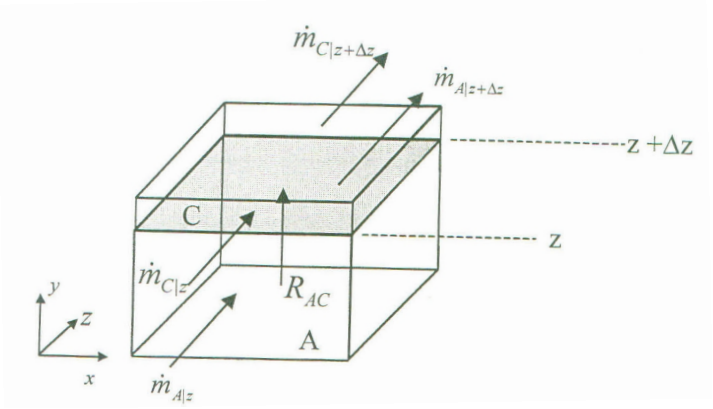

Figure 4.11: Mass balances over the solid-melt interface.

$$\dot{m}_{C|z+\Delta z}=\dot{m}_{C|z}+R_C \tag{4.21}$$

where:

$$\dot{m}_{C|z} = W_C \rho_m \int_0^{\delta_C} V_z dy \tag{4.22}$$

$$R_C = \rho_s V_{sy} \Delta z W_C \tag{4.23}$$

where ρ_s is the solid bed density and the indices $C|z$ and $C|z + \Delta z$ refer to the down-channel increment z and $z + \Delta z$, respectively, in zone C.

The mass flow rate in the solid bed $\left(\dot{m}_{A|z+\Delta z}\right)$ is:

$$\dot{m}_{A|z+\Delta z} = \dot{m}_{A|z} - R_C \tag{4.24}$$

where:

$$\dot{m}_{A|z} = \rho_s V_{sz} \left(H_{s|z} W_s\right) \tag{4.25}$$

and $H_{s|z}$ is the solid bed height. Consequently, the total mass flow rate $(\dot{m}_T)$ is:

$$\dot{m}_T = \dot{m}_{A|z+\Delta z} + \dot{m}_{C|z+\Delta z} \tag{4.26}$$

At last, a heat balance over the melting interface can be expressed as:

$$k_m \left(\frac{\partial T}{\partial y}\right)\Big|_{y=H-\delta_C} - k_s \left(\frac{\partial T}{\partial y}\right)\Big|_{y=H-\delta_C} = \rho_s \lambda V_{sy} \tag{4.27}$$

Pressure generation

The computation of the pressure profile for this zone is made by doing an identical force and torque balances similar to the ones carried out for the solids conveying zone. In this case, a viscous force must replace the friction force at the barrel wall (Kacir and Tadmor, 1972).

$$F_1 = \tau W_b dz \tag{4.28}$$

where τ is the shear stress. For isotropic pressure distribution and constant channel depth:

$$P = P_0 \exp\left(\frac{B_1' + A_1' K}{B_2 + A_2 K} \Delta z\right) + \frac{\tau W_b \left(\cos\bar{\theta} - K \sin\bar{\theta}\right)}{B_1' + A_1' K} \left[\exp\left(\frac{B_1' + A_1' K}{B_2 + A_2 K} \Delta z\right) - 1\right] \tag{4.29}$$

where A_1', A_2, B_1', B_2 and K are constants.

Power consumption

Following the procedure presented for the solids conveying zone, but replacing the contact with the barrel by a melt film, the mechanical power consumption can be calculated in the delay zone I. Therefore, Equation 4.12 becomes:

$$e_w^{'} = e_{wb}^{'} + e_{ws} + e_{wf} + e_{wp} \tag{4.30}$$

where e_{wb}' is the power dissipated on the barrel surface.

4.4.2 *Delay zone II*

This zone can be considered as a particular case of melting where the five distinct sections represented in Figure 4.12 can be identified (Elbirli et al., 1984; Lindt and Elbirli, 1985). Thus, physical compatibility between adjacent functional zones is ensured.

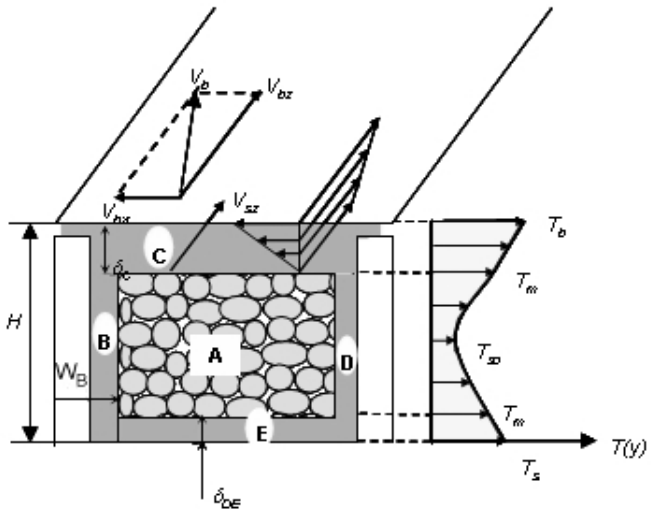

Figure 4.12: Cross-section for delay zone II.

The solid bed (A) is surrounded by melt films adjacent to the barrel wall (C), the screw root (E) and the active (B) and trailing (D) screw flights. Diference between the delay zone II and the melting zone is only in terms of melt pool B. When, the thickness of melt film B reaches the channel depth occurs transition from delay zone II to melting zone. In the delay

zone II section B is a melt film and calculations are carried out in the x-direction. However, in the melting zone, section B is a melt pool where the melt recirculates and, therefore, a two-dimensional approach need to be followed. The next section describes the model for melting zone.

4.5 MELTING

Figure 4.13 shows a schematic representation of the melting mechanism in a rectangular channel cross-section.

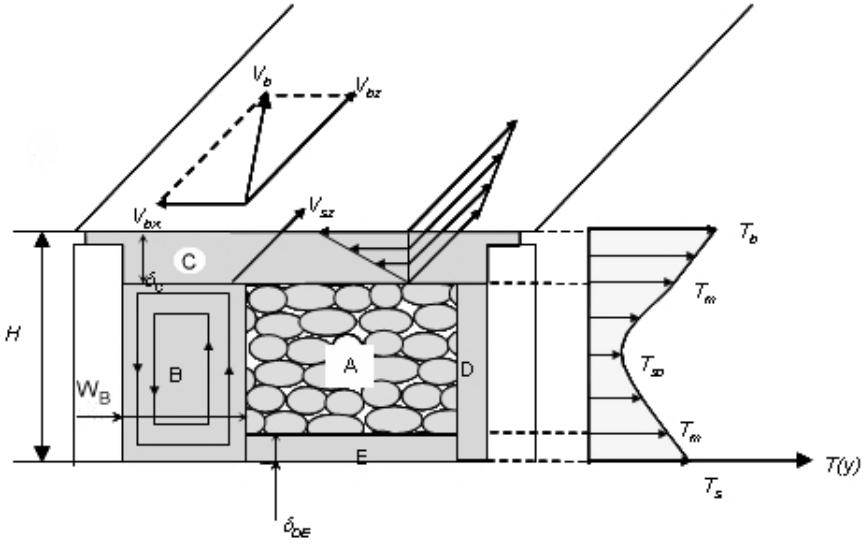

Figure 4.13: Cross-section for melting.

Each one of the five individual regions are described by different forms of the momentum and energy equations. To complete the equations available, boundary conditions and force, heat and mass balances are calculated. In addition to the simplifications made in the delay zone I is necessary to introduce new ones for the calculations in the melting zone (Elbirli et al., 1984; Lindt and Elbirli, 1985):

- The temperature field, of the melt films is fully developed in the cross channel direction (i.e., $\frac{\partial T}{\partial x} = 0$), but not in the down channel direction (i.e., $\frac{\partial T}{\partial z} \neq 0$);
- Heat conduction in the down channel direction is neglected (i.e., $\frac{\partial^2 T}{\partial z^2} << \frac{\partial^2 T}{\partial y^2}$);
- The solid bed velocity is constant.

Momentum and energy equations

A. Melt films (C, D and E)

The momentum and energy equations for films C, D and E are identical due to the assumptions made and the development of cross-channel melt circulation around the solid bed. As suggested by previous experimental work, Elbirli et al. (1984), Region D can be considered as an extension of region E. The flow and the thermal behavior of regions C and DE can be described by Equation 4.14 to Equation 4.17 with the following boundary conditions:

$$\begin{cases} V_x(y=0)=0 \\ V_x(y=\delta_C)=-V_{bx} \end{cases} \quad \begin{cases} V_z(y=0)=V_{sz} \\ V_z(y=\delta_C)=V_{bz} \end{cases} \quad \begin{cases} T(y=0)=T_m \\ T(y=\delta_C)=T_b \end{cases} \tag{4.31}$$

for region C and

$$\begin{cases} V_x(y=0)=0 \\ V_x(y=\delta_{DE})=0 \end{cases} \quad \begin{cases} V_z(y=0)=0 \\ V_z(y=\delta_{DE})=V_{sz} \end{cases} \quad \begin{cases} T(y=0)=T_s \\ T(y=\delta_{DE})=T_m \end{cases} \tag{4.32}$$

for region DE.

B. Melt pool (zone B)

Melt recirculation takes place when the melt pool width (W_B) is equal or greater than the screw channel depth , i.e., $\frac{\partial V_z}{\partial y} \neq 0$. Otherwise, B will behave as C (i.e., delay zone prevails). During melting, the momentum in the z direction and energy equations (Equation 4.16 and Equation 4.17) take the form:

$$\frac{\partial P}{\partial z} = \frac{\partial}{\partial y}\left(\eta \frac{\partial V_z}{\partial x}\right) + \frac{\partial}{\partial y}\left(\eta \frac{\partial V_z}{\partial y}\right) \tag{4.33}$$

$$\rho_m c_p V_z \frac{\partial T}{\partial z} = k_m \left(\frac{\partial^2 T}{\partial x^2} + \frac{\partial^2 T}{\partial y^2}\right) + \eta \dot{\gamma}^2 \tag{4.34}$$

The boundary conditions are:

$$\begin{cases} V_x(y=0)=0 \\ V_x(y=H)=-V_{bx} \end{cases} \quad \begin{cases} V_z(x=0)=0 \\ V_z(x=W_b)=V_{sz} \\ V_z(y=0)=0 \\ V_z(y=H)=V_{bz} \end{cases} \quad \begin{cases} T(x=0)=T_s \\ T(x=W_b)=T_m \\ T(y=0)=T_s \\ T(y=H)=T_b \end{cases} \tag{4.35}$$

c. Solid bed (zone A)

The solid bed is considered to move in the down channel direction at constant velocity:

$$V_{sz} = \frac{\dot{m}_T H W}{\rho_s} \tag{4.36}$$

An asymmetrical temperature distribution is caused by different heat conduction and dissipation rates occuring in the two opposite sides of the solid bed. Therefore, region A can be subdivided in two subregions (see Figure 4.14):

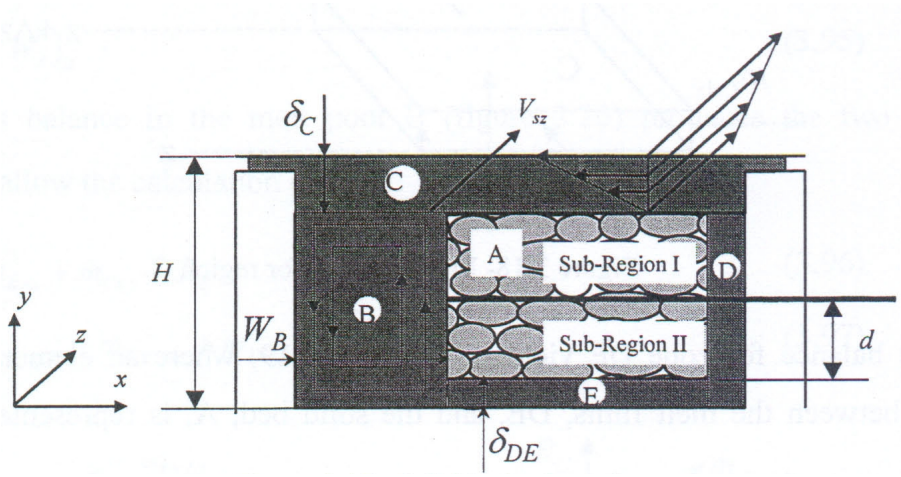

Figure 4.14: Solid bed sub-regions.

$$-\frac{V_{sy1}}{\alpha_s}\frac{\partial T_{s1}}{\partial y} + \frac{V_{sz}}{\alpha_s}\frac{\partial T_{s1}}{\partial z} = \frac{\partial^2 T_{s1}}{\partial y^2} \qquad \left(d \le y \le H_{s|z}\right) \tag{4.37}$$

$$\frac{V_{sy2}}{\alpha_s}\frac{\partial T_{s2}}{\partial y} + \frac{V_{sz}}{\alpha_s}\frac{\partial T_{s2}}{\partial z} = \frac{\partial^2 T_{s2}}{\partial y^2} \qquad (0 \le y \le d) \tag{4.38}$$

where V_{sy1} and V_{sy2} are the solid polymer velocities in the direction of the melt films C and E, respectively, T_{s1} and T_{s2} are the temperature profiles for sub-regions 1 and 2, respectively, and d is the distance in the y direction such that $T_{s1}(y=d) = T_{s2}(y=d)$.

The boundary conditions for these regions are:

$$\begin{cases} T_{s1}\left(y = H_{s|z}, z\right) = T_m \\ \qquad\qquad\qquad\qquad \text{for sub-region I} \\ \dfrac{\partial T_{s1}(y = d, z)}{\partial y} = 0 \end{cases}$$

$$\begin{cases} T_{s2}\left(y = 0, z\right) = T_m \\ \qquad\qquad\qquad\qquad \text{for sub-region II} \\ \dfrac{\partial T_{s2}(y = d, z)}{\partial y} = 0 \end{cases} \tag{4.39}$$

An iterative process is used to calculate distance d, starting with an initial value $\left(\text{for example, } \frac{H_{s|z}}{2}\right)$ until the temperature at d for the two regions is equal, i.e., $T_{s_1}\left(y = d\right) = T_{s_2}\left(y = d\right)$.

Mass and heat balances

Figure 4.15 represents an elemental portion of the interface of the melt film, C, and the solid bed, A.

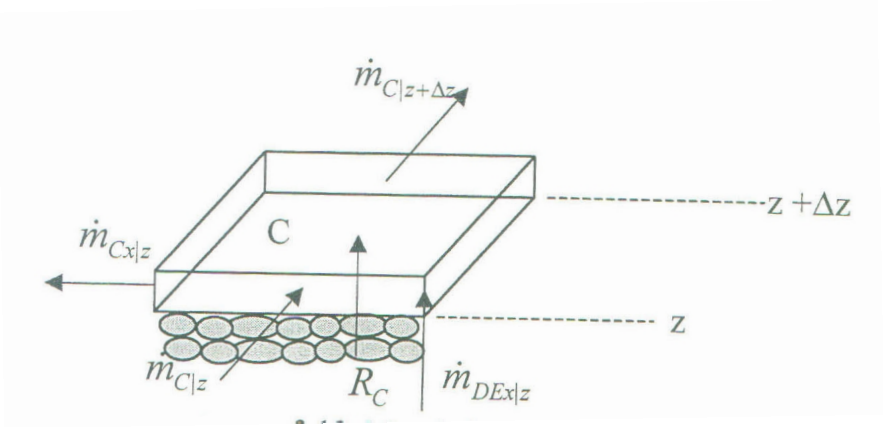

Figure 4.15: Mass balance for region C.

The mass balance for region C is calculated taking into account melt recirculation around the solid bed and is given by:

$$\dot{m}_{C|z+\Delta z} = \dot{m}_{C|z} - \dot{m}_{Cx|z} + \dot{m}_{DEx|z} + R_C \tag{4.40}$$

$$\dot{m}_{C|z} = W_{s|z}\rho_m \int_0^{\delta_{C|z}} V_z^{(C)} dy \tag{4.41}$$

$$\dot{m}_{Cx|z} = \Delta z \rho_m \int_0^{\delta_{C|z}} V_x^{(C)} dy \tag{4.42}$$

$$\dot{m}_{DEx|z} = \Delta z \rho_m \int_0^{\delta_{DE|z}} V_x^{(DE)} dy \tag{4.43}$$

$$R_C = \rho_s V_{sy1|z} \Delta z W_{s|z} \tag{4.44}$$

where $\dot{m}_{C|z}$ down-channel mass flow rate, $\dot{m}_{Cx|z}$ net flow rate to the melt pool, in the x direction and $\dot{m}_{DEx|z}$ cross-channel flow rate into the film from DE. In the above equations $\delta_{DE|Z}$ is the thickness of melt film DE.

Figure 4.16 shows an elemental portion of the interface between the melt films, DE, and the solid bed, A.

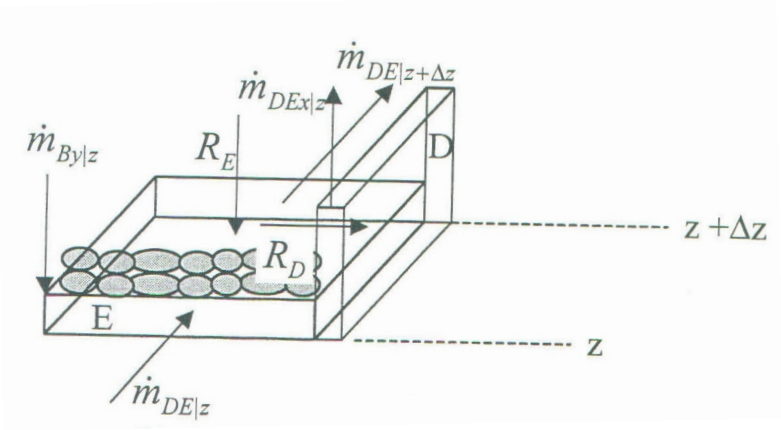

Figure 4.16: Mass balance for region DE.

The mass balance for zone DE yields:

$$\dot{m}_{DE|z+\Delta z} = \dot{m}_{DE|z} - \dot{m}_{DEx|z} + \dot{m}_{By|z} + R_D + R_E \tag{4.45}$$

where $\dot{m}_{DE|z}$ is down-channel mass flow rate, $\dot{m}_{By|z}$ is rate of melt circulation through the melt pool in the x-y plane, R_D is melting rate over the interface A-D for an increment Δz and R_E is melting rate over the interface A-E for an increment Δz, defined as:

$$\dot{m}_{DE|z} = (W_s + H_s)_{|z} \rho_m \int_0^{\delta_{DE|z}} V_z^{(DE)} dy \tag{4.46}$$

$$R_D + R_E = \rho_s V_{sy2|z} \Delta z \left(W_s + H_s\right) \tag{4.47}$$

Figure 4.17 shows a portion of the interface between the melt pool, B, and the solid bed, A.

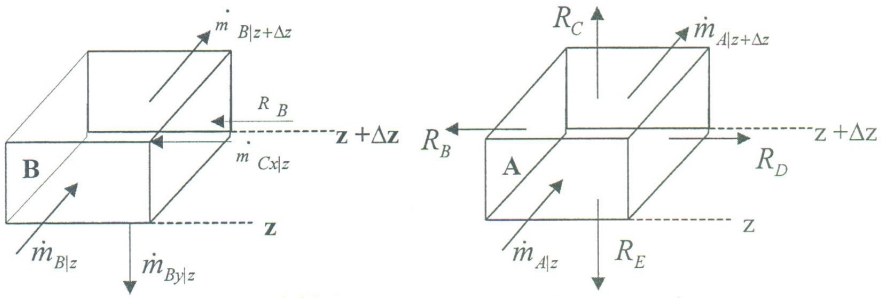

Figure 4.17: Mass balances for regions A and B.

The mass balance for the solid bed A is:

$$\dot{m}_{A|z+\Delta z} = \dot{m}_{A|z} - \left(R_C + R_B + R_D + R_E\right) \tag{4.48}$$

where:

$$\dot{m}_{A|z} = \rho_s V_{sz} \left(W_s H_s\right)_{|z} \tag{4.49}$$

At last, for the calculation of $\dot{m}_{By|z}$, the mass balance in the melt pool B (Figure 4.17) produces the two following equations:

$$\dot{m}_{B|z+\Delta z} = \dot{m}_{B|z} - \dot{m}_{By|z} + \dot{m}_{Cx|z} + R_B \tag{4.50}$$

$$\dot{m}_{B|z+\Delta z} = \dot{m}_T - \left(\dot{m}_{A|z+\Delta z} + \dot{m}_{C|z+\Delta z} + \dot{m}_{DE|z+\Delta z}\right) \tag{4.51}$$

Heat balances over the interfaces A-C and A-DE are useful to calculate the solid polymer velocity in the direction of the melt films C $\left(V_{sy1}\right)$ and DE $\left(V_{sy2}\right)$. The corresponding equations are, respectively:

$$k_m \left.\frac{\partial T}{\partial y}\right|_{A-C,\,melt} - k_s \left.\frac{\partial T}{\partial y}\right|_{A-C,\,solid} = \rho_s \lambda V_{sy1} \tag{4.52}$$

$$k_s \left.\frac{\partial T}{\partial y}\right|_{A-DE,\,solid} - k_m \left.\frac{\partial T}{\partial y}\right|_{A-DE,\,melt} = \rho_s \lambda V_{sy2} \tag{4.53}$$

Force balances

To complete the analysis the equilibrium of forces acting on the solid bed in the x and y directions are made:

$$\frac{\partial P^{(C)}}{\partial x} + \frac{\partial P^{(DE)}}{\partial x} = \frac{2\left(\tau_{yx|DE} + \tau_{yx|C}\right)}{H_s} \tag{4.54}$$

$$\frac{\partial P^{(C)}}{\partial z} + \frac{\partial P^{(DE)}}{\partial z} = \frac{\partial P}{\partial z}\left(= \frac{\partial P^{(B)}}{\partial z}\right) \tag{4.55}$$

and a condition of pressure continuity along the solid bed is defined:

$$\frac{\partial P^{(C)}}{\partial x} W_s = \frac{\partial P^{(DE)}}{\partial x} (W_s + H_s) \tag{4.56}$$

where $\tau_{yx|DE}$ and $\tau_{yx|C}$ are the shear stresses acting on the interfaces A-DE and A-C, respectively.

Finnaly, the various system of equations are subjected to the following geometric constraints:

$$\delta_C + H_s + \delta_{DE} = H \tag{4.57}$$

$$W_B + W_s + \delta_{DE} = W \tag{4.58}$$

Power consumption

The mechanical power consumption for the melting zone (e_m), results from the contributions of the power dissipated on the melt films C (e_{mfC}) and DE (e_{mfDE}), on the melt pool (e_{mp}), on the flight clearance (e_{mcl}) and the power required to build up pressure (e_{mbp}):

$$e_m = e_{mfC} + e_{mfDE} + e_{mp} + e_{mcl} + e_{mbp} \tag{4.59}$$

4.6 MELT CONVEYING

After melting is completed the melt conveying, or pumping zone, is developed . In this zone, mixing and generation of the required pressure to force the polymer through the die at a

specific output are acomplished. A two-dimensional analysis of developing non-isothermal non-Newtonian flow will be described bellow. Figure 4.18 presents the velocity and the temperature profiles for this zone.

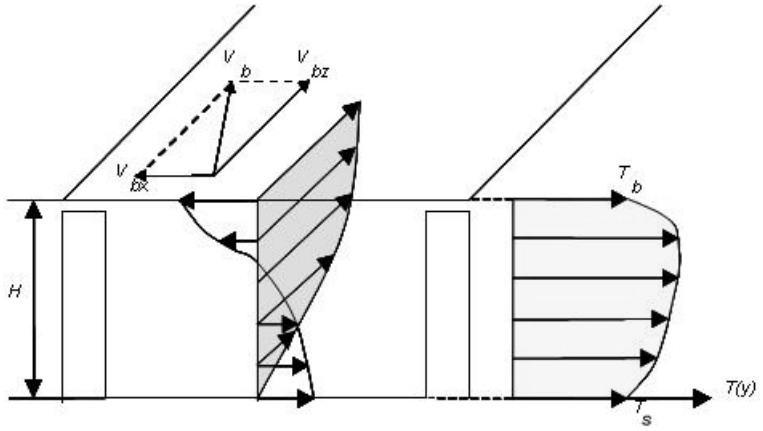

Figure 4.18: Cross-section for melt conveying zone.

The following assumptions are made (Fenner, 1977, 1979):

- Gravitational and inertial forces are neglected;
- The molten polymer is a viscous fluid obeying to the power-law;
- The flow is steady;
- Leakage flow and wall slip are neglected;
- The flow is fully developed in the down and cross channel directions (i.e. $\frac{\partial V_x}{\partial x} = 0$ and $\frac{\partial V_z}{\partial z} = 0$);
- The temperature field is fully developed in the cross channel direction (i.e. $\frac{\partial T}{\partial x} = 0$);
- Heat conduction in the down channel direction can be neglected (i.e. $\frac{\partial^2 T}{\partial z^2} << \frac{\partial^2 T}{\partial y^2}$).

Momentum and energy equations

Taking into account these conditions, the governing equations are similar to those for the melt pool in the melting zone (equations 4.14, 4.15, 4.33 and 4.34). The relevant boundary conditions are:

$$\begin{cases} V_x(y=0)=0 \\ V_x(y=H)=-V_{bx} \end{cases} \quad \begin{cases} V_z(x=0)=0 \\ V_z(x=W)=0 \\ V_z(y=0)=0 \\ V_z(y=H)=V_{bz} \end{cases} \quad \begin{cases} T(x=0)=T_s \\ T(x=W)=T_s \\ T(y=0)=T_s \\ T(y=H)=T_b \end{cases} \tag{4.60}$$

Power consumption

The power consumption (e_p) results from the contribution of the power dissipated on the screw channel (e_{psc}) on the flight clearance (e_{pcl}) and from the power required to build up pressure (e_{pp}):

$$e_p = e_{psc} + e_{pcl} + e_{pp} \tag{4.61}$$

5

MODELLING OF PLASTICATING INJECTION MOULDING - EXPERIMENTAL ASSESSMENT

Abstract[1]

A computational model for the description of polymer flow during the plasticating phase of the injection moulding process is proposed. The polymer behaviour is determined during the dynamic and static phases of the process. The model takes into account the backwards movement of the screw, the presence of a non–return valve and the conduction of heat during the idle times. Results for the dynamic and static phases of the plasticization are presented. The model is also used to study the influence of some important operative process parameters, such as, screw speed, backpressure, barrel temperatures and injection chamber length. The assessment of the computational results is made experimentally by comparing the average temperature calculated with measurements made in front of the screw nozzle using both, an Infrared (IR) camera and an IR thermometer.

5.1 INTRODUCTION

Injection moulding represents the most important process for manufacturing plastic parts. This processing technique is appropriate for mass production of plastic items, since raw material can be transformed into a moulding by a single procedure. In most cases finishing operations are not required. An important benefit of injection moulding is the possibility of making complex geometries automatically in one production step. Typical injection mouldings can be found everywhere in daily life, examples include automotive parts, toys, household articles, consumer electronic goods and micro parts.

Screw in-line plastic injection moulding machines have been used for the production of most products. However, existing studies were mainly on extruders, which are simpler to model and differ by neglecting the transient effects. There are a number of reasons for this, one of which is that model for reciprocating extruders is more complex. Up to now, many of

1 C. Fernandes, A.J. Pontes, J.C. Viana, J.M. Nóbrega and A. Gaspar-Cunha (2012). Modelling of Plasticating Injection Moulding - Experimental Assessment, in final phase of preparation.

the studies on the inline injection process take the simpler course of an extruder. This over-simplification of the inline injection process leaves out the most vital aspect of reciprocation, which changes the process model from steady extrusion to that of a discontinuous process.

In a typical reciprocating injection moulding cycle, first the screw is located in the forward position in the barrel, then the screw begins to rotate (screw recharge), conveying plastic material forward and developing a pressure ahead of the screw. This pressure forces the screw back to the desired volume of the moulded part. The screw is then idle in the back position while the previously moulded plastic cools down in the mould and the mould is opened and the part ejected. After the mould closes again, the screw is forced forwards by hydraulic pressure, causing the newly recharged shot at the head of the screw to flow into the empty mould. A valve, such as a check ring, prevents back-flow during injection. The screw then maintains the pressure on the moulded plastic for a specific time (the holding time). This completes the cycle.

Hence the injection cycle can be divided into three stages: the feeding (the screw rotating and moving backwards), stop (no screw movement) and injecting (the screw moving forwards without rotation).

Plasticization in a reciprocating-screw injection moulding machine has been generally assumed to be analogous to that of a single-screw extruder. That is, the screw can be divided into three functional zones of solid-conveying, melting and metering. Plastic melts predominantly in the melting zone, located between the solid-conveying and metering zones. The plastic granules are joined into a single solid piece (solid-bed), before entering the melting zone, in which the solid-bed is constantly deformed.

A considerable progress in optimization of plasticating systems of screw machines can be obtained not only in an experimental way, but also by means of mathematical modelling of transport phenomena in such systems. Due to the character of plasticization in the injection moulding process the resulting equations of continuity, motion and energy are strongly coupled and they can be solved only numerically. Therefore, mathematical models of transport phenomena can be successfully applied only by computer process simulation.

In the literature is possible to find some computer models for simulation of polymer plastication during extrusion (Tadmor and Klein, 1968; Chung, 1971; Tadmor, 1974; Torner, 1977; Tadmor and Gogos, 1979; Agur and Vlachopoulos, 1982; Zawadzky and Karnis, 1985; Rao, 1986). The present work consists of different modifications of the extrusion model formulated by Tadmor and Klein (1968). However there are distinctive differences between

melting in reciprocating extruders and non-reciprocating extruders. First, there are three stages in injection cycle of reciprocating screws. This causes the full melting process to be composed of discrete stages. Unlike non-reciprocating extruders, where one simple model (linear in time area) can be applied to describe the whole process, only a non-linear model can be used to describe the injection cycle. Second, there are axial movements of the screw in reciprocating extruders, when compared with non-reciprocating ones and both the solids and melt conveying rates through feeding are reduced because of the axial screw velocity. Third, the time for each stage is limited. For this reason the melting processes in these stages (including the rotating stage) act in a transient manner as an alternative of being steady-state as in non-reciprocating extruders. Consequently, the resultant balance equations are a lot more complicated in comparison with the similar ones for extrusion. This fact is probably the most important reason because there are less data in the literature about modelling of plasticization during injection moulding (Donovan, 1974; Lipshitz et al., 1974; Rauwendaal, 1992; Potente et al., 1993; Yung and Xu, 2001; Yung et al., 2003; Steller and Iwko, 2008). Some models presented include just a few problems connected with plasticization, such as changes in solid bed profile during the injection cycle, without taking into account the reciprocating screw movement (Rao, 1986). Rauwendaal (1992), described quantitatively the solids conveying, melting and melt conveying in a single screw extruder with both axial and rotational motion of the screw. The theoretical description of this extrusion process can be considered as an extension of the theory for non-reciprocating extruders. Yung et al. (2003) studied the transient models for the melting process in the three stages (melting, injection and stop stages) in the reciprocating extruder. Finally, Steller and Iwko (2008) presented a mathematical model of polymer plastication in a reciprocating screw injection moulding machine that takes into account all characteristic features of working of a real injector, such as periodical action of the three zones screw, to-and-from screw motion with controlled stroke and static and dynamic melting.

These newest mathematical models for injection moulding are being created with high complexity but some simplifying assumptions were made. The most important is a semi-empirical approach in the case of pressure calculations, if the screw channel is almost completely filled with solid polymer.

In this work the software available at the Department of Polymer Engineering of University of Minho (Gaspar-Cunha, 2000) to model the extrusion plasticating was modified in order to take into account the backwards movement of the screw, the presence of a non–return valve

and the conduction of heat during the idle times. The model uses the Tadmor formulation for temperature description during the plasticating and 3D transient equation of heat conduction is applied for the polymer in the injection chamber during the idle times. In this model the computation of the pressure profile is done by force and torque balances. The modelling routine developed was used to study the influence of some important operative process parameters, such as, barrel temperature profile, screw speed, backpressure, flow rate during injection and cycle times. Experimental assessment of the computational results was also done.

The paper is organized as follows. First, a description of the injection moulding process (injection cycle, system geometry, operating conditions and polymer properties) is presented. Then, the mathematical models adopted for the plasticating and stationary phases of the injection moulding process are proposed and described in detail. The mathematical models are applied to a case study. Finally, the modelling results for the dynamic and static phases are presented and discussed and the computational results are assessed experimentally.

5.2 PLASTICATING IN INJECTION MOULDING

5.2.1 *Injection cycle*

Injection moulding is a process of polymer transformation involving several steps, which are performed in an order that is repeated at each cycle. Below, a complete cycle of the injection moulding process was described (Figure 5.1).

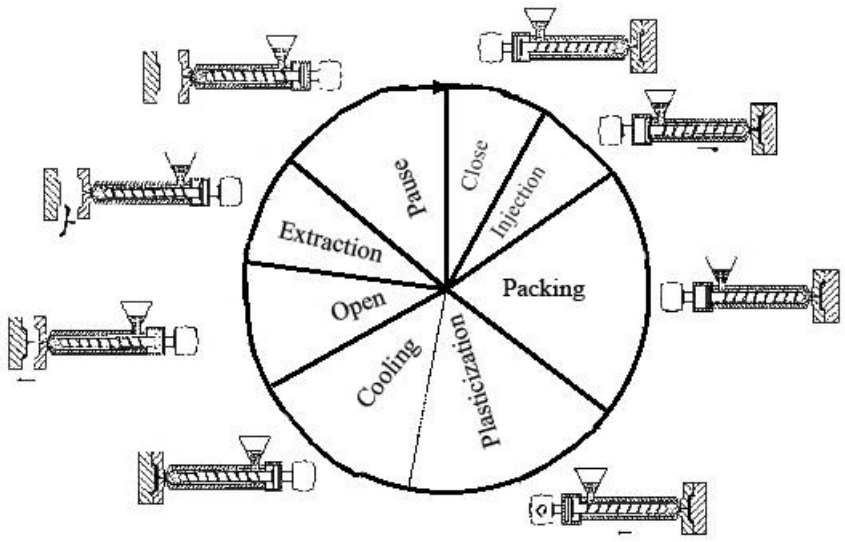

Figure 5.1: Injection moulding cycle (adapted from Zavaliangos (2001)).

When the screw turns, the solid material coming from the hopper is dragged against the inner wall of the cylinder. Thus, the friction force created heats up and pushes the material through the channel in direction of the tip of the screw. The polymer plasticization occurs due to the heat generated by friction and the heat conducted from the electric resistances that involve the external wall of the cylinder. When no more solid particles exists the plasticization finishes.

Since injection nozzle needs to be adjacent to the mould (that must be closed and filled), the plasticized material cannot exit the cylinder and accumulates in front of the screw. The pressure of the material pushes the screw back until it reaches a position pre-determined by the operator. At this point, the screw stops and the plasticization end. The mass of plasticised material, which is accumulated between the injection nozzle and the tip of the screw, should be enough to completely fill the cavity and the mould supply system.

Next the material must be injected, that is, transported to the closed mould cavity. The screw moves forward creating the necessary pressure so that material can pass through the injection nozzle channel, mould supply channel, entrance point of the cavity and fill the cavity. Since mould walls have channels for circulation of water or oil, gradually the moulded part and the material inside injection channel are cooled. After filling, occurs packing: the screw is maintained advanced until the material entrance point in the cavity is solidified. Cooling of the injected part continues and cavity and supply channel are completely solidified.

Since during cooling the screw is idle and the press is closed, the cooling time can be used for plasticating the material that will be injected in the next cycle.

5.2.2 *System geometry*

In a typical plasticating unit an Archimedes type screw rotates inside a heated barrel. The screw has (at least) three distinct geometrical sections (Figure 5.2): the feed zone, where the channel depth is constant (H_1); the compression zone, where the channel depth changes along the axis; and the metering zone, where the channel depth is again constant but smaller (H_2).

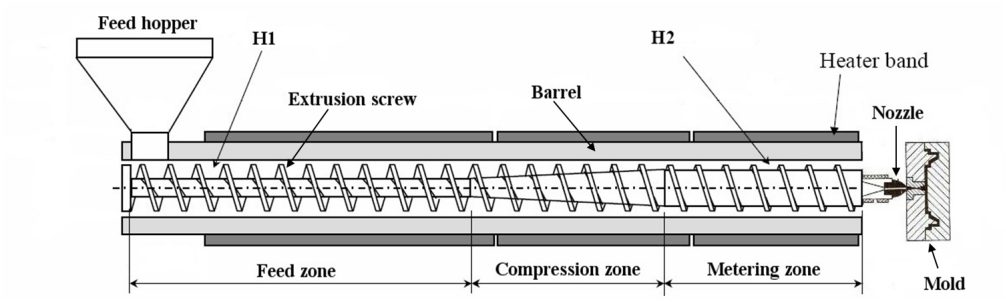

Figure 5.2: Typical injection screw machine.

Figure 5.3 illustrates a portion of the screw and barrel that is used to define the geometry of a single screw extruder. The internal barrel diameter is D_b, the internal and external screw diameters are D_i and D_s, respectively, and the screw pitch is S. The channel depth H, is given by:

$$H = \frac{D_b - D_i}{2} \tag{5.1}$$

The flight clearance is δ_f. The helix angle (θ) and the channel width (W) vary in the radial direction. At the root of the screw, θ_s and W_s, and at the barrel surface, θ_b and W_b:

$$\theta_s = \arctan\left(\frac{S}{\pi D_i}\right) \tag{5.2}$$

$$\theta_b = \arctan\left(\frac{S}{\pi D_s}\right) \tag{5.3}$$

$$W_s = S\cos\theta_s - e \tag{5.4}$$

$$W_b = S\cos\theta_b - e \tag{5.5}$$

The flight width (e) is calculated in a direction normal to the flights (as the channel width). Generally, the number of screw flights in parallel (p) is 1.

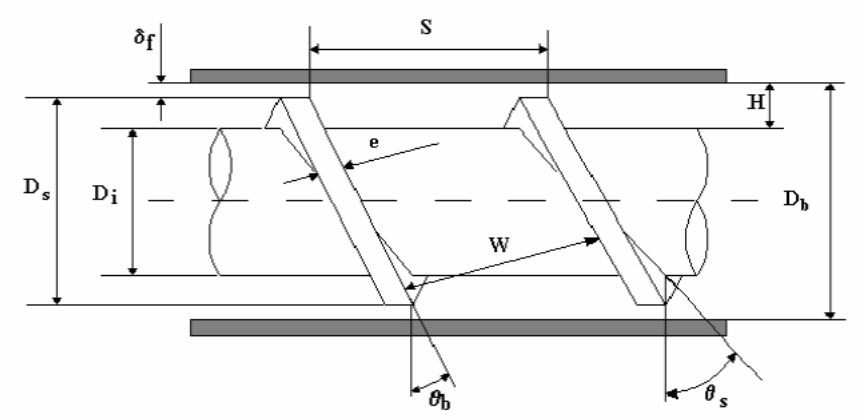

Figure 5.3: Geometry of a reciprocating injection screw.

5.2.3 *Operating conditions*

The barrel heating bands temperatures are identified as T_{b_i}, $i = 1, \ldots, N_{heatbands}$. Also, the nozzle can have a specific temperature value, identified here as T_{nozzle}.

The other operating parameters are screw speed N, back pressure in front of the screw during rotation (plasticization pressure) P_{plast}, time of the screw rest in the backwards position (analogous with the cooling time) t_{stop}. This time establish the polymer static melting in the heated part of the barrel. In contrast with the static melting phase, the time of dynamic melting (rotating and withdrawing screw) t_{plast} is not constant, but it depends on process conditions and can be calculated by:

$$t_{plast} = \frac{\pi \left(\frac{D_b}{2}\right)^2 \Delta L}{Q} \tag{5.6}$$

where ΔL is the incremental step in the injection chamber defined by:

$$\Delta L = \frac{L_{injchamber}}{N_{injchamber}} \tag{5.7}$$

with $L_{injchamber}$ being the length of the injection chamber and $N_{injchamber}$ the number of intervals in which the length of injection chamber is divided. To calculate the volumetric output (Q) the algorithm estimates first two initial output values using the screw geometry in the melt conveying zone and the screw speed. Next, calculations along the down-channel

direction using the extrusion models are done. Finally, the predicted pressure at the die exit is used as a convergence criterion to obtain the final volumetric output. If this pressure is lower than a pre-defined small value the program stops and the volumetric output is found. Otherwise, new output values are defined by the secant method and the computations with the extrusion models are carried out until convergence is reached.

5.2.4 *Polymer properties*

During polymer flow in the screw channel changes in the polymer physical state occurs. Thus, the description of flow phenomena occurring requires some physical data reflecting both the transition conditions of a polymer and its properties in the solid or liquid state. The material parameters used are the following: solid polymer density (ρ_s), melt polymer density (ρ_m), solid polymer thermal conductivity (k_s), melt polymer thermal conductivity (k_m), solid polymer specific heat capacity $\left(c_{p_s}\right)$, melt polymer specific heat capacity $\left(c_{p_m}\right)$, heat of fusion (λ), melting or flow temperature (T_m), barrel and screw friction factors of solid polymer (f_b) and (f_s), respectively, and rheological parameters of the melt. The rheological characterization of the melt behaviour was described by the constitutive equation of the Carreau-Yasuda model:

$$\eta\left(\dot{\gamma}\right) = \frac{\eta_0 f}{\left[1 + \left(K_1 f \dot{\gamma}\right)^a\right]^{\left(\frac{1-n}{a}\right)}} \tag{5.8}$$

where η_0 means zero-shear viscosity, $\dot{\gamma}$ is shear rate, $\eta\left(\dot{\gamma}\right)$ represents the shear rate-dependent viscosity, K_1, n and a are empirical constants and f stands for the exponential relations embracing the temperature and pressure sensitivity. In this study we have chosen the exponential expression widely used in polymer engineering calculations and modelling of nonisothermal injection moulding flows,

$$f = e^{\frac{E}{R}\left(\frac{1}{T} - \frac{1}{T_0}\right)} \tag{5.9}$$

where E/R means temperature coefficient of viscosity, T and T_0 are testing and reference temperatures, respectively.

5.3 MATHEMATICAL MODEL

5.3.1 *Global model*

Plasticating reciprocating extruders receives the polymer from the hopper, melts, homogenises and injects it into the mould. The physical phenomena developed inside the machine are complex. They correspond to a set of sequential functional zones that are usually identified as (Figure 5.4):

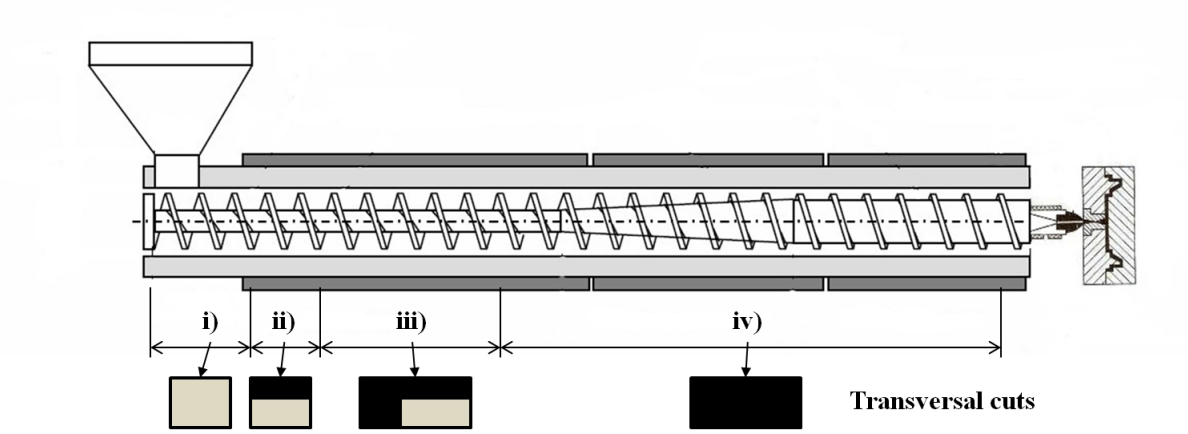

Figure 5.4: Physical phenomena inside the plasticating injection unit.

i) feed port and solids conveying zone;

ii) transient zone;

iii) melting zone;

iv) melt conveying zone.

They are qualitatively comparable to the correspondent zones in the extrusion process (Tadmor and Klein, 1970). Differences for steady conditions of extrusion are that lengths and positions of these zones change in time during the injection cycle. The present paper describes these changes in two strictly coupled states (Figure 5.5): at the end of screw rotation (beginning of static melting, $N = 0$) and at the beginning of screw rotation (beginning of dynamic melting, $N > 0$). During the plasticating time the screw retracts from the position L_0 (initial position) to the position L_1 (final position). Then, the screw stops rotating and melting due only to conduction occurs. Next, during injection time the material is forced to flow inside the mould and the screw advances forward to the initial position L_0. In this

position, packing and cooling of the polymer in the mould will take place. This completes a single injection moulding cycle.

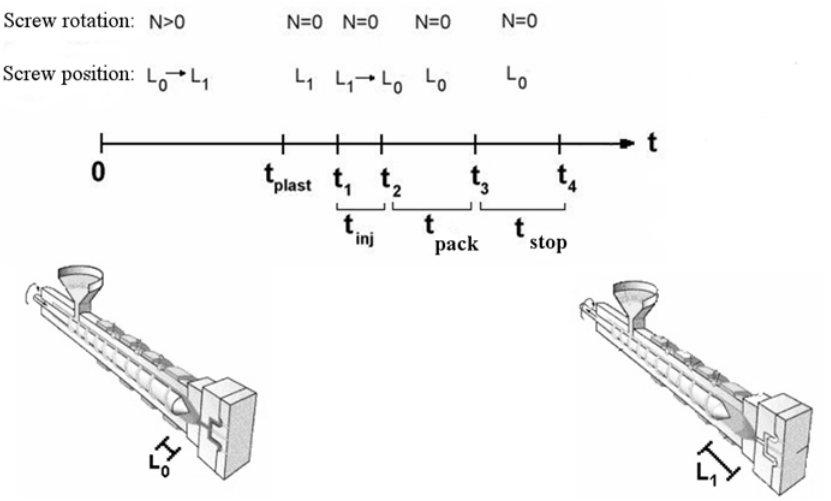

Figure 5.5: Time scale in injection moulding process (t_{plast} - plasticating time, t_{inj} - injection time, t_{pack} - packing time and t_{stop} - cooling time, adapted from *The Encyclopedia Britannica* (2000)).

This paper presents a modification of an extruder simulation code (Gaspar-Cunha, 2000) to in order to take into account the backwards movement of the screw, the presence of a non–return valve, the conduction of heat during the idle times. The global program structure of the plasticating simulation code is represented in figure Figure 5.6.

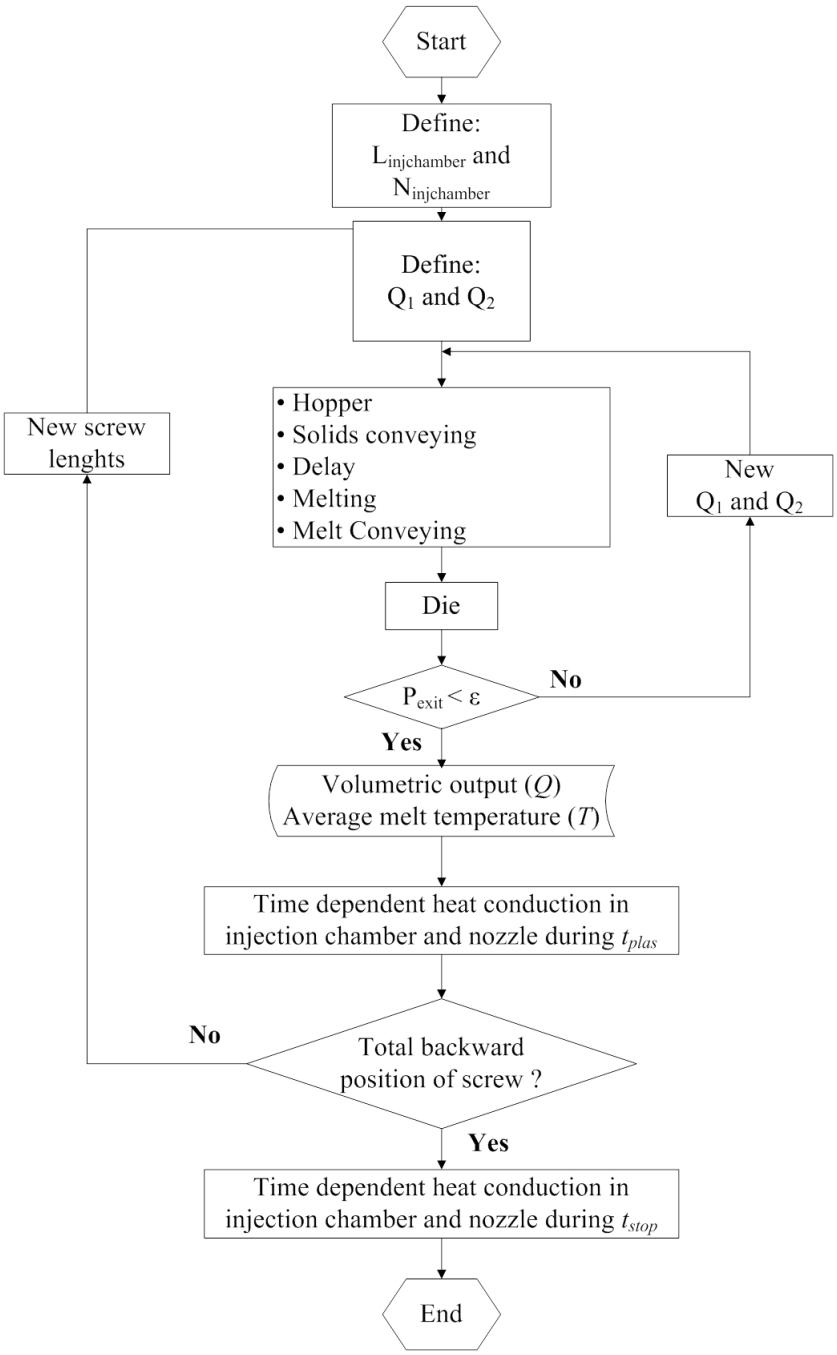

Figure 5.6: Global program structure.

First, the length of the injection chamber is divided in several intervals called computation step intervals (ΔL) which are given by Equation 5.7. When the screw is located in position L_0 (initial position), the steady-state extrusion model (Tadmor and Klein, 1970) is used to obtain the temperature profile of the polymer in all zones, as shown in Figure 5.4. Next, the screw moves backwards to position $L_0 + \Delta L$, since a quantity of melted polymer (Q) is accumulated in front of the screw. At this point, average melt temperature $(\overline{T})$ and plasticating time (t_{plast}) (see Equation 5.6) needed to fill the chamber with Q volumetric quantity of melt polymer are calculated.

The polymer starts to accumulate in the barrel chamber at the front of screw. For this polymer the melting and heating processes can be treated as a static melting/heating, assuming that the rotational screw movement does not affect the melted polymer accumulated. Then, only heating due to conduction from the heated barrel bands was considered. The main difference with the modelling made in the screw channel is it dependence from the time. The heat conduction equation is used to compute the polymer temperature changes during the plasticating time. For that purpose, the average melt temperature $\left(\overline{T}\right)$ calculated in the previous step is used as initial temperature for the subsequent step. After, the new location of the screw is updated by reducing the length of feed zone due to backward movement of screw. The process is repeated until the screw reaches position L_1, that is the total backward position. In this location the screw stops and only heat due to conduction is considered during the stop time $\left(t_{stop}\right)$ that is pre-defined by the user.

5.3.2 *Plasticating phase*

During the plasticating phase the screw moves backward and for each ΔL the extrusion model describing the polymer flow along the screw is applied. In the solids conveying zone the cross temperature profile in each differential element along the screw channel can be described by Equation 5.10, where the left term represents heat convection and the right term represents heat conduction.

$$V_{sz}\frac{\partial T}{\partial z} = \alpha_s \frac{\partial^2 T}{\partial y^2} \tag{5.10}$$

V_{sz} is the solid bed velocity, T is the cross temperature profile (direction y) and α_s is the thermal diffusivity of the solid plug. The temperature of the solid plug increases due to friction at the polymer-barrel and polymer-screw walls and to heat conduction from the barrel.

The models used for calculating the temperature profiles flow behaviour in the film and in the solid bed for the delay zone used here are based on the models proposed by Kacir and Tadmor (1972), which is described by equations 5.11 and 5.12:

$$\rho_m c_p V_z\left(y\right)\frac{\partial T}{\partial z} = k_m \frac{\partial^2 T}{\partial y^2} + \eta\dot{\gamma}^2 \tag{5.11}$$

$$V_{sy}\frac{\partial T}{\partial y} + V_{sz}\frac{\partial T}{\partial z} = \alpha_s \frac{\partial^2 T}{\partial y^2} \tag{5.12}$$

where ρ_m is the melt density, c_p is the melt specific heat, k_m is the melt thermal conductivity, η is the melt viscosity and $\dot{\gamma}$ is the shear rate.

For the melting and melt conveying zones a non-isothermal two-dimensional flow of a non-Newtonian fluid in the presence of convection is considered. During melting, the energy equation takes the form::

$$\rho_m c_p V_z\,(y)\,\frac{\partial T}{\partial z} = k_m\left(\frac{\partial^2 T}{\partial x^2} + \frac{\partial^2 T}{\partial y^2}\right) + \eta\dot{\gamma}^2 \tag{5.13}$$

Equations 5.11 and 5.13 are non-linear, since the viscosity depends on the temperature and on the velocity field. The solutions of those equations were obtained by using the Crank-Nicholson finite difference implicit scheme (Gaspar-Cunha, 2000).

5.3.3 *Stationary phase*

After the application of the melting models described in plasticating phase, the temperature of melted polymer accumulated in front of screw can be calculated by solving the energy conservation equation, given by:

$$\rho_m c_p \frac{\partial T}{\partial t} = k_m\left(\frac{\partial^2 T}{\partial x^2} + \frac{\partial^2 T}{\partial y^2} + \frac{\partial^2 T}{\partial z^2}\right) \tag{5.14}$$

The governing Equation 5.14 is solved with the finite volume method described in Nóbrega et al. (2004). Basically, the solution domain is decomposed in many adjacent control volumes over which those equations are integrated and transformed into algebraic form. The discretized system of equations is solved iteratively, for the dependent variable T, with conjugate gradient solvers.

5.4 CASE STUDY

The modelling routine developed was validated through the comparison of the computational results with experimental measurements of the temperature in the front of screw nozzle. These measurements were made using both an infrared camera (ThermaCAM SC640) and an

infrared thermometer (model Fluke 62 Mini). A study concerning the influence of operative process parameters, such as, screw rotation speed, backpressure, barrel temperatures and injection chamber length, was also performed. The computational runs carried out are shown in Table 5.1.

RUN	SCREW ROTATION (RPM)	BACK PRESSURE (MPA)	BARREL TEMPERATURES (°C)	LENGTH OF INJECTION CHAMBER (MM)
1	50	15	190-200-210-220-220	100
2	60	15	190-200-210-220-220	100
3	100	15	190-200-210-220-220	100
4	150	15	190-200-210-220-220	100
5	200	15	190-200-210-220-220	100
6	100	3	190-200-210-220-220	100
7	100	8	190-200-210-220-220	100
8	100	15	190-200-210-220-220	100
9	100	20	190-200-210-220-220	100
10	100	30	190-200-210-220-220	100
11	100	15	185-187-187-190-190	100
12	100	15	187-190-190-200-200	100
13	100	15	190-200-210-220-220	100
14	100	15	210-220-230-240-240	100
15	100	15	240-250-260-270-270	100
16	100	15	190-200-210-220-220	15
17	100	15	190-200-210-220-220	30
18	100	15	190-200-210-220-220	60
19	100	15	190-200-210-220-220	100
20	100	15	190-200-210-220-220	150

Table 5.1: Set of computational runs.

The polymer used in this work was polypropylene, PPH 5060, from TOTAL Petrochemicals. Table 5.2 gives a summary of the relevant polymer properties used in the calculations.

PROPERTY	VALUE UNIT
Polymer solid density - ρ_s	900.3 Kg/m^3
Polymer melt density - ρ_m	734.1 Kg/m^3
Thermal conductivity of solid polymer - k_s	0.2 $W/m.^oC$
Thermal conductivity of polymer melt - k_m	0.17 $W/m.^oC$
Specific heat capacity of solid polymer - c_{p_s}	1700 $J/Kg.^oC$
Specific heat capacity of polymer melt - c_{p_m}	2700 $J/Kg.^oC$
Heat of fusion - λ	64100 J/Kg
Melting or flow temperature - T_m	165 ^oC
Barrel friction factor of solid polymer - f_b	0.45
Screw friction factor of solid polymer - f_s	0.25
Zero-shear viscosity - η_0	1323.71 Pa/s
Reference temperature - T_0	243.3 ^oC
Temperature coefficient of viscosity - E/R	12272.59
Empirical constant - K_1	0.0247
Empirical constant - n	0.272
Empirical constant - a	0.7326

Table 5.2: Typical properties of PPH 5060.

For the case of the viscosity properties, the Carreau-Yasuda parameters (η_0, E/R, K_1, n and a) were determined at typical injection shear rates (between 10 and 1000 s^{-1}) and temperatures (190, 216.7, 243.3 and 270 ^oC). Cross-WLF viscosity parameters of PPH 5060 obtained in Moldflow database allows to compute viscosity parameters for Carreau-Yasuda model by fitting the values between the two viscosity models. Carreau-Yasuda viscosity model is used in our simulations instead of the Cross-WLF model due to the implementation of Carreau-Yasuda model in the originally steady-state extruder routines.

An injection machine, Klockner Ferromatic K85 of 85 tonnes of clamp force, fitted with a conventional three-zone screw was used. The injection machine is able to control four independent barrel temperature zones plus the nozzle, as shown in Figure 5.7. Table 5.3 presents a summary of the geometric characteristics (as described in Section 5.2.2) for the injection plasticating screw.

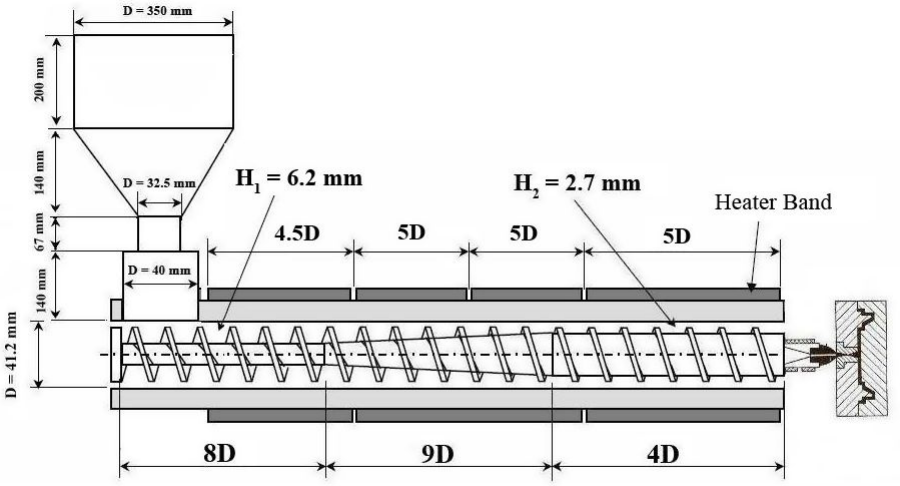

Figure 5.7: Geometry of the injection plasticating screw used in the experiments.

PROPERTY	VALUE UNIT
Internal barrel diameter - D_b	41.2 mm
Internal screw diameter - D_i	28.8 mm in feed zone
	$[29.1, 35.3] mm$ in compression zone
	35.8 mm in metering zone
External screw diameter - D_s	41 mm
Screw pitch - S	41 mm
Flight width - e	5 mm

Table 5.3: Geometric values of injection plasticating screw.

Channel depth (H_1) in the feed zone, channel depth (H_2) in the metering zone and flight clearance (δ_f) can be calculated using the geometrical values presented in Table 5.3.

5.5 RESULTS AND DISCUSSION

In this section, three different categories of results were presented and discussed. Initially, typical plasticating modelling results were shown (corresponding to run 3 of Table 5.1). These results includes pressure, solid bed and average melt temperature profiles along the plasticating screw. Then, the melt temperature profile obtained from the 3D transient equation of heat conduction during the static phase were presented and discussed. Finally, the influence of the operating conditions, such as, screw speed, backpressure, set barrel temperature profiles and injection chamber length, in the evolution of the average melt temperature in front of the screw nozzle was studied. These results (average melt temperature)

were assessed experimentally through measurements made using both an IR camera and an IR thermometer.

5.5.1 *Plasticating results*

As shown in Figure 5.8 the number of intervals $(N_{injchamber})$, in which the length of injection chamber is divided, has no effect in the average melt temperature of the polymer in injection chamber. Thus, due to the lower computation time the results presented below were made using 6 intervals, being the calculations made until the screw reaches the backward position.

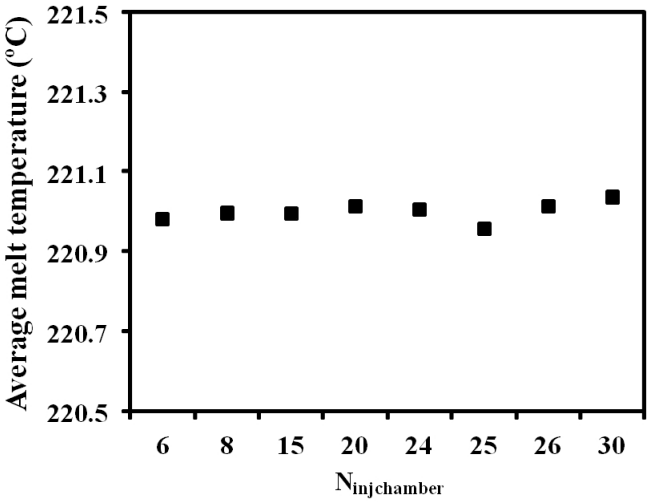

Figure 5.8: Effect of the number of intervals in which the length of injection chamber is divided on the average melt temperature.

Figure 5.9 shows the pressure, solid bed and average melt temperature profiles developed during the dynamic phase, i.e., the screw backwards movement computed in the plasticating iterations. As expected, the maximum pressure (Figure 5.9-A) decreases with the iterations since the length of the screw is smaller and back pressure is maintained constant. Melting starts earlier and is faster (Figure 5.9-B) since due to the screw backwards the compression zone of the screw also moves back, which helps the melting process. Finally, average melt temperature (Figure 5.9-C) decreases with the iterations because the viscous dissipation decreases as the pressure is smaller.

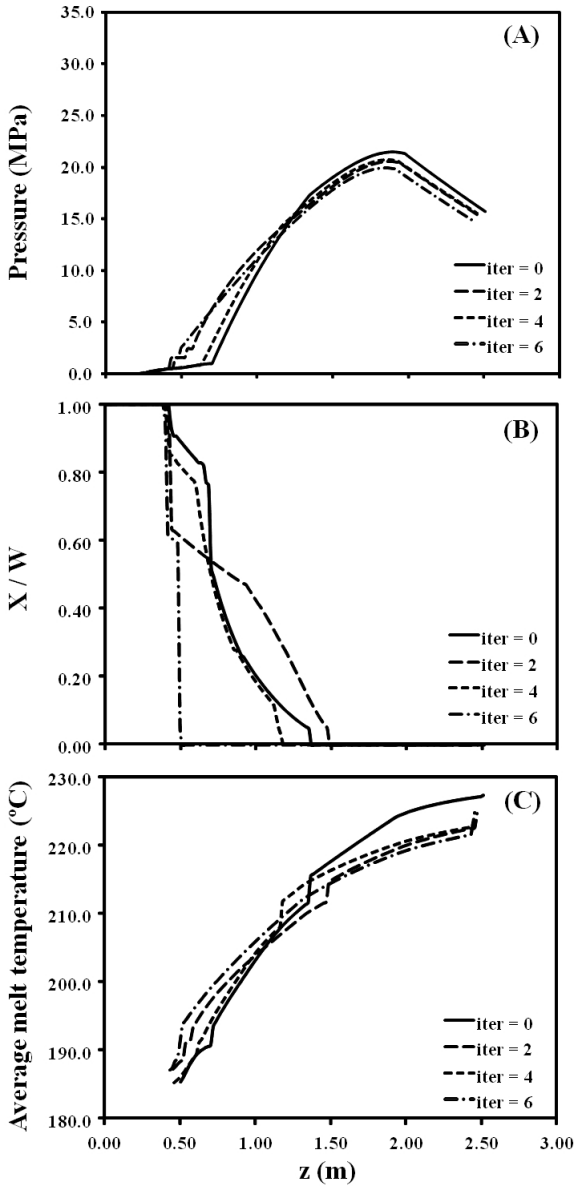

Figure 5.9: Effect of the screw backwards movement in the pressure profile (A), in the solid bed profile (B) and in the average melt temperature profile (C).

The results for the static phase, i.e., for the situation in which the polymer reaches the injection chamber during the successive iterations, were presented in Figure 5.10. As referred above, these results were obtained by the resolution of the 3D transient equation of heat conduction. In this figure only a transversal cut made in the intermediate position of the x axis was made. As can be seen, during the successive iterations the maximum value of the melt temperature approximates to the value of last heating band. This results of the heat due to conduction since the time that the polymer spends in the chamber is increasing. As a consequence, the values of the average melt temperature in the injection chamber (shown in Figure 5.11) have, also, the same behaviour.

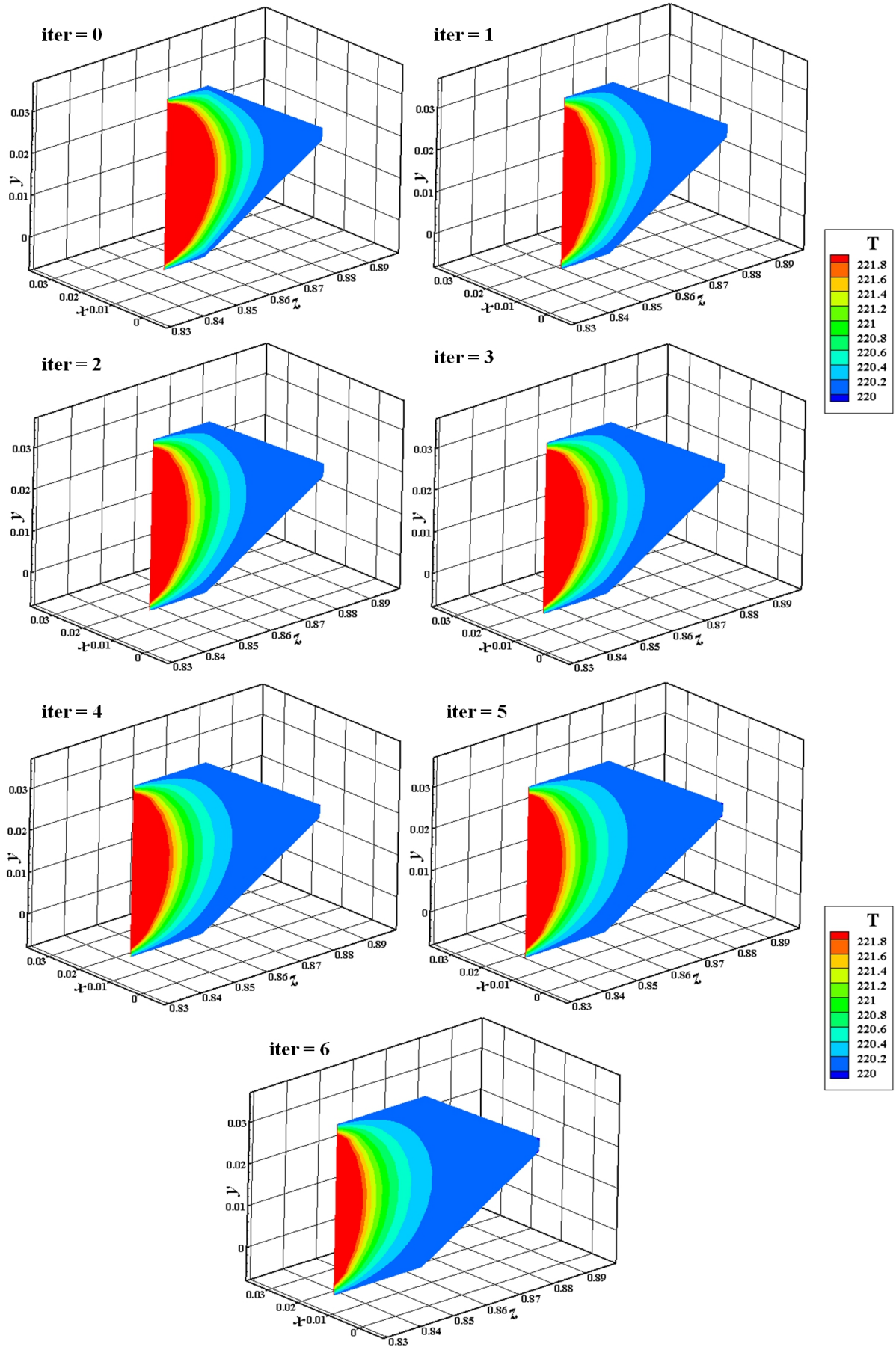

Figure 5.10: Effect of the screw backwards movement in the melt temperature profile of polymer in the injection chamber.

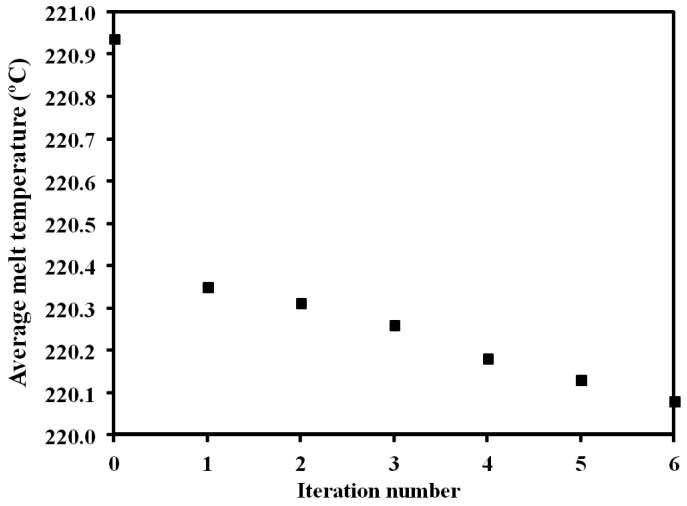

Figure 5.11: Effect of the screw backwards movement in the average melt temperature of polymer in the injection chamber.

5.5.2 *Experimental assessment*

The computational (before and after the static calculations made) and experimental results showing the effect of screw speed in melt temperatures in the injection chamber are compared in Figure 5.12. As expected, the average melt temperature increases slightly with screw speed due to the increase in the viscous heat dissipation. However, all these values are approximately equal to the set barrel temperature of the last heating zone, which is where the barrel chamber is located. This means that during the static phase and mainly for high screw speeds, the heat generated by viscous dissipation during the plasticating phase is transferred to the barrel. The temperature of the melt in the chamber decreases as can be observed in Figure 5.12.

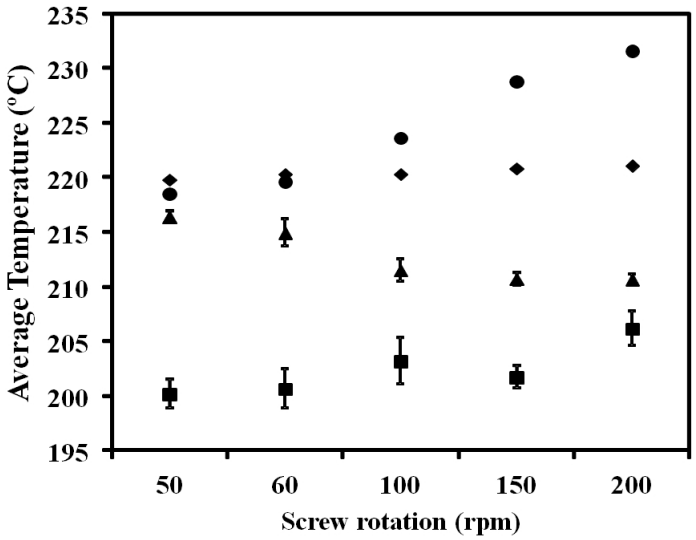

Figure 5.12: Effect of screw speed in the average melt temperature (circle - computation before static phase; diamond – computation after static phase; square – IR thermometer; triangle – IR camera).

The existing differences between the two experimental methods used are due to the way how the measurements were made. The IR camera measurements were obtained from the images taken immediately after the polymer emerges from the front of the screw nozzle. The IR thermometer measurements were made by inserting the probe inside a portion of melted polymer after it emerges from the injection nozzle, which are made some instants later than the IR camera measurements. These instants are enough to the polymer reduce the temperature to the values observed in the case of the IR thermometer. Thus, it is possible to conclude that the IR camera measurement is a more efficient method. However, the average temperature decreases with screw speed but, for the case of higher screw speeds, a comparison with the computational results shows differences lower than 5%. Hence, the computational results are able to replicate the correct behaviour concerning the melt temperature inside the injection chamber.

Figure 5.13 shows the effect of back pressure in the average melt temperature, using a constant screw speed of 100 rpm. The behaviour of the computational results and the *IR* camera measurements is similar, as the average melt temperature does not change with back pressure. The differences are the identical to those of Figure 5.12 and were discussed therein.

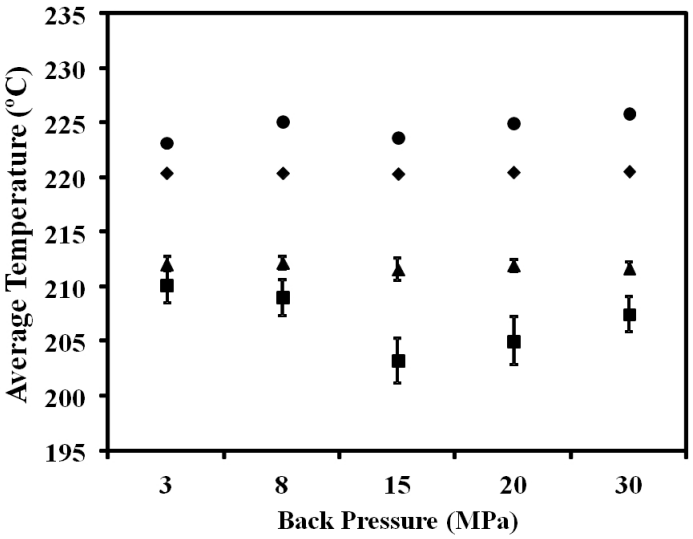

Figure 5.13: Effect of back pressure in the average melt temperature (circle - computation before static phase; diamond – computation after static phase; square – *IR* thermometer; triangle – *IR* camera).

The effect of set barrel temperatures is shown in Figure 5.14. The behaviour observed for the computational and experimental results is very similar. However, for a linear change on the set barrel temperatures, a non-linear behaviour is observed for the average melt temperature in both, the computational and the experimental results. Also, the average melt temperature in the chamber is very similar to that of the temperature after the plasticating, except in the case of the higher set barrel temperature for which is higher. This is what is expected since when the barrel temperature is increased the viscous dissipation is smaller and the melt temperature in the chamber is also lower.

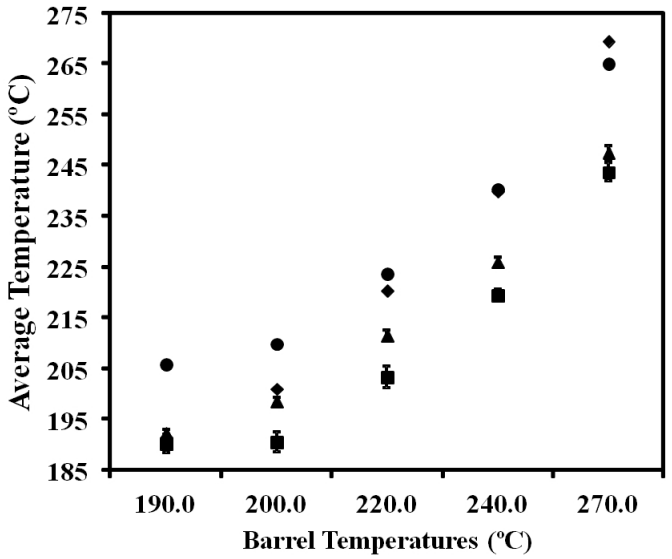

Figure 5.14: Effect of barrel temperatures in the average melt temperature (circle - computation before static phase; diamond – computation after static phase; square – *IR* thermometer; triangle – *IR* camera).

Finally, the length of injection chamber, shown in Figure 5.15, has no effects on the average melt temperature in both cases, computational and experimental results.

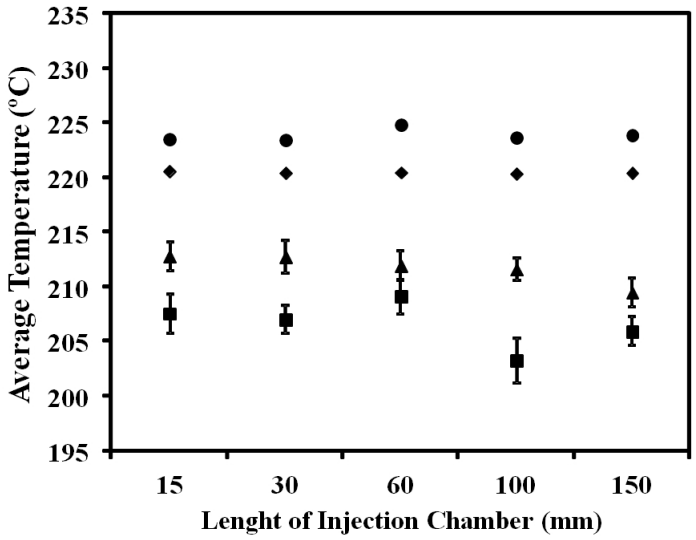

Figure 5.15: Effect of length of injection chamber in the average melt temperature (circle - computation before static phase; diamond – computation after static phase; square – IR thermometer; triangle – IR camera).

In all cases shown the differences between the computational results and the IR camera measurements are below 5%, which validates the computational program developed for the plasticating of the injection moulding process, including both the rotation and the static phases.

5.6 CONCLUSIONS

In this work a mathematical model for the modelling of the plasticating phase of the injection moulding process is proposed. This model is a modification of the steady-state extrusion model previously developed, by taking into account the backwards movement of the screw, the presence of a non–return valve and the conduction of heat during the idle times.

The validity of the model is assessed experimentally using two different methods (an IR camera and an IR thermometer) for measuring the average melt temperature that leaves the injection chamber. The effect of some operative variables (e.g., screw speed, backpressure, set barrel temperature profiles and injection chamber length) in the average melt temperature is presented. The experimental measurements made validated the computational results, as the differences obtained for the average melt temperature are below 5% when the IR camera method is used.

Part IV

OPTIMIZATION OF INJECTION MOULDING CYCLE - CASE STUDIES

INTRODUCTION TO PART IV

The lesser the knowledge about existing relationships between the requirement and the form to satisfy those requirements, the more a design problem tends towards creative design.

— Michael Rosenman

In this part MOEAs are used to optimize the injection moulding process. The aim of these studies are the optimization of the operating conditions (Chapter 6), the cooling system (Chapter 7) and the gate location (Chapter 8). The use of MOEAs was adopted due to the complexity of the process, since it is necessary to take into account various objectives simultaneously. In these chapters this type of optimization algorithms were used as an optimization tool and, thus, a previously developed MOEA, called Reduced Pareto Set Genetic Algorithm with Elitism (RPSGAe) was used (Gaspar-Cunha and Covas, 2004).

6

USING MULTI-OBJECTIVE EVOLUTIONARY ALGORITHMS IN THE OPTIMIZATION OF OPERATING CONDITIONS OF POLYMER INJECTION MOULDING

Abstract[1]

A Multi-objective Optimization Genetic Algorithm, denoted as RPSGAe, has been applied to the optimization of the polymer injection moulding process. The aim is to implement an automatic optimization scheme capable of defining the values of important process operating conditions (such as melt and mould temperatures, injection time and holding pressure), yielding the best performance in terms of prescribed criteria (such as temperature difference on the moulding at the end of filling, the maximum cavity pressure, the pressure work, the linear shrinkage and the cycle time). The methodology proposed was applied to some case studies. The results produced have physical meaning and correspond to a successful process optimization.

6.1 INTRODUCTION

Injection moulding of polymeric materials is a high throughput process adequate to manufacture thermoplastic components of complex geometry with tight dimensional tolerances. This process is an intricate dynamic and transient process, involving convoluted melting-flow-pressure-solidification phases and a complex material behavior strongly affecting the quality and properties of the final moulded component.

In injection moulding, the thermomechanical environment imposed to the polymer melt is controlled by the definition of the operative processing variables (e.g. plasticating temperatures, cycle times, injection and holding pressures) and/or system geometry (e.g., plasticating screw, injection gate location, water lines layout, etc.). These thermomechanical conditions control the microstructure and morphology of the final moulded component (Viana et al., 2002; Viana, 2004), which determines, in turn, their dimensions (shrinkage), dimensional

1 C. Fernandes, A.J. Pontes, J.C. Viana and A. Gaspar-Cunha (2010). Using Multi-Objective Evolutionary Algorithms in the Optimization of Operating Conditions of Polymer Injection Moulding, *Polymer Engineering and Science* **50 Issue 8** 1667–1678.

stability (distortion and warpage) and properties (e.g., mechanical behavior, permeability, appearance) (Chang and Faison, 2001; Viana et al., 2004). If the thermomechanical history variables (pressure, temperature, flow and cooling rate), can be monitored directly or indirectly in the impression, the moulded product properties can be accurately and consistently predicted.

In recent research, the pressure at the impression has been regarded as the most important parameter to establish a correlation with the dimensions and the weight of the moulded part (Jensen, 1981), been considered a finger print of the process (Winterthur, 1998). Figure 6.1 shows a typical pressure evolution inside the mould impression and its main characteristics.

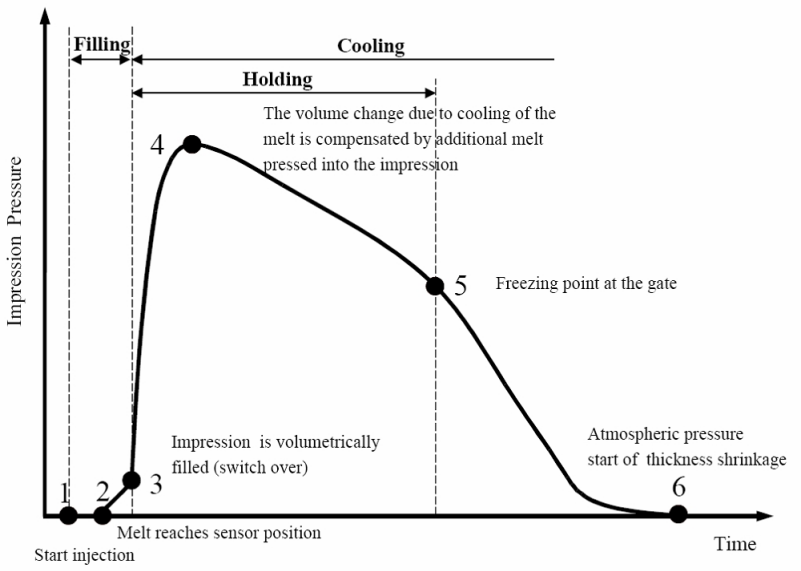

Figure 6.1: Typical pressure evolution inside the mould impression.

The shape of this pressure profile is strongly affected by some changes in the injection moulding process, such as temperature, flow rate, holding pressure and time. The establishment definition of the adequate processing conditions, to mould a high quality plastic component, is therefore a complex task due to the significant number of processing variables, to the high level of interactions between these variables and to the numerous moulding features and end-use properties to improve.

The use of computer simulations on the design stages of engineering plastic components for the injection moulding process is very frequent (Cmold, 1999; Moldflow, 2010). Initially, a finite element mesh representative of the part geometry is defined, the materials are selected, the gate location is defined and the initial processing variables are introduced. Then, after launching the simulation the outputs are analyzed. A trial-and-error process is applied, where the initial conditions, in what concerns geometry, material and/or processing

conditions are modified until the desired results are obtained. This process can be very complex since in most cases multiple criteria are to be optimized simultaneously. Also, the finding of a global optimum solution is not guaranteed.

Various optimization strategies using different methodologies to optimize the injection moulding process have been reported in the literature. Lam and Seow (2000) proposed a method for flow path generation using the Moldflow software. This algorithm was combined with an optimization routine based on hill-climbing approximation method in order to perform automatic cavity balancing. Yarlagadda and Khong (2001) applied an ANN to optimize the injection time and injection pressure in order to improve the quality of the part produced. Lotti and Bretas (2003) applied ANN to predict the morphology and the mechanical properties of an injection moulded part as a function of the processing conditions (mould and melt temperatures and flow rate). A central composite design of experiments approach was used to predict the moulding morphology as a function of the processing conditions using the Moldflow software. Castro et al. (2003) used ANN and statistical analysis to find the optimal compromise between multiple performance measures (minimization of maximum injection pressure, time to freeze, range of volumetric shrinkage, maximum shear stress at the wall and bulk temperature range) to define the setting of injection moulding variables (melt temperature, mould temperature, ejection temperature) and the gate location. Kim et al. (1996) applied a GA in the optimization of some injection moulding process parameters, (e.g., mould temperature, melt temperature and filling time) using the results of a flow simulation code. The performance of the process was quantified using a weighted sum of the temperature difference, "overpack" and frictionally overheating criteria. Turng and Peic (2002) proposed an integrated CAE optimization tool coupling a process simulation program with various optimization algorithms, such as, SQP, SAE, DE and SA, to determine the optimal design and process variables. Alam and Kamal (2003) suggested that the maximum difference in shrinkage among the parts is an appropriate measure of product quality in the runner-balancing problem. They proposed a new approach to runner balancing, which accounts for product costs by including runner system volume and cycle time. The optimization problem was solved with a multi-objective genetic algorithm (NSGA-II). Lam et al. (2004) proposed an approach to optimize both the cooling channel design and the process conditions through the use of an EA. The aim being to optimize the coordinates of centers of the cooling channels, the sizes of the cooling channels, the flow rate and the inlet temperature in each channel, the packing time, the cooling time and the clamp open time in order to obtain the most uniform

cavity surface temperature. Ozcelik and Erzurumlu (2006) proposed an hybrid optimization methodology based on ANN and GA in order to minimize the warpage of thin shell plastic parts. The parameters used are mould temperature, melt temperature, packing pressure, packing time, runner type, gate location and cooling time. A predictive model, based on ANN, for warpage was created using these process parameters. ANN model was interfaced with an effective genetic algorithm to find the optimum process parameter values.

The main limitations of the above methodologies are twofold. First, most of the approaches proposed either consider one objective or use an aggregation function of the various objectives. This is not the better way to deal with the multi-objective nature of these optimization problems since this implies the aggregation in a single function of very different measures with different meanings. Second, the methodologies proposed are not totally integrated, i.e., they do not consider the optimization and modeling processes as a whole process.

Therefore, the development of a global integrated optimization methodology able to facilitate the definition of the processing window and the maximization of the moulding properties is, therefore, of high importance. In particularly, the aim of this work is to apply this methodology to the proper setting of the processing variables to manufacture injection moulded components (process optimization).

This was the strategy followed in a previous paper Gaspar-Cunha and Viana (2005), where an automatic optimization methodology based on MOEA for the maximization of the mechanical response of injection mouldings was used. For that purpose an MOEA was linked to an injection moulding simulator code (C-Mold). This allows the optimization of the processing conditions (injection flow rate, melt temperature and mould temperature) for a desired morphological state or for an enhanced mechanical response.

An automatic optimization methodology based on MOEA (Gaspar-Cunha and Covas, 2004) to define the processing window in injection moulding is proposed in Section 6.2. For that purpose a MOEA is linked to an injection moulding simulator code (in this case C-Mold). In Section 6.3 the proposed optimization methodology was used to set the processing conditions of the moulding in polystyrene (STYRON 678E). The optimization results obtained have been validated experimentally. Finally, the optimization results achieved by the global optimization of operating conditions in polymer injection moulding are presented in Section 6.4.

6.2 MULTI-OBJECTIVE EVOLUTIONARY ALGORITHMS

The methodology proposed in this work integrates the computer simulations of the injection moulding process, an optimization methodology based on evolutionary algorithm and multi-objective criteria in order to establish the set of operative processing variables leading to a good moulding process. The optimization methodology adopted is based on a MOEA (Gaspar-Cunha and Covas, 2004), due to multi-objective nature of most real optimization problems, where the simultaneous optimization of various, often conflicting, criteria is to be accomplished (Goldberg, 1989; Gaspar-Cunha, 2000). The solution must then result from a compromise between the different objectives. Generally, this characteristic is taking into account using an approach based on the concept of Pareto frontiers (i.e., the set of points representing the trade-off between the objectives) together with an MOEA. This enabled the simultaneously accomplishment of the several solutions along the Pareto frontier, i.e., the set of non-dominated solutions (Deb, 2001; Coello et al., 2002).

The link between the MOEA and the problem to solve is made in two different steps (see flowchart of Figure 6.2). First, the population is random initialized, where each individual (or chromosome) is represented by the binary value of the set of all variables. Then, each individual is evaluated by calculating the values of the relevant objectives using the modeling routine (in this case C-Mold). Finally, the remaining steps of a MOEA are to be accomplished. To each individual is assigned a single value identifying its performance on the process (fitness). This fitness is calculated using a Multi-Objective approach as described in details elsewhere (Goldberg, 1989; Coello et al., 2002). If the convergence objective is not satisfied (e.g., a pre-defined number of generations), the population is subjected to the operators of reproduction (i.e., the selection of the best individuals for crossover and/or mutation) and of crossover and mutation (i.e., the methods to obtain new individuals for the next generation). The RPSGAe uses a real representation of the variables, a simulated binary crossover, a polynomial mutation and a roulette wheel selection strategy (Gaspar-Cunha and Covas, 2004; Deb, 2001).

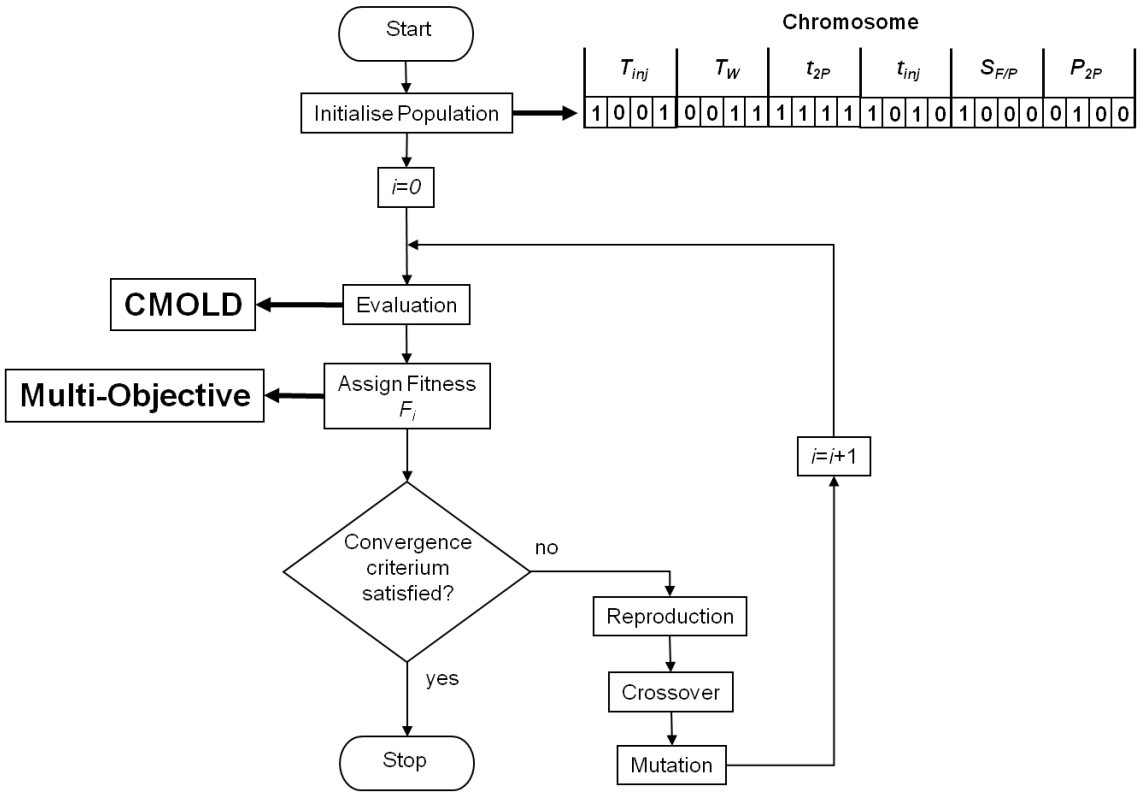

Figure 6.2: Flowchart of the MOEA applied for the optimization of the injection moulding process.

6.3 CASE STUDY

The optimization methodology proposed will be used for setting the processing conditions of the moulding shown in Figure 6.3, which will be moulded in polystyrene (STYRON 678E). The relevant polymer properties used for the flow simulations were obtained from the software (C-Mold) database. The models for the simulations, implemented in the C-Mold simulation package are based on a hybrid finite-element/finite-difference/control-volume numerical solution of the generalized Hele-Shaw flow of a compressible viscous fluid under non-isothermal conditions. The rheological and Pressure-Volume-Temperature (PVT) description therein implied is obtained by the Cross-WLF and the Tait modified equation, respectively. More details about the software are described in the company technical and related literature (Hieber and Shen, 1980; Chiang et al., 1991b; Viana, 1999; Chiang et al., 1991a).

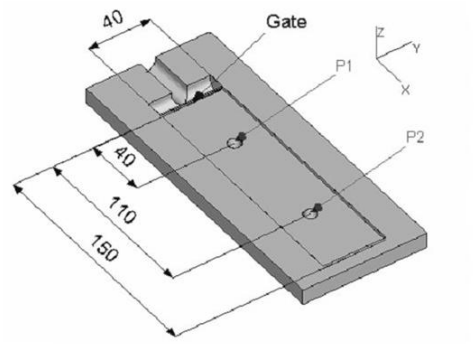

Figure 6.3: Moulding insert of injection moulding part with 2 mm of thickness (dimensions in mm).

The geometric model of the plate for the simulations consisted of 408 triangular elements. The runner and impression mesh used in the simulations is shown in Figure 6.4.

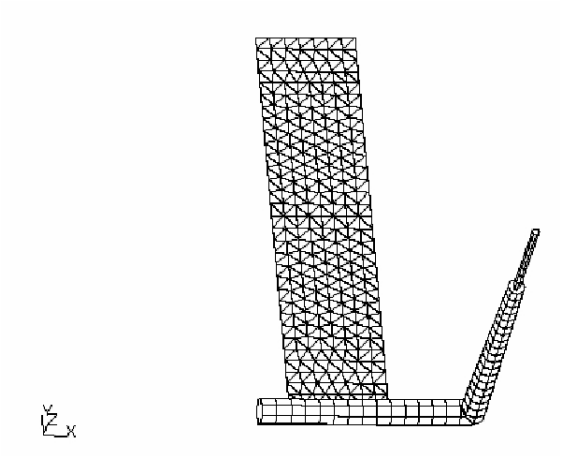

Figure 6.4: Mesh of the C-Mold model for the edge gated plate (408 elements).

The simulations considered the mould filling and holding (post-filling) stages. A node near the P1 position, pressure sensor position (see Figure 6.3) was selected as a reference point for this study. The processing variables to optimize and allowed to varied in the simulations in the following intervals were: injection time, $t_{inj} \in [0.5; 3]$ s (corresponding to flow rates of 24 and 4 cm^3/s, respectively), melt temperature, $T_{inj} \in [180; 280]$ ºC, mould temperature, $T_w \in [30; 70]$ ºC, holding pressure, $Ph \in [7; 38]$ % of maximum machine injection pressure, with fixed switch-over point, SF/P, at 99 %, timer for hold pressure of 15 s and cooling time of 15 s.

For the results produced by the modeling programme two process restrictions were imposed: i) the moulding has to be completely filled, obviously no short-shots were admitted and ii) the computed values of the maximum shear stress and strain-rate were limited to their critical values (defined on the C-Mold database) in order to avoid potential defects (e.g., melt fracture). The objectives used are the following:

- The temperature difference on the moulding at the end of filling, $dT = (T_{max} - T_{min})$, was minimized to avoid part distortions and warpage due to different local cooling rates, $dT \in [0;20]\,^{o}C$;

- The linear shrinkage (LS) of the mouldings, defined as:

$$LS = \frac{D_{mould} - D_{part}}{D_{mould}} \times 100 \tag{6.1}$$

  where D_{mould} is the dimension of the mould and D_{part} is the corresponding part dimension, was minimized, $LS \in [0;15]\,\%$;

- The maximum cavity pressure was minimized, reducing the clamping force, $P_{max} \in [1;70]\,MPa$;

- The cycle time was minimized, increasing productivity, $t_c \in [30;35]\,s$;

- The pressure work (PW), defined as the integral of pressure, P, along the time, t:

$$PW = \int_0^{t_c} P\,(t)\,dt \tag{6.2}$$

  was to be minimized in order to diminish the residual stress, the energy consumption and to reduce the mechanical efforts supported by the equipment, $PW \in [0;200]\,MPa.s$.

Since the aim of this work is to study the applicability of the optimization methodology in the establishment of the adequate processing conditions in injection moulding process taking into account the various criteria identified above, the 20 optimization runs identified in Table 6.1 were carried out.

RUN	OPTIMIZED CRITERIA
1	PW and LS
2	PW and dT
3	PW and P_{max}
4	PW and t_c
5	LS and dT
6	LS and P_{max}
7	LS and t_c
8	t_c and dT
9	t_c and P_{max}
10	PW, LS and dT
11	PW, LS and P_{max}
12	PW, LS and t_c
13	PW, dT and P_{max}
14	PW, dT and t_c
15	PW, P_{max} and t_c
16	LS, dT and P_{max}
17	LS, dT and t_c
18	LS, P_{max} and t_c
19	t_c, dT and P_{max}
20	All objectives

Table 6.1: Objectives used in each process optimization run.

The first studies (runs 1 to 9) addressed only the simultaneous optimization of pairs of objectives. Then we considered three objectives (runs 10 to 19) and we will present the 3-dimensional Pareto frontiers of this runs. Finally, we consider the simultaneous optimization of the five objectives and a five-dimensional Pareto frontier in the objectives domain is obtained.

The RPSGAe was applied using the following parameters: 50 generations, crossover rate of 0.8, mutation rate of 0.05, internal and external populations with 100 individuals (except in the optimization of 3 and 5 objectives where 200 individuals are used), limits of the clustering algorithm set at 0.2 and NRanks at 30. These values resulted from a carefully analysis made in a previous paper (Gaspar-Cunha and Covas, 2004).

6.4 RESULTS

6.4.1 *Experimental Assessment*

First the optimization methodology proposed was validated experimentally. A single optimization run using two different objectives, the minimization of pressure work and of linear shrinkage, has been carried out. These objectives were chosen due to the possibility of measuring them experimentally on the available injection machine. Six points were chosen from the Pareto frontiers obtained for the initial and the final populations of the EA (Figure 6.5). These solutions were experimentally tested in an injection moulding machine and the corresponding results were compared with the computational ones (Figure 6.6). As can be seen the general behavior (i.e., its relative location) of the experimental and computational solutions is very similar, the differences being due to the capacity of the simulation program (C-Mold) in reproducing the reality.

Figure 6.7 shows the simulation vs. experimental pressure curves of the six points chosen. As can be seen the experimental results are very similar to those of the simulation except on the case of point 3, which confirms the results shown if Figure 6.6.

The deviation of point 3 is due to the higher pressure in cavity that occurs when is applied a higher holding pressure. It is usually to measure a residual pressure in the cavity when is applied a higher pressure in a material with lower shrinkage. This could be due to the elastic deformation of mould that is not considered in commercial software's like C-Mold (Pontes, 2002).

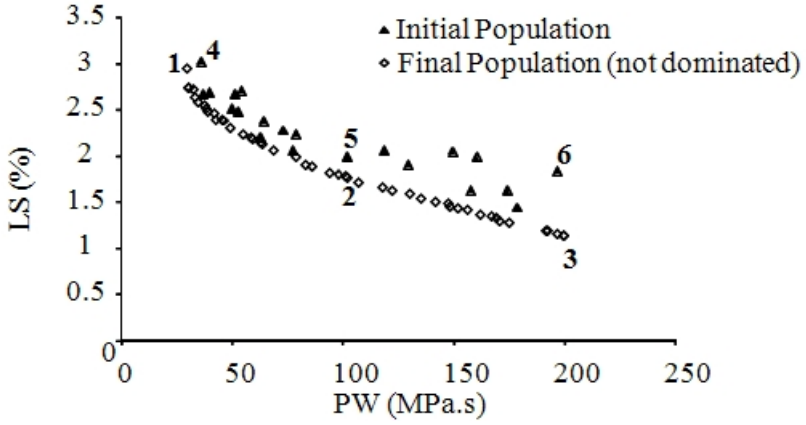

Figure 6.5: Pareto frontier - optimization results.

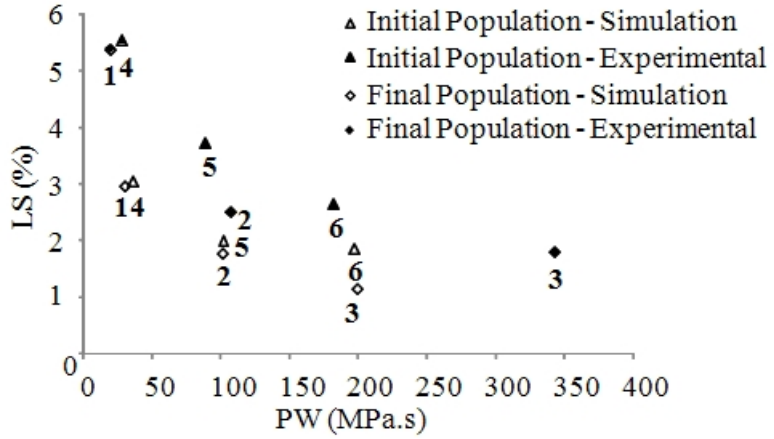

Figure 6.6: Pareto frontier - optimization vs. experimental results.

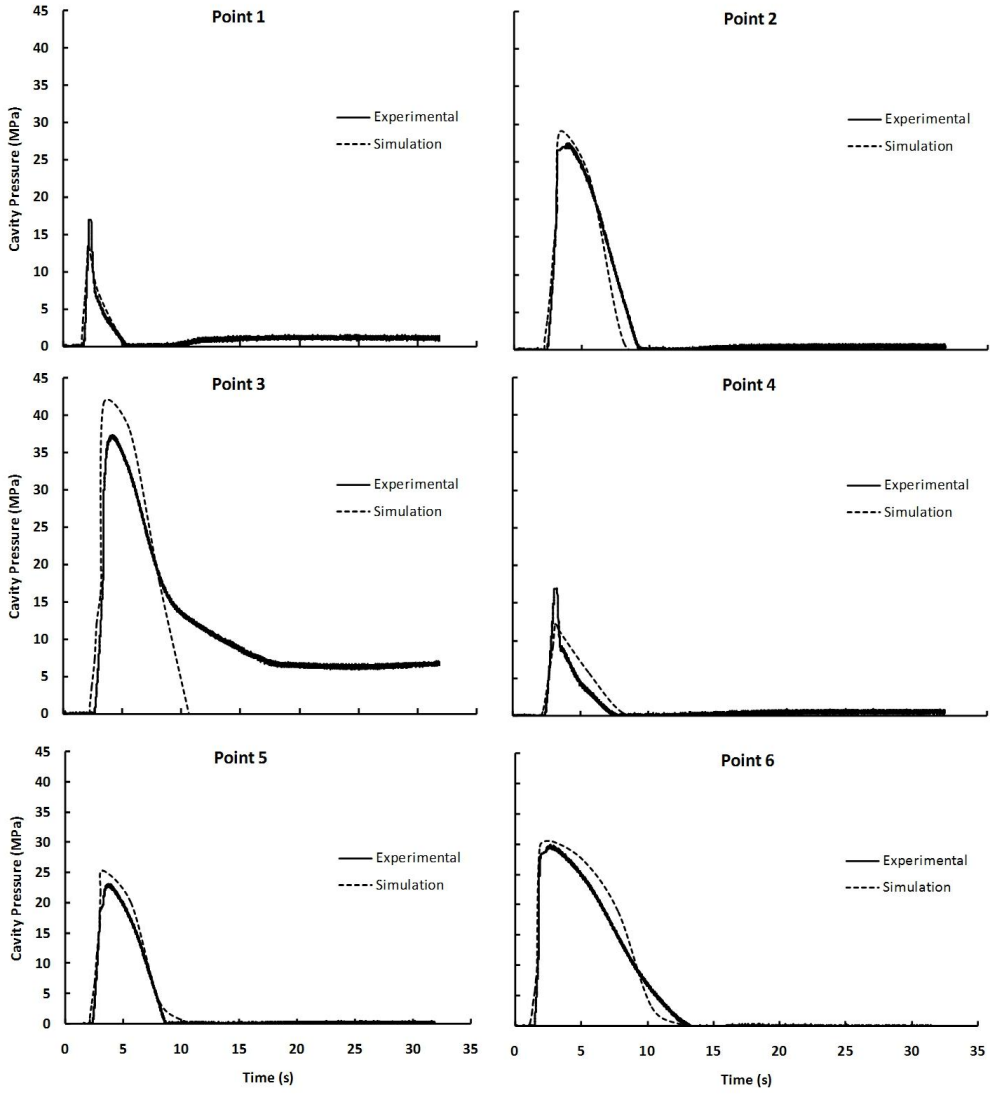

Figure 6.7: Presssure curves - optimization vs. experimental results.

6.4.2 *Optimization considering two objectives*

Figure 6.8 illustrates the trade-off between each objective of runs 1 to 4 against power work.

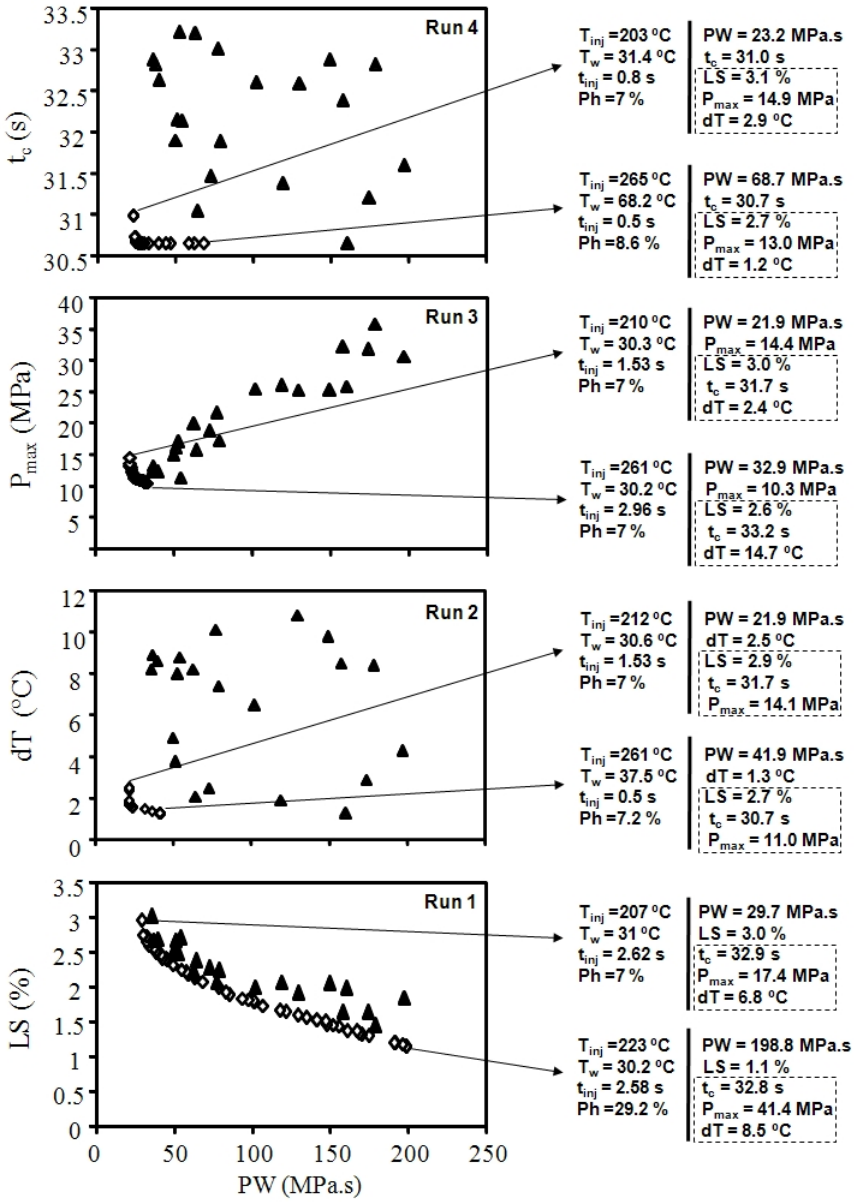

Figure 6.8: Optimization results for two objectives, runs 1 to 4. Open symbols: Pareto frontier at 50th generation; full symbols: initial population (PW – power work, LS – linear shrinkage, t_c – cycle time, P_{max} – maximum pressure, dT – temperature difference).

The optimization algorithm is able to evolve during the 50 generations and to produce a good approximation to the Pareto frontier in all the cases.

As expected, power work conflicts with linear shrinkage of the mouldings. Interestingly, cycle time (t_c), maximum pressure (P_{max}) and temperature difference (dT) slightly decrease with power work (PW).

In run 1, PW and LS are simultaneously optimized (PW – LS plot of Figure 6.8). The PW values range between 29.7 – 198.8 MPa.s and LS between 1.1 – 3 %. The resulting optimized Pareto frontier is highly non-linear: the highest variations of PW occur for their lowest values (29.7 – 70 MPa.s); the highest variations of LS are obtained for their highest values (2 – 3 %). For the extreme optimized points, the following setting of processing variables should be used: T_w at 30 – 31 ºC and the injection time at 2.58 – 3 s. The processing variables allowed to vary in a wide range are: the melt temperature that can be adjusted between 207 – 260 ºC; and the holding pressure at 7 – 29.2 % of maximum value of the machine injection pressure. When T_{inj} is at 222.7 ºC, Ph should be set at 29.17 %. In these conditions, LS is minimized (low melt viscosity) and PW is maximum (high holding pressure).

Run 2 optimized simultaneously PW and dT (PW – dT plot of Figure 6.8). The optimized power work and dT varies only slightly from 21.9 – 41.9 MPa.s and 1.3 – 2.5 ºC, respectively. These conditions are met for: the low setting of holding pressure (Ph = 7 % of maximum value of the machine injection pressure) and for mould temperatures between 30 – 38 ºC. The injection time and melt temperature can be varied in a wider range: t_{inj} between 0.5 – 1.5 s and T_{inj} between 211.8 – 260.5 ºC. When injection time is lower the injection flow rate, Q_{inj}, is higher. Therefore, the melt temperature is higher and more uniform. Consequently, dT is minimum. In another point of view, for high injection time the injection flow rate is lower. Then, the melt cools quickly during injection stage resulting in a higher temperature variation in the moulding. Hence dT is maximum.

In run 3, both PW and P_{max} were optimized at the same time (PW – P_{max} plot of Figure 6.8). The PW and P_{max} values range slightly from 21.9 – 32.9 MPa.s and 10.3 – 14.4 MPa, respectively. These objectives are simultaneously met for the adjustment on the mould temperature and holding pressure on their minimal values (30 ºC and 7 % of maximum value of the machine injection pressure, respectively). The processing variables allowed to vary in a wide range are: the melt temperature that can be adjusted between 210 – 261 ºC; and the injection time, which can be set between 1.5 – 3 s. When T_{inj} is at 210 ºC, t_{inj} should be set at 1.5 s. In these conditions P_{max} is maximum (high melt viscosity and high pressure) and PW is minimized because cycle time is also minimized due to high cooling rate.

Finally, run 4 optimized simultaneously PW and t_c (PW – t_c plot of Figure 6.8). The PW values range between 23.2 – 68.7 MPa.s and t_c between 30.6 – 31 s. These conditions are met for: the low setting of injection time that ranges between 0.5 – 0.8 s and for holding pressure between 7 – 8.6 % of maximum value of the machine injection pressure. The melt

and mould temperatures can be varied in a wider range: T_{inj} between 203 – 266 °C and T_w between 31 – 68 °C. When T_{inj} is at 266 °C and T_w at 68 °C their maximum values achieved in this optimization, the t_c is minimized (high cooling rate) and PW is maximum due to lower melt viscosity that promote a better packing of the material during holding phase, hence increasing the pressure.

Figure 6.9 illustrates the trade-off between each objective of runs 5 to 7 against linear shrinkage and Figure 6.10 illustrates the trade-off between each objective of runs 8 and 9 against cycle time. A physical analysis similar to those of runs 1 to 4 can be done to understand the relationship between the objectives involved on runs 5 to 9.

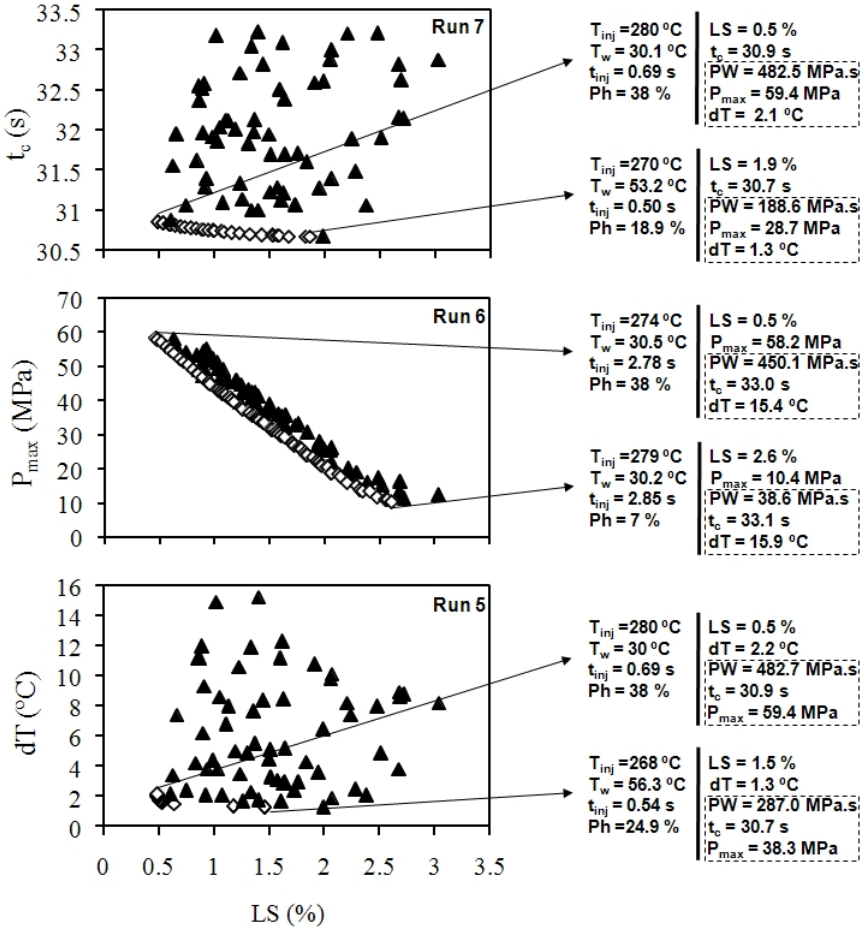

Figure 6.9: Optimization results for two objectives, runs 5 to 7. Open symbols: Pareto frontier at 50th generation; full symbols: initial population (LS – linear shrinkage, t_c – cycle time, P_{max} – maximum pressure, dT – temperature difference).

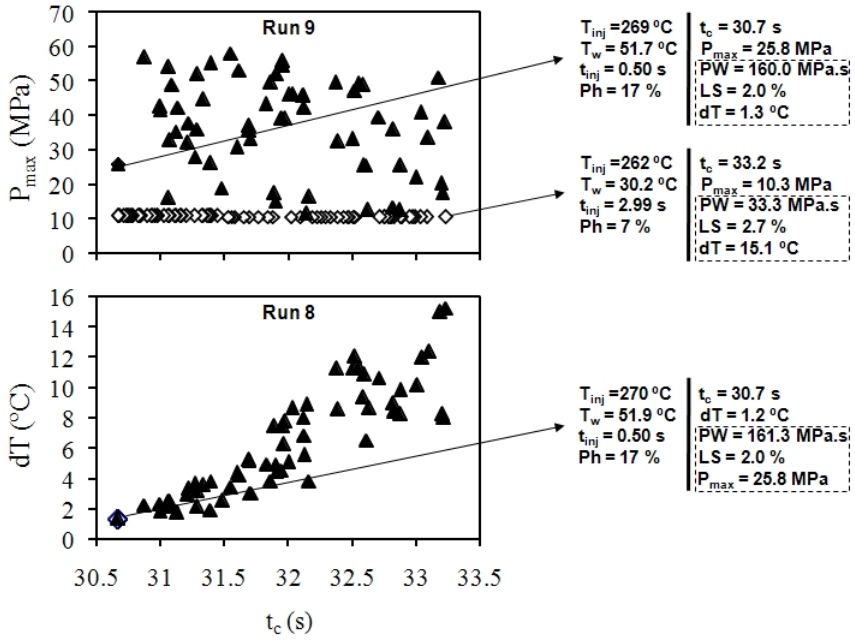

Figure 6.10: Optimization results for two objectives, runs 8 and 9. Open symbols: Pareto frontier at 50th generation; full symbols: initial population (t_c – cycle time, P_{max} – maximum pressure, dT – temperature difference).

6.4.3 *Optimization considering three objectives*

Figure 6.11 illustrates the trade-off between each objective of runs 10 to 15. Similar data was also obtained for the other runs.

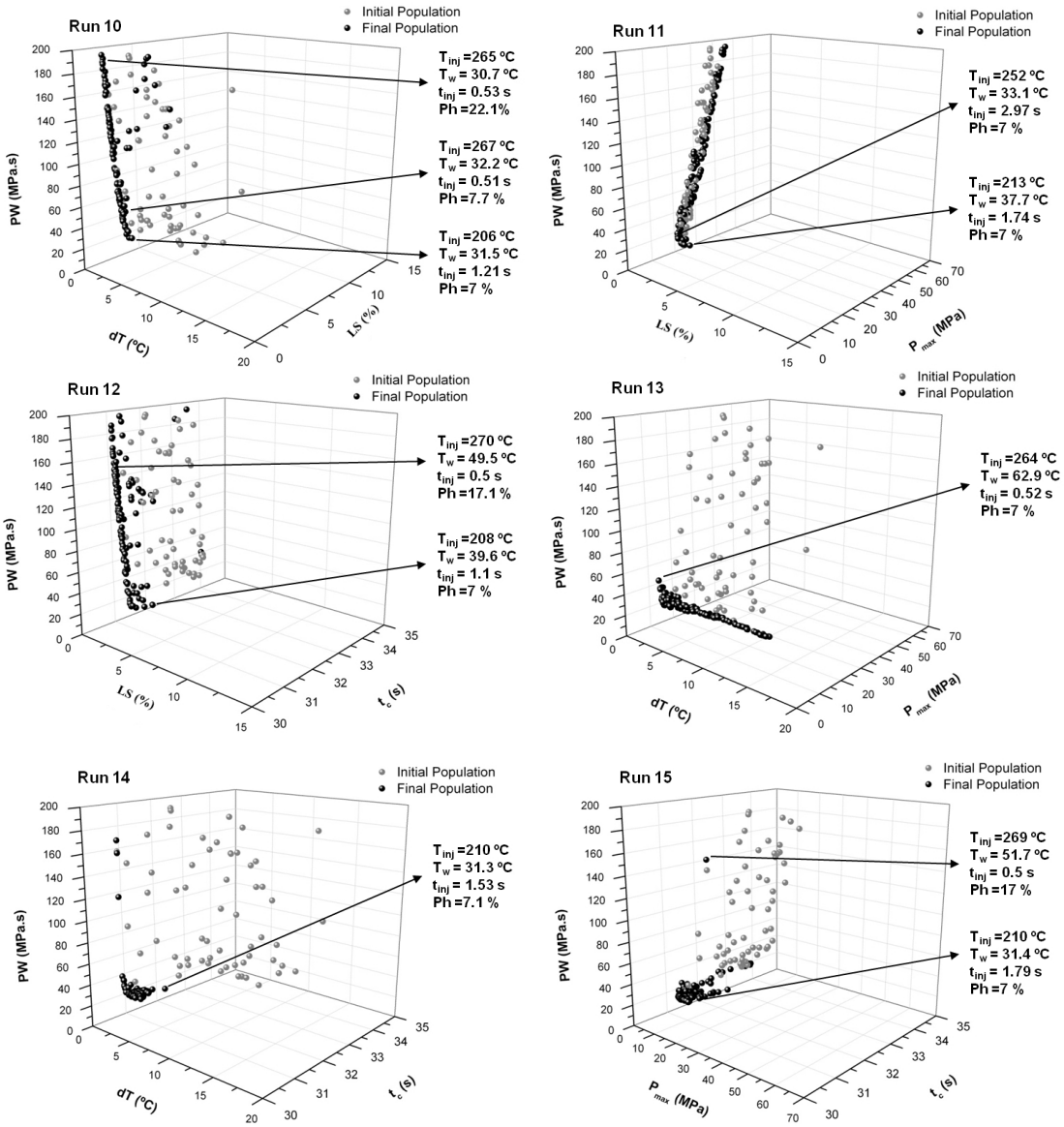

Figure 6.11: Optimization results for three objectives, run 10 to 15, in the objectives domain. Black symbols: Pareto frontier at 50th generation; grey symbols: initial population (PW – power work, LS – linear shrinkage, t_c – cycle time, P_{max} – maximum pressure, dT – temperature difference).

In run 10, PW, LS and dT are simultaneously optimized (dT – LS – PW plot of Figure 6.11). The PW values range between 23.2 – 199.6 MPa.s, LS between 1.2 – 3.1 % and dT between 1.4 – 9.6 °C. The highest variations occur in the objectives PW and dT. If pressure work is considered as the most important objective (i.e., the point with the lower pressure work) we have that LS = 3.1 % (the highest linear shrinkage value) and dT = 2 °C (a reasonable lower value for temperature difference on the moulding at the end of filling). In this case the injection moulding machine must operate with injection time of 1.2 s, melt and mould temperatures of 206 °C and 31.5 °C, respectively, and holding pressure at 7 % of maximum value of the machine injection pressure. Therefore, this solution is unsatisfactory when an

objective such as linear shrinkage is considered. In other hand, if dT is considered as the most important objective (i.e., the point with the lower temperature difference on the moulding at the end of filling) we can consider either PW = 187.9 MPa.s and LS = 1.6 % or PW = 46.4 MPa.s and LS = 2.7 %. In the first case, PW assume a high value and LS a lower value and injection machine must operate with injection time of 0.53 s, melt and mould temperatures of 265 ºC and 30.7 ºC, respectively, and holding pressure at 22.1 % of maximum value of the machine injection pressure. In the second case, PW is lower and LS is high with injection machine operating with injection time of 0.51 s, melt and mould temperatures of 267 ºC and 32.2 ºC, respectively, and holding pressure at 7.7 % of maximum value of the machine injection pressure. Hence, the first solution is unsatisfactory relativity to pressure work and the second solution is unsatisfactory relativity to linear shrinkage.

Run 11 optimized simultaneously PW, P_{max} and LS (LS – P_{max} – PW plot of Figure 6.11). The PW values range between 22.8 – 195.3 MPa.s, P_{max} between 10.4 – 40.7 MPa and LS between 1.2 – 3.1 %. The highest variations occur in the objective's PW and P_{max}. If pressure work is considered as the most important objective (i.e., the point with the lower pressure work) we have that P_{max} = 13.9 MPa (a reasonable lower value for maximum mould pressure) and LS = 3.1 % (the highest linear shrinkage value). In this case the injection moulding machine must operate with injection time of 1.74 s, melt and mould temperatures of 213 ºC and 37.7 ºC, respectively, and holding pressure at 7 % of maximum value of the machine injection pressure. This solution is unsatisfactory relativity to linear shrinkage. If maximum mould pressure is considered as the most important objective (i.e., the point with the lower maximum mould pressure) we have that PW = 31.5 MPa.s and LS = 2.7 % (reasonable values for both objective's). In this case the injection moulding machine must operate with injection time of 2.97 s melt and mould temperatures of 252 ºC and 33.1 ºC, respectively, and holding pressure at 7 % of maximum value of the machine injection pressure.

In run 12, PW, t_c and LS are simultaneously optimized (LS – t_c – PW plot of Figure 6.11). The PW values range between 23.6 – 197.2 MPa.s, t_c between 30.7 – 33.2 s and LS between 1.2 – 3 %. The highest variations occur in the objective's PW and t_c. If pressure work is considered as the most important objective (i.e., the point with the lower pressure work) we have that t_c = 31.3 s (a reasonable lower value for cycle time) and LS = 3 % (the highest linear shrinkage value). In this case the injection moulding machine must operate with injection time of 1.1 s, melt and mould temperatures of 208 ºC and 39.6 ºC, respectively, and holding pressure at 7 % of maximum value of the machine injection pressure. This solution is

unsatisfactory relativity to linear shrinkage. If cycle time is considered as the most important objective (i.e., the point with the lower cycle time) we have that PW = 159.8 MPa.s (high value for pressure work) and LS = 2 % (reasonable value for linear shrinkage). In this case the injection moulding machine must operate with injection time of 0.5 s, melt and mould temperatures of 270 ºC and 49.5 ºC, respectively, and holding pressure at 17.1 % of maximum value of the machine injection pressure. This solution is unsatisfactory relativity to pressure work.

In run 13, PW, P_{max} and dT are simultaneously optimized (dT – P_{max} – PW plot of Figure 6.11). The PW values range between 21.8 – 48.1 MPa.s, P_{max} between 10.3 – 14.3 MPa and dT between 1.2 – 14.8 ºC. The highest variations occur in the objective dT. If temperature difference on the moulding at the end of filling is considered as the most important objective (i.e., the point with the lower temperature difference on the moulding at the end of filling) we have that P_{max} = 10.8 MPa (a reasonable lower value for maximum mould pressure) and PW = 48.1 MPa.s (the highest pressure work value). In this case the injection moulding machine must operate with injection time of 0.52 s, melt and mould temperatures of 264 ºC and 62.9 ºC, respectively, and holding pressure at 7 % of maximum value of the machine injection pressure. This solution is unsatisfactory relativity to pressure work.

Run 14 optimized simultaneously PW, t_c and dT (dT – t_c – PW plot of Figure 6.11). The PW values range between 22.1 – 169.9 MPa.s, t_c between 30.7 – 31.7 s and dT between 1.2 – 3 ºC. The highest variations occur in the objective PW. If pressure work is considered as the most important objective (i.e., the point with the lower pressure work) we have that t_c = 31.7 s (the highest cycle time value) and dT = 2.4 ºC (a reasonable value for temperature difference on the moulding at the end of filling). In this case the injection moulding machine must operate with injection time of 1.53 s, melt and mould temperatures of 210 ºC and 31.3 ºC, respectively, and holding pressure at 7.1 % of maximum value of the machine injection pressure. This solution is unsatisfactory relativity to cycle time.

Finally, run 15 optimized simultaneously PW, t_c and P_{max} (P_{max} – t_c – PW plot of Figure 6.11). The PW values range between 21.9 – 160.1 MPa.s, t_c between 30.7 – 33.1 s and P_{max} between 10.3 – 25.8 MPa. The highest variations occur in the objective's PW and t_c. If pressure work is considered as the most important objective (i.e., the point with the lower pressure work) we have that t_c = 32 s and P_{max} = 14.7 MPa (reasonable values for both objective's). In this case the injection moulding machine must operate with injection time of 1.79 s, melt and mould temperatures of 210 ºC and 31.4 ºC, respectively, and holding pressure

at 7 % of maximum value of the machine injection pressure. If cycle time is considered as the most important objective (i.e., the point with the lower cycle time) we have that PW = 160.1 MPa.s and P_{max} = 25.8 MPa (highest values for both objective's). In this case the injection moulding machine must operate with injection time of 0.5 s, melt and mould temperatures of 269 ºC and 51.7 ºC, respectively, and holding pressure at 17 % of maximum value of the machine injection pressure. This solution is unsatisfactory relativity to pressure work and maximum mould pressure.

In Figure 6.12 a comparison between the Pareto plots of an optimization run with two objectives (run 2) with the 2D Pareto plots of optimization runs (runs 10, 13 and 14) considering three objectives. As expected, when a third objective is introduced the number of non-dominated solutions increase, i.e., the size of the optimal region increases. It is clear that this difficult the selection of the single solution to be used on the process.

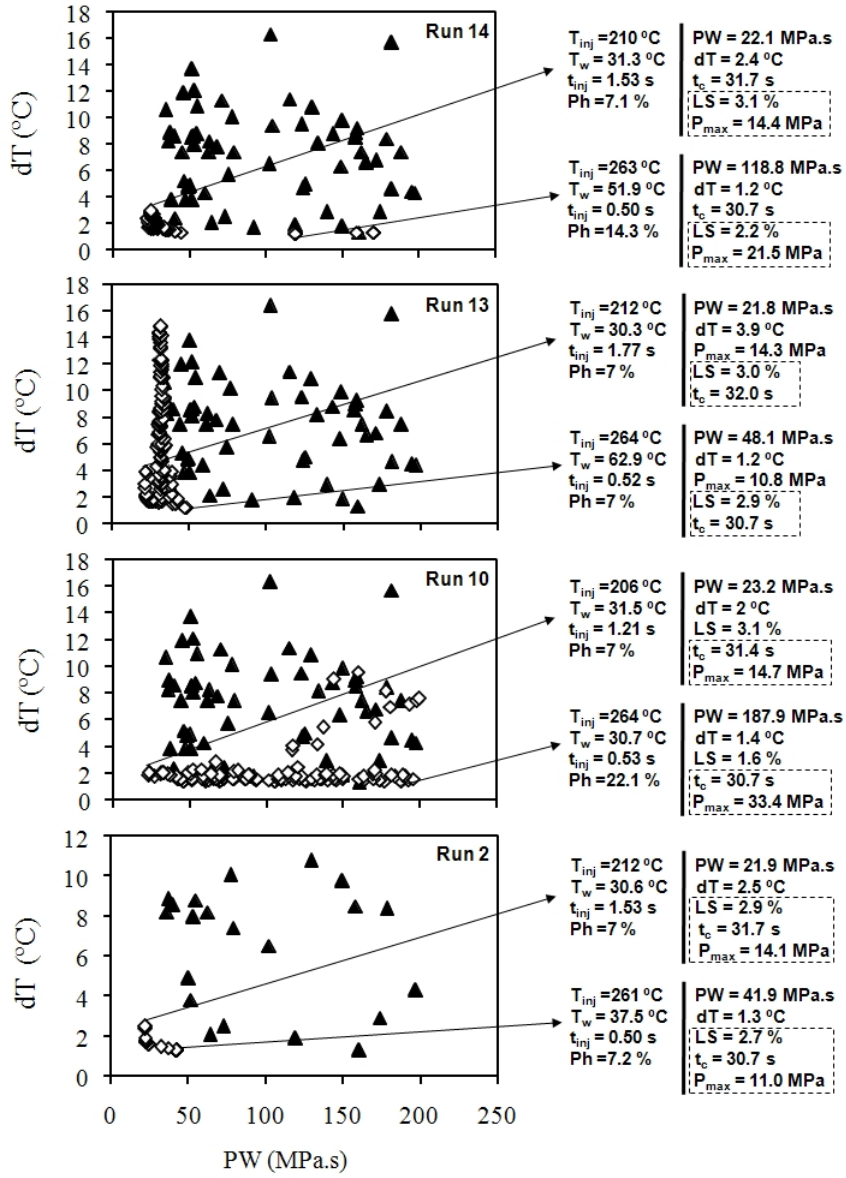

Figure 6.12: Comparison between the optimization results with two objectives, run 2, with results with three objectives, run 10, 13 and 14, in the objectives domain. Open symbols: Pareto frontier at 50th generation; full symbols: initial population (PW – power work, LS – linear shrinkage, t_c – cycle time, P_{max} – maximum pressure, dT – temperature difference).

6.4.4 *Optimization considering all objectives*

Run 20 consider the simultaneous optimization of the five objectives. In this case, a five-dimensional Pareto frontier in the objectives domain is obtained (Figure 6.13). It is difficult to choose a solution from this multidimensional Pareto frontier since the location of one possible solution in the various graphical representations is not evident. However, one must remember that a table identifying all the Pareto solutions is available. The decision maker

must define a working point (or region) in the objectives domain curves (Figure 6.13) and select the corresponding solution in the parameters to optimize domain (Figure 6.14).

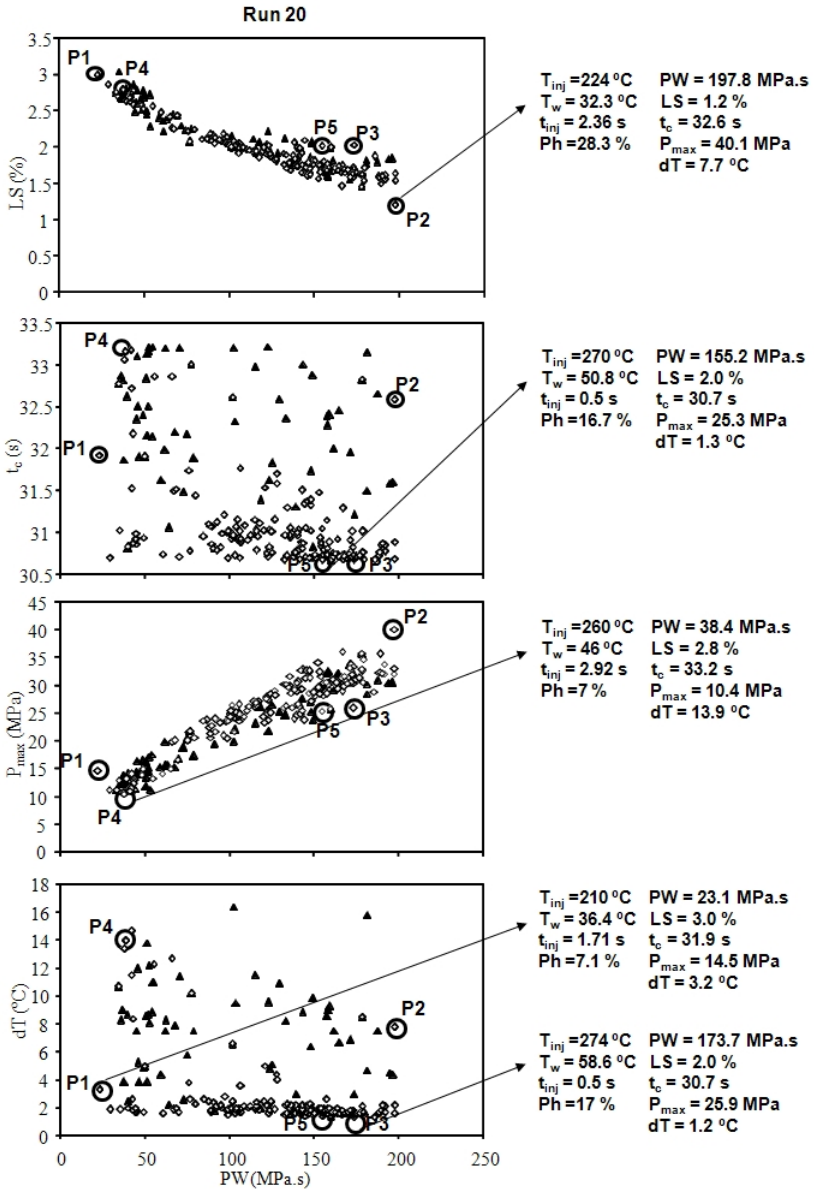

Figure 6.13: Optimization results for five objectives, run 20, in the objectives domain. Open symbols: Pareto frontier at 50th generation; full symbols: initial population (PW – power work, LS – linear shrinkage, t_c – cycle time, P_{max} – maximum pressure, dT – temperature difference).

For example, if pressure work is again considered as the most important objective, point P1 in Figure 6.13 (i.e., the point with the lower pressure work) can be defined and the corresponding solution chosen in Figure 6.14. In this case, the injection moulding machine must operate with injection time of 1.7 s (corresponding to flow rate of 7.06 cm^3/s), melt and mould temperatures of 210 °C and 36 °C, respectively, and holding pressure at 7 % of maximum machine injection pressure. This is done using the tabular form of the solutions represented in Figure 6.14. This set of processing variables leads to relative high linear

shrinkage equal to 3 % and cycle time of 31.9 s. The maximum mould pressure, P_{max}, and temperature difference on the moulding at the end of filling, dT, achieve low values equals to 14.5 MPa and 3.2 ºC, respectively. Finally, pressure work assume the minimum value possible equal to 23 MPa.s. Therefore, it is clear that this solution is unsatisfactory when objectives such as cycle time and linear shrinkage are considered.

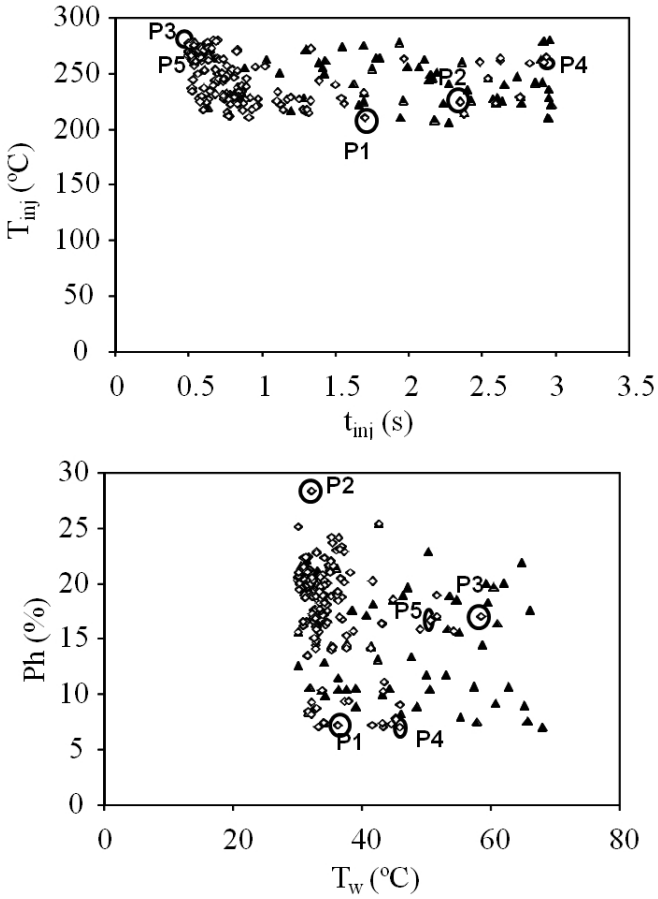

Figure 6.14: Optimization results for five objectives, run 20, in the parameters to optimize domain. Open symbols: Pareto frontier at 50th generation; full symbols: initial population (t_{inj} – injection time, T_{inj} – melt temperature, T_w – mould temperature, P_h – holding pressure).

Alternatively, if linear shrinkage is considered as the most important objective, point P2 in Figure 6.13 (i.e., the point with the lower linear shrinkage) can be chosen and the corresponding solution (Figure 6.14) selected (injection time of 2.4 s, melt and mould temperatures of 224 ºC and 32 ºC, respectively, and holding pressure of 28 % of maximum value of the machine injection pressure). This set of processing variables leads to a high pressure work (PW = 198 MPa.s) and maximum mould pressure (P_{max} = 40 MPa). Also, the cycle time and temperature difference on the moulding at the end of filling have relative high values (t_c = 32.5 s and dT = 7.7 ºC), but linear shrinkage is minimum (LS = 1.2 %). In this case, this solution is unsatisfactory when objectives such as pressure work and maximum

mould pressure are considered. A similar study can be done for the other points shown in Figure 6.13.

Hence, the selected objectives cannot be all optimized simultaneously, but graphical and tabular Pareto frontiers are a powerful tool enabling the decision maker to select different solutions representing different compromises between the objectives considered.

6.5 CONCLUSIONS

In this work, a multi-objective optimization methodology based on Evolutionary Algorithms (MOEA) was applied to the optimization of the operating conditions of polymer injection moulding process. The algorithm is able to take into account the multiple objectives used and, with a single run, to obtain a complete trade-off of solutions. The results obtained showed that the optimization methodology proposed is able to find solutions with physical meaning.

7

USING MULTI-OBJECTIVE EVOLUTIONARY ALGORITHMS FOR OPTIMIZATION OF THE COOLING SYSTEM IN POLYMER INJECTION MOULDING

Abstract[1]

The cooling process in polymer injection moulding is of great importance as it has a direct impact on both productivity and product quality. In this paper a Multi-objective Optimization Genetic Algorithm, denoted as RPSGAe, was applied to optimize both the position and the layout of the cooling channels in the injection moulding process. The optimization model proposed in this paper is an integration of genetic algorithms and Computer-Aided Engineering, CAE, technology applied to polymer process simulations. The main goal is to implement an automatic optimization scheme capable of defining the best position and layout of the cooling channels and/or setting the processing conditions of injection mouldings. In this work the methodology is applied to a L-shape moulding with the aim of minimizing the part warpage quantified by two different conflicting measures. The results produced have physical meaning and correspond to a successful process optimization.

7.1 INTRODUCTION

The injection moulding cycle consists of three important stages: mould filling, melt packing and part cooling. The cooling system design is of considerable importance since about 60-70 % of the cycle time is taken up by the cooling phase. An efficient cooling system design aiming at reducing cycle time must minimize undesired defects such as sink marks, part warpage and differential shrinkage.

In cooling system design, the design variables typically include the size of cooling channel and its layout, the thermal properties, temperature and flow rate of the coolant fluid. With so many design parameters involved, the determination of the optimum cooling system is extremely difficult. For an optimum design, the designer needs a powerful tool integrating the

1 C. Fernandes, A.J. Pontes, J.C. Viana and A. Gaspar-Cunha (2012). Using Multi-Objective Evolutionary Algorithms for Optimization of the Cooling System in Polymer Injection Moulding, *Journal of International Polymer Processing* **Issue 2012/02** 213–223.

cooling analysis and optimization programs into the design process. Therefore, it is necessary to develop computer-based methods to achieve efficient cooling system designs that optimize channel dimensions and layout as well as the processing conditions. The application of computer tools on the various designing stages of the injection moulding process is very frequent (e.g., Duff (2000); Menges and Mohren (1986)). Usually, the sequential steps of this design process are the following: definition of a finite element mesh representative of the part geometry and cooling system (in the case of a cooling analysis), selection of materials, definition of the gate location and of the initial processing variables. Finally, after launching the simulation the outputs are analyzed. Various optimization strategies using different methodologies to optimize the shape and locations of cooling channels in injection moulding have been reported in the literature. Tang et al. (1997, 1998) used 2D transient *FEM* simulations coupled with Powell's optimization method to optimize the cooling channel geometry to get uniform temperature in the polymer part. Park and Kwon (1998b) developed 2D and 3D stationary *BEM* simulations in the injection moulds coupled with 1D transient analytical computation in the polymer part (throughout the moulding thickness). The heat transfer integral equation is differentiated to get sensitivities of a cost function to the parameters (Park and Kwon, 1998c). The calculated sensitivities are then used to optimize the position of linear cooling channels for simple layouts (Park and Kwon, 1998a). Mathey et al. (2004) developed an optimization procedure to improve cooling of injection moulds. The model uses a mathematical programming method, *SQP*, to modify and improve automatically the geometry and the process parameters according to an objective function (e.g. cooling time or temperature uniformity). The *SQP* method was coupled with the *BEM* to solve thermal problems of cooling during injection. Lam et al. (2004) explored an approach to optimize both cooling channel design and process condition selection simultaneously through an evolutionary algorithm. The design variables used were: centers coordinates of cooling channels, sizes of cooling channels, flow rate and inlet temperature of the coolant in each cooling channel, packing time, cooling time and mould opening time. The work integrated genetic algorithm and *CAE* tool with the objective of achieving the most uniform cavity surface temperature to assure product quality. Qiao (2006) implemented a systematic computer-aided methodology for the optimization of cooling system design. Cycle-averaged cooling analysis, perturbation-based sensitivity analysis and the hybrid simulated annealing and Davidon–Fletcher–Powel method optimizer were applied to search for the optimal design. Significant uniformity of the temperature distribution along the cavity surface was

obtained as a result of the optimization process. Pirc et al. (2007) used *BEM* and *DRM* applied to unsteady heat transfer of injection moulds. The *BEM* code was combined with an adaptive reduced modelling and applied to a practical methodology for optimizing both the position and the layout of the cooling channels in injection moulding process. For that, the direct computation was coupled with an optimization algorithm such as *SQP*, where a potential problem is defined in a 2D unbounded domain. Later, Pirc et al. (2008) extended that methodology to optimize both the position and the layout of the cooling channels in 3D simulations of the injection moulding process. The optimization variables used were the position and shape parameters of the cooling channels and the outputs were the temperature of the moulded part surface and the variation of the temperature along this surface.

An important limitation of these optimization methodologies resides in the use of single objective optimization strategies, where the various objectives are either optimized alone or using an aggregation function. This type of methodology is not able to capture the trade-off between the objectives, which can bias the solution found. Therefore, an automatic optimization methodology based on Multi-Objective Evolutionary Algorithm - *MOEA* (Gaspar-Cunha and Covas, 2004) to define the best position and layout of cooling channels and/or defining the values of important operating conditions in injection moulding is proposed in this work. For that purpose a *MOEA* is linked to an injection moulding simulator code (in this case C-Mold). The methodology proposed here is general enough to be used with any injection moulding simulator code. The limitation of their applicability lies on the necessity of communicating the data in both directions (i.e., from the *MOEA* to the simulator and from the simulator to the *MOEA*).

The proposed optimization methodology was applied to a case study where the layout of the cooling channels and/or the processing conditions are established in order to minimize the part warpage quantified by two conflicting objectives as described below. This methodology proposed here is general enough to be used with any other injection moulding simulator code.

7.2 DEVELOPMENT OF THE OPTIMIZATION SYSTEM

7.2.1 *Framework*

In this work a methodology integrating computer simulations of the injection moulding process, an optimization methodology based on EA and multi-objective criteria is proposed. This methodology is used to establish the configurations of the cooling circuits and/or define the best processing conditions that lead to a part with lower warpage. *EA*s are a class of metaheuristics based on the concepts of the natural evolutions. The selection, crossover and mutation operators are applied to the current population that evolves during the successive generations (or iterations). The initial generation of chromosomes (initial population) indicating the configurations of the cooling circuits and/or the set of operative processing variables is randomly generated within the feasible search space and evaluated by the C-Mold modelling routine. The quality of the cooled part is quantified by the fitness function (angle deformation) of each chromosome. Then a new generation is produced though *EA* reproduction and re-evaluated. The process iterates until an optimal or near optimal cooling system design and/or processing conditions are found.

Figure 7.1 shows the interface for integrating C-Mold and the *EA*-based optimization routine. A design with cooling circuit coordinates and/or processing conditions are sent to C-Mold and shrinkage and warpage analysis is done through command files provided by C-Mold software. When the analysis is finished, the optimization routine will read the C-Mold results and calculations are done to measure the deformation angle along the part.

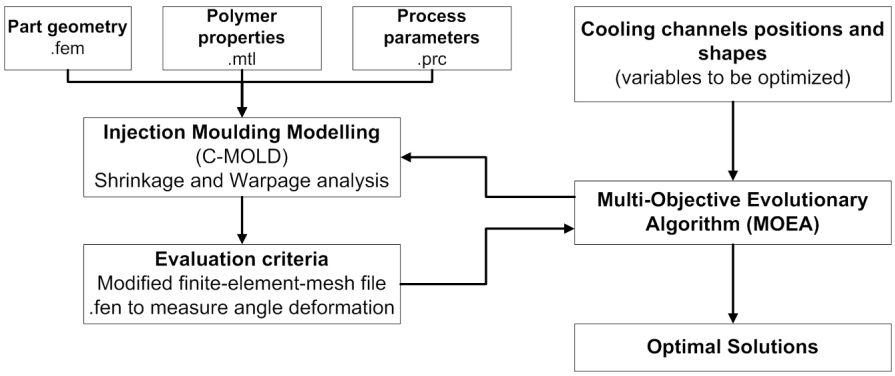

Figure 7.1: Interfacing optimization routine and C-Mold software.

7.2.2 *MOEA*

Based on the above described interface, the framework of the prototype system for mould cooling design optimization can be constructed, as shown in Figure 7.2. First, the population is randomly initialized, where each individual (or chromosome) is represented by the binary or real value of the set of all selected design variables (see Figure 7.3). In the presented case study, real representation is used. Then, each individual is evaluated by C-Mold shrinkage and warpage analysis. Based on the simulation results the deformation of the part is computed for that chromosome. Then, to each individual is assigned a single value identifying its performance on the process (fitness). A Multi-Objective approach, described in details elsewhere (Gaspar-Cunha and Covas, 2004), is used to calculate the fitness of each individual. If the convergence objective is not satisfied (e.g., a pre-defined number of generations), the population is subjected to the operators of selection (i.e., the choice of the best individuals for crossover and/or mutation), crossover and mutation in order to obtain new individuals for the next generation/iteration (Goldberg, 1989; Coello et al., 2002; Gaspar-Cunha, 2009).

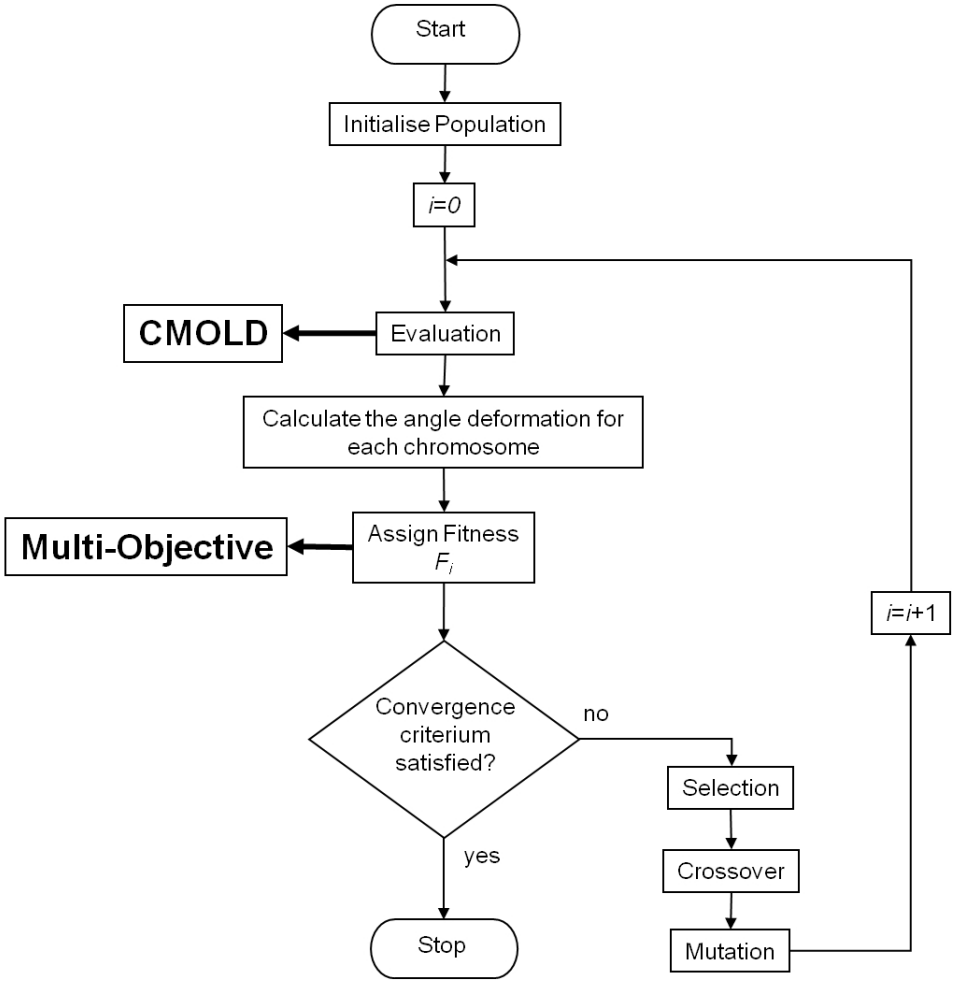

Figure 7.2: Flowchart of the MOEA applied for the optimization of the cooling system design.

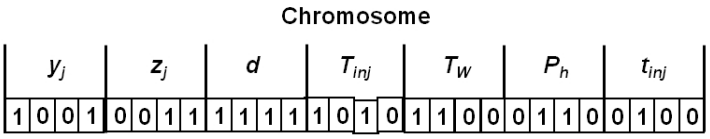

Figure 7.3: Chromosome representation.

In order to illustrate how the EAs work we will use a small example showing the application of selection, crossover and mutation operators (Gaspar-Cunha, 2009). The selection defines which of the individuals of the present population will act as parents of the next generation. This selection is based on the value of the global objective function determined for each individual. Different selection schemes exist, however they are all based on the concept of giving more opportunity to the individuals (or chromosomes) with higher fitness of being selected (Goldberg, 1989; Gaspar-Cunha, 2009).

The crossover allows the algorithm to produce new individuals for the next generation. For example, if two individuals represented in binary code (7 bits each) are selected for crossover, individual 1 [1010111] and individual 2 [1000011] and the crossover is to be applied in the

position 3. Then, two new offspring are generated by exchanging the information between the parents as illustrated next: offspring 1 [101 | 0011] and offspring 2 [100 | 0111], where the sign " | " represents here the crossover point. These new individuals can be or not inserted in the new population depending if they improve or not the value of the objective function, respectively. The crossover is applied with a given rate, meaning that only a percentage of the new population will be generated by crossover. Finally, the mutation consists in changing a single bit in a selected parent with a very low rate in order to obtain an offspring that will be incorporated in the new population.

7.2.3 *Objective function*

Essentially, the optimization problem in the present investigation is to minimize the warpage of the part measured by the deformation angle. In the present study warpage is quantified using two conflicting objectives as described below. First, twenty four coordinates in total were taken through the C-Mold model (Figure 7.4), near of the specific points located at 5, 15, 25 and 35 mm from the right side of the plate (as shown in Figure 7.4), before and after part moulding.

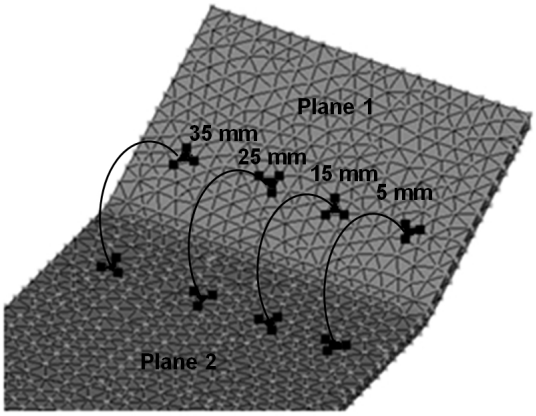

Figure 7.4: Coordinates and angles between planes on C-Mold model (before and after moulding).

Then the equations of eight planes defined by the specified points (Figure 7.4) are computed:

$$ax + by + cz + d = 0 \tag{7.1}$$

where $\overrightarrow{n} = (a, b, c) \in \mathbb{R}^3 \setminus \{(0, 0, 0)\}$ is the normal vector to the plane and d is a real number.

The corresponding angles between planes (Figure 7.4) were calculated by:

$$cos\theta_i = \frac{|n_1 \cdot n_2|}{\|n_1\| \times \|n_2\|}, \; i = 1, \ldots, 4, \tag{7.2}$$

where n_1 and n_2 are normal vectors to the planes 1 and 2, respectively.

The angle of the cavity moulding is 28.227 degrees. After moulding, the following two objectives with respect to the deformation angle deformation were defined:

1. Minimize dispersion (σ_1) of angular measurements after moulding relatively to the angle of the cavity moulding (28.227 degrees):

$$\min \sqrt{\frac{\sum_{i=1}^{4} (28.227 - \theta_i)^2}{3}} \tag{7.3}$$

2. Minimize dispersion (σ_2) of differences $d\theta_i = 28.227 - \theta_i$, $i = 1, \ldots, 4$, relatively to their mean value $\overline{d\theta_i}$:

$$\min \sqrt{\frac{\sum_{i=1}^{4} \left(d\theta_i - \overline{d\theta_i}\right)^2}{3}} \text{ where } \overline{d\theta_i} = \frac{\sum_{i=1}^{4} d\theta_i}{4} \tag{7.4}$$

The goal of each objective is:

1. to obtain a part with an angle closer as much to 28.227, after moulding (angle warpage);
2. to maintain unchanged the differences $d\theta_i$, $i = 1, \ldots, 4$ along the specific points (5, 15, 25 and 35mm) in order to minimize the effect of plane warpage.

These two objectives are conflicting and will be optimized simultaneously. Concerning the modelling programme, the geometric and process constraints considered were:

- geometric constraints:
  - upper/lower-bound constraints on the coordinates of the cooling channels;
  - limits on the distance between the cooling channels;
  - limits on the distance between each channel and the cavity boundary.
- process restrictions:
  - the moulding has to be completely filled, obviously no short-shots were admitted;

– the computed values of the maximum shear stress and strain-rate were limited to their critical values (defined on the C-Mold database) in order to avoid other potential defects (e.g., shark skin).

7.3 CASE STUDY

The cooling system considered in this investigation uses cylindrical cooling channels and water as coolant fluid. The geometry is a rectangular L-shape moulding with a curved end as shown in Figure 7.5. The moulding has the following nominal dimensions: 1.5 mm of thickness, 40 mm of width and 134 mm of length. The finite element mesh has 874 triangular elements. The initial cooling system layout is presented in Figure 7.5.

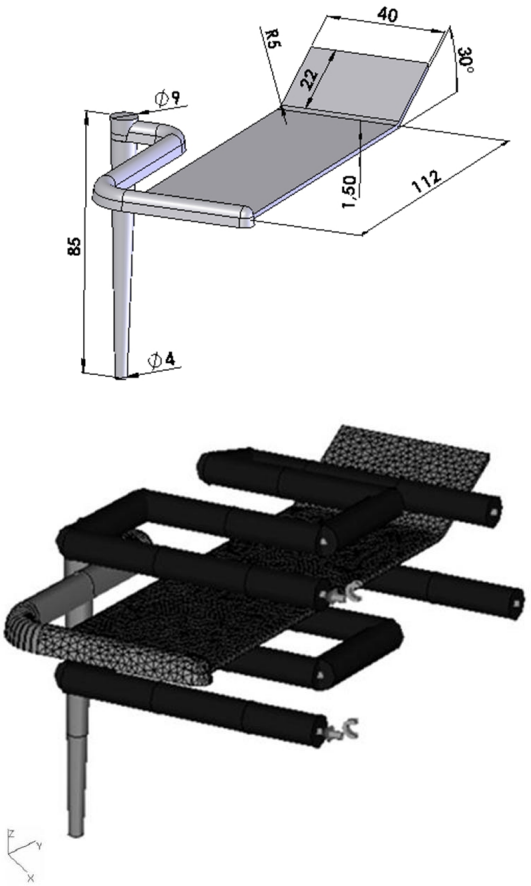

Figure 7.5: Moulding geometry, mesh and initial cooling system (dimensions in mm).

The part is moulded in polystyrene, STYRON 678E, from Bayer. Table 7.1 gives a summary of the relevant polymer properties used for the flow simulations (C-Mold database).

PROPERTY	VALUE UNIT
Melt density	$968.6\,kg/m^3$
Typical melt temperature	$503\,K$ or $230\,^oC$
Maximum shear stress	$2.4 \times 10^5\,Pa$
Maximum shear rate	$4 \times 10^4\,s^{-1}$
Specific heat	$2100\,J/kg.K$
Thermal conductivity	$0.15\,W/m.K$

Table 7.1: Typical properties of STYRON 678E.

Mould material selected is P20 steel and concerning the processing conditions two cases were considered, one where they are constant and other where they are optimized. The simulations in C-Mold are based on a hybrid finite-element/finite-difference/control-volume numerical solution of the generalized Hele-Shaw flow equation of a compressible viscous fluid under non-isothermal conditions. The polymer rheological and PVT description were modelled by a Cross-WLF and the Tait modified equations, respectively. More details about the software are described in related literature (Hieber and Shen, 1980; Chiang et al., 1991a,b; Viana, 1999). The simulations considered the C-Mold Integrated Shrinkage & Warpage analysis that includes polymer melt flow and mould cooling analysis, residual stress calculations and structural analysis.

The cooling system was modelled by sixteen coordinates describing the locations of the two cooling channels, one in each mould side. Each location is defined by the y and z coordinates of the cooling line center in the y-z plane and by the x coordinate describing the depth of the cooling line along the x axis (x is maintained constant along the optimization process, see Figure 7.5). Another selected design variable is the cooling channel diameter. Four processing variables were also selected, namely, the injection time, the melt and mould temperatures and the holding pressure, based on their potential relevance on the part quality. Table 7.2 resumes the selected design variables and their corresponding values ranges.

DESIGN VARIABLE	VALUE RANGE
Y coordinate (mm) - $y_1, \ldots, y_{16}$	$[0, 160]$ subject to constraint
Z coordinate (mm) - $z_1, \ldots, z_{16}$	$[-20, 50]$ subject to constraint
Cooling channel diameter (mm) - d	$[5, 10]$
Injection time (s) - t_{inj}	$[0.5, 3]$
Melt temperature (ºC) - T_{inj}	$[180, 280]$
Mould temperature (ºC) - T_w	$[30, 70]$
Holding pressure (% of maximum machine injection pressure)	$[7, 38]$

Table 7.2: Design and processing variables and their value ranges.

The RPSGAe uses a real representation of the variables, a simulated binary crossover, a polynomial mutation and a roulette wheel selection strategy (Gaspar-Cunha and Covas, 2004; Goldberg, 1989; Coello et al., 2002; Deb, 2001). The RPSGAe was applied using the following parameters: 50 generations (or iterations), crossover rate of 0.8, mutation rate of 0.05, internal and external populations with 200 individuals, limits of the clustering algorithm set at 0.2 and N_{Ranks} at 30. These values resulted from a carefully analysis made in a previous work (Gaspar-Cunha and Covas, 2004).

The proposed optimization methodology will be used for setting the diameter and coordinates of the cooling channels and/or to define the selected processing conditions.

7.4 RESULTS

Three different studies were performed. First, an analysis of variance (ANOVA and MANOVA) was made considering simulation results with the aim to check if the parameters considered are statistically significant for the objectives used. This ANOVA/MANOVA analysis only was made for comparison purposes and is not necessary in the optimization scheme based on EAs proposed. Then, the RPSGAe algorithm was used to optimize the process considering two different situations, one considering the operating conditions constant and other where these conditions are optimized simultaneously with cooling channels design.

At this point is important to clarify that the computation time for an optimization run only depends on the number of times the C-Mold software is called. In the present case is possible to get a complete optimization in circa of 10 hours in a personal computer with an

Intel i7 processor at 2.67 Mhz. An optimal solution is obtained after a RPSGAe optimization runs (where the C-Mold software is called hundreds of times).

7.4.1 *Analysis of modelling results*

The moulding program includes changes of the injection time, melt and mould temperatures and holding pressure, in two levels (Table 7.2) according to design of analytical simulations plan. A total of 16 different mouldings were obtained, as listed in Table 7.3.

RUN	$t_{inj}\,(s)$	$t_{inj}\,(^{o}C)$	$t_w\,(^{o}C)$	$ph\,(\%)$
1	0.5	180	30	7
2	0.5	180	30	38
3	0.5	180	70	7
4	0.5	180	70	38
5	0.5	280	30	7
6	0.5	280	30	38
7	0.5	280	70	7
8	0.5	280	70	38
9	3	180	30	7
10	3	180	30	38
11	3	180	70	7
12	3	180	70	38
13	3	280	30	7
14	3	280	30	38
15	3	280	70	7
16	3	280	70	38

Table 7.3: Design of analytical simulations (independent variables).

The effect of the processing conditions on the angular measurements after moulding is listed in Table 7.4.

RUN	σ_1	σ_2
1	0.01876	0.00136
2	0.02614	0.00387
3	0.00851	0.00227
4	0.02456	0.00733
5	0.02696	0.00140
6	0.05494	0.00680
7	0.01914	0.00184
8	0.06589	0.01293
9	0.01599	0.00179
10	0.02178	0.00556
11	0.00956	0.00220
12	0.01989	0.00706
13	0.02058	0.00076
14	0.03960	0.00797
15	0.01274	0.00169
16	0.05391	0.01505

Table 7.4: Angular measurements resulting from variation of the processing conditions (dependent variables).

Two types of analysis were performed with these simulation results, namely ANOVA and MANOVA (Chatfield and Collins, 1996). In the former, the analysis is performed on each of the dependent variables. In the MANOVA analysis the four variables are considered simultaneously in order to detect a potential degree of correlation between them.

Table 7.5 presents the results for the responses of the analytical modeling package. The table lists the significant terms (5% level) for the multivariate (MANOVA) and univariate (ANOVA) analysis. These results were obtained using the SPSS software considering different multivariate tests (Pillai's trace, Wilk's Lambda, Hotteling's trace and Roy's Largest Root).

EFFECT	MULTIVARIATE ANALYSIS	UNIVARIATE ANALYSIS	
		σ_1	σ_2
Intercept	*	*	*
t_{inj}	*	*	–
T_{inj}	*	*	*
T_w	*	–	*
Ph	*	*	*
$t_{inj} * T_{inj}$	–	–	–
$t_{inj} * T_w$	–	–	–
$t_{inj} * Ph$	–	–	–
$T_{inj} * T_w$	–	–	–
$T_{inj} * Ph$	*	*	*
$T_w * Ph$	–	*	*

Table 7.5: Significant processing factors from ANOVA and MANOVA analysis (* statistically significant, – statistically nonsignificant).

According to MANOVA, all the main effects are statistically significant and only the two–way interaction between T_{inj} and Ph is statistically significant. However, when the effects of variables are considered individually, one can conclude that injection time is not important on dispersion (σ_2) of differences $d\theta_i = 28.2 - \theta_i, i = 1, \ldots, 4$, and mould temperature is not important on dispersion (σ_1) of angular measurements after moulding. Also, the two-way interactions between T_{inj}*Ph and T_w*Ph are statistically significant.

Figure 7.6 shows the effects of some interactions between factors (t_{inj}*T_{inj}, t_{inj}*T_w, t_{inj}*Ph) on the dispersion coefficients σ_1 and σ_2. In general, the values of σ_1 decreases with injection time and the values of σ_2 increase with it except when holding pressure equals 7%. The values of σ_1 are lower when melt temperature and holding pressure decreases and mould temperature increases. σ_2 values are lower for lower values of all shown factors.

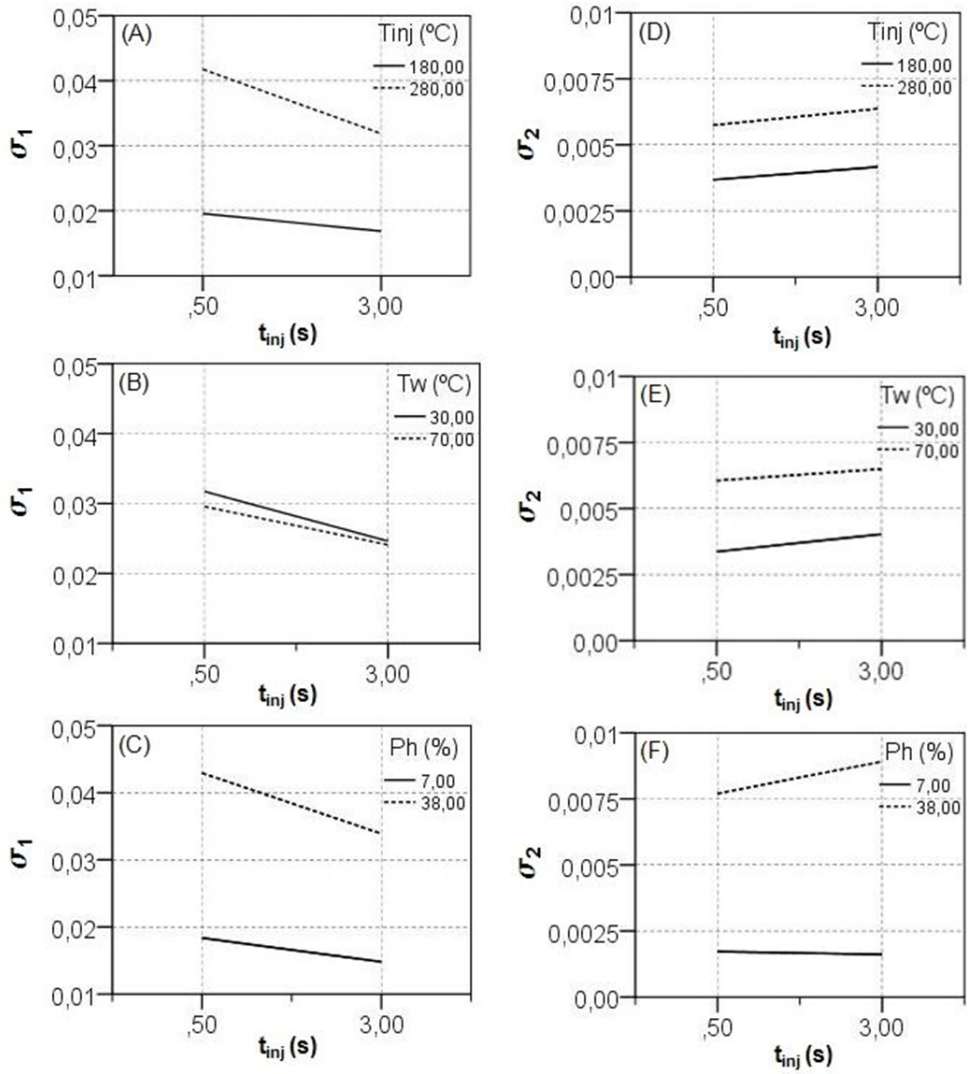

Figure 7.6: Effect graphs for dispersion one and two vs. injection time for different levels of T_{inj}, T_w and Ph.

The main conclusion from this analysis is that there is an interaction between both objectives considered (σ_1 and σ_2), i.e., is not indifferent to consider these objectives separately or simultaneously.

7.4.2 *Processing conditions optimization results*

Firstly, the optimization methodology proposed was used for setting the processing conditions of the case study moulding in order to accomplish the objectives given by equations 7.3 and 7.4, i.e., to minimize the part warpage and distortion. The results obtained in the objectives space are shown in Figure 7.7 and the associated processing conditions for points P1 to P7 are shown in Table 7.6.

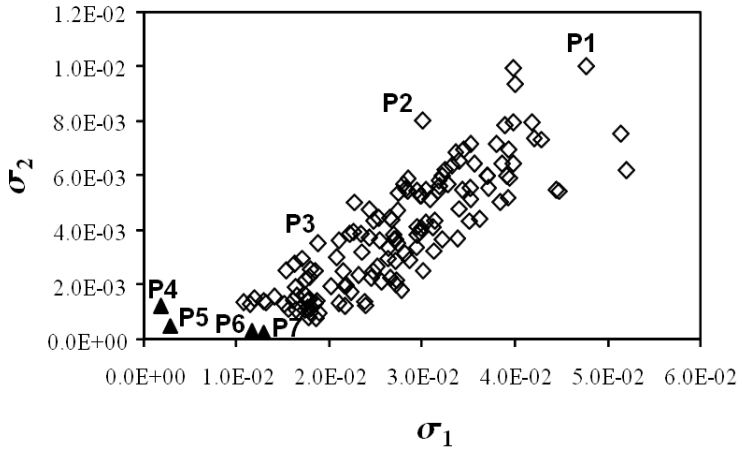

Figure 7.7: Processing conditions optimization results. Full symbols: Pareto frontier at 50th generation; Open symbols: initial population (σ_1 – dispersion of angular measurements after moulding, σ_2 – dispersion of differences $d\theta_i$, $i = 1, \ldots 4$, relatively to their mean value $\overline{d\theta_i}$).

	VARIABLES				OBJECTIVES	
SOLUTIONS	t_{inj} (s)	T_{inj} (ºC)	T_w (ºC)	Ph (%)	σ_1 (º)	σ_2 (º)
P1	1.21	265	70	35.1	0.04762	0.01001
P2	2.87	225	67	34.9	0.02998	0.00802
P3	2.43	225	65	21.9	0.01866	0.00353
P4	2.65	226	56	8.1	**0.00169**	0.00126
P5	2.60	229	54	7.9	0.00275	0.00051
P6	2.64	222	69	7.1	0.01156	**0.00034**
P7	2.53	229	65	7,3	0.01281	**0.00026**

Table 7.6: Optimal processing conditions to minimize the deformation angle and plane distortion of the moulding.

From Figure 7.7 can be observed that points P1, P2 and P3 (open symbols), that belong to the initial population, have significantly higher holding pressure values than points P4, P5, P6 and P7 that belong to the final population (filled symbols). This fact indicates that to minimize the deformation angle and distortion a lower holding pressure must be applied. Points P4 and P5 are the solutions with minimal deformation angle (i.e. higher minimization of σ_1) and points P6 and P7 represent the solutions with minimal part distortion (i.e. higher minimization of σ_2).

Analyzing Table 7.6, it is clear that injection time and melt temperature values are very similar in all solutions (except for P1), but mould temperatures of solutions P4 and P5 are lower than the mould temperatures of solutions P6 and P7; and holding pressures of solutions P1 to P3 are higher than holding pressures of solutions P4 to P7. Thus, solutions with injection times of 2.45-2.87 s, melt temperatures of 222-229 ºC, mould temperature

of 54-56 ºC and holding pressure equal to 7.9-8.1 % results in a moulding with the lowest deformation angle and the solutions with mould temperature of 65-70 ºC and holding pressure of 22-35 % leads to a lower part distortion.

These results are in accordance with the statistical analysis done in the previous section. The best results (i.e., that minimize simultaneously both objectives) are achieved for lower holding pressure, intermediate mould and injection temperatures and higher injection times.

7.4.3 *Cooling channels design optimization results*

Secondly, the proposed optimization methodology is applied to find the best cooling channels design variables. In this optimization procedure, the processing conditions were maintained constant, according to Table 7.7. To measure the optimality of the solutions, the objectives given by equations 7.3 and 7.4 were again used.

This study was divided in two parts: firstly, the simulations consider a cold runners system; second, the simulations consider a direct hot runner.

PARAMETER	VALUE UNIT
Injection temperature	230 ^{o}C
Mould temperature	50 ^{o}C
Holding pressure	17 % of the maximum machine injection pressure
Holding time	15 s
Injection time	0.5 s

Table 7.7: Processing conditions used in the simulations.

7.4.3.1 *Optimization with cold runners*

The results obtained in the criteria's space for the initial and final generations are presented in Figure 7.8 and the cooling channels locations of points P1 to P6 are shown in Figure 7.9.

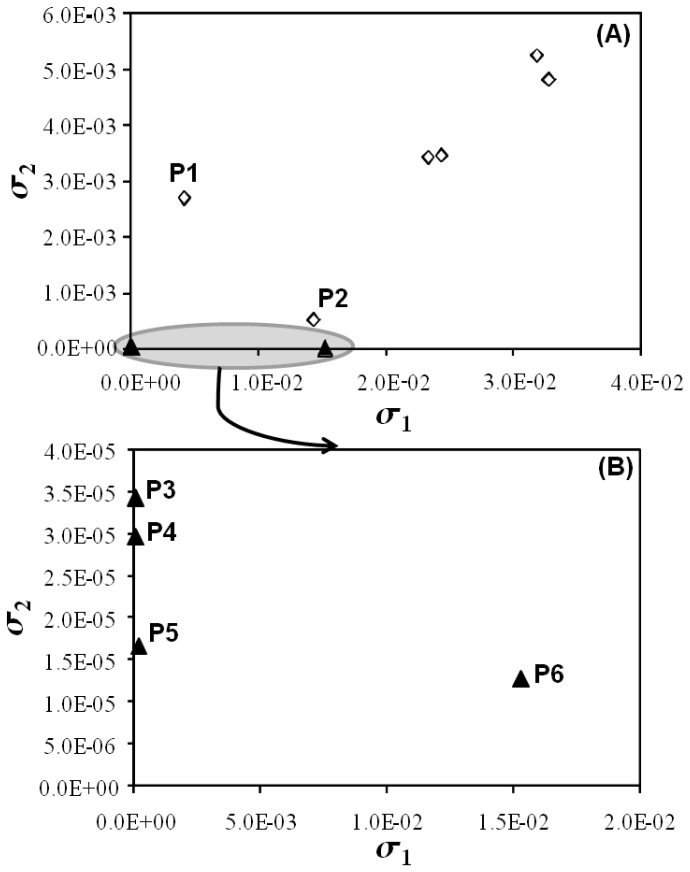

Figure 7.8: Cooling channels design optimization results: (A) Initial population and Pareto frontier at 50th generation; (B) Pareto frontier at 50th generation (σ_1 – dispersion of angular measurements after moulding, σ_2 – dispersion of differences $d\theta_i$, $i = 1, \ldots 4$, relatively to their mean value $\overline{d\theta_i}$).

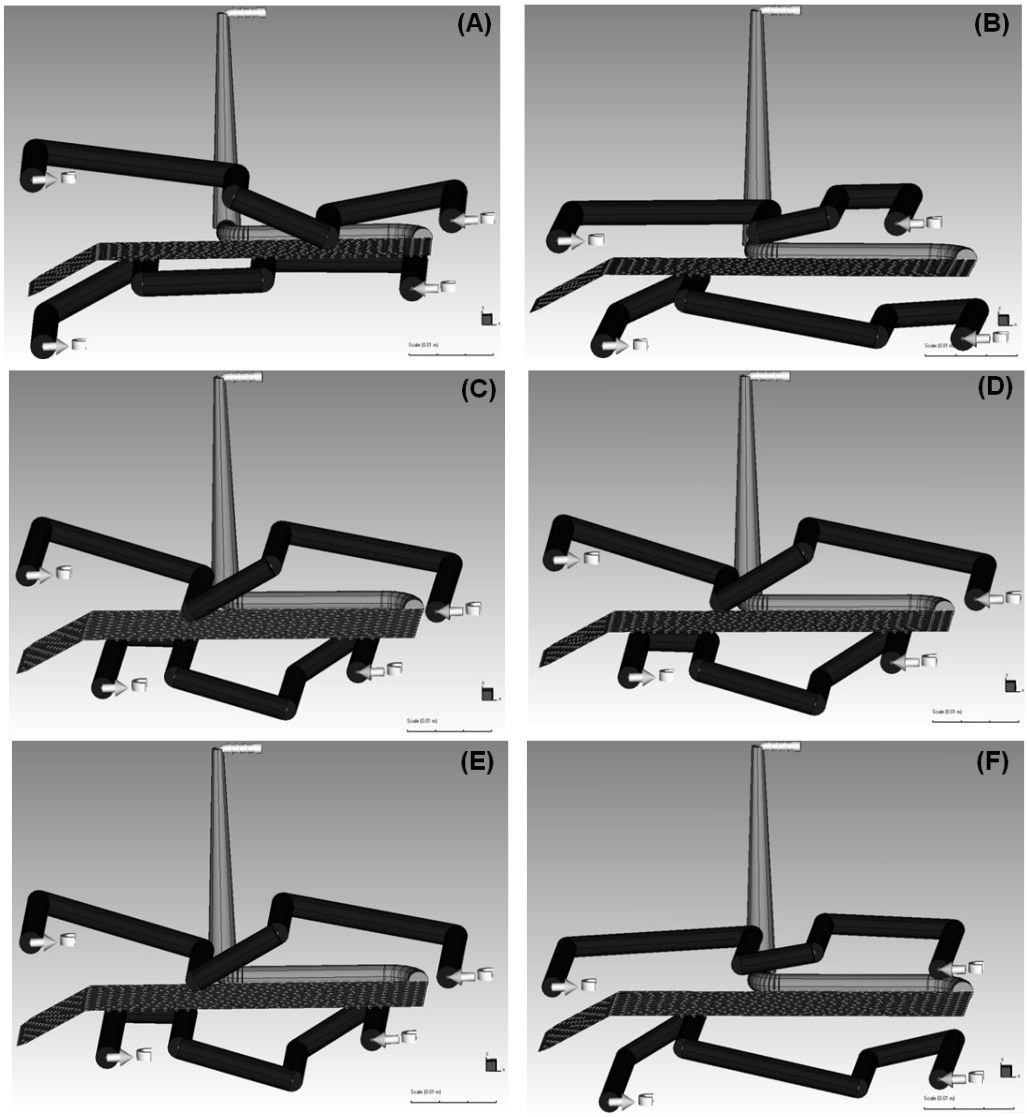

Figure 7.9: Optimal cooling channels designs: solutions corresponding to points P1 to P6 represented in Figure 7.8.

As an example, points P1 and P2 (belonging to the initial population) were picked in Figure 7.8, in order to study their evolution along the optimization process. The cooling channels designs of these points are, also, represented in Figure 7.9. The evolution of point P1 trough the optimization process originates solutions represented by point P3, P4 and P5 in the final population and point P2 originates solution P6 in final population. Cooling channels locations represented on Figure 7.9 (points P3, P4 and P5 in Figure 7.8, respectively) provide a higher minimization of σ_1 and cooling channel location of Figure 7.9 (point P6 in Figure 7.8) assure a higher minimization of σ_2. Points P3, P4 and P5 have cooling channels designs with similar shape. On the other hand, point P6 has a cooling channel design with a different shape. This means that solutions of points P3, P4 and P5 are more efficient to obtain a polymeric part with an angle similar to 28.2° after processing, i.e., lower deformation angle

and the solution of point P6 is more indicated to minimize the effect of distortion of the part because it is better in maintaining unchanged the difference $d\theta_i$, $i = 1, \ldots, 4$, along the width of the part. It is also important to note that the cooling channel diameter of solutions who guarantee a higher minimization of σ_1 is of 8 mm and cooling channel diameter of solution that assure a higher minimization of σ_2 is of 7 mm.

7.4.3.2 *Optimization with direct hot runner*

The results obtained in the criteria's space for the initial and final generations are presented in Figure 7.10 and the cooling channels locations of points P1 to P4 are shown in Figure 7.11.

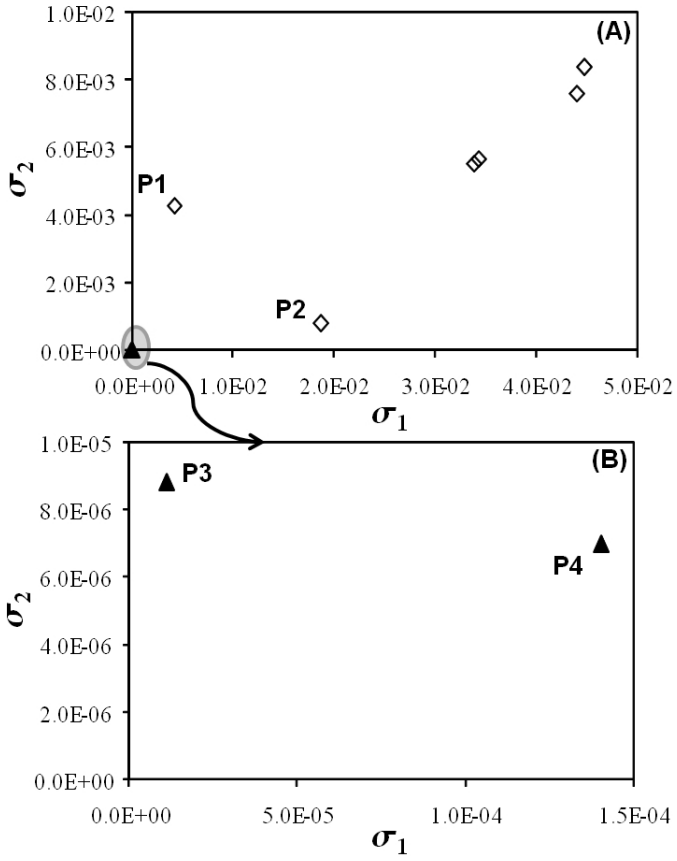

Figure 7.10: Cooling channels design optimization results: (A) Initial population and Pareto frontier at 50th generation; (B) Pareto frontier at 50th generation (σ_1 – dispersion of angular measurements after moulding, σ_2 – dispersion of differences $d\theta_i$, $i = 1, \ldots 4$, relatively to their mean value $\overline{d\theta_i}$).

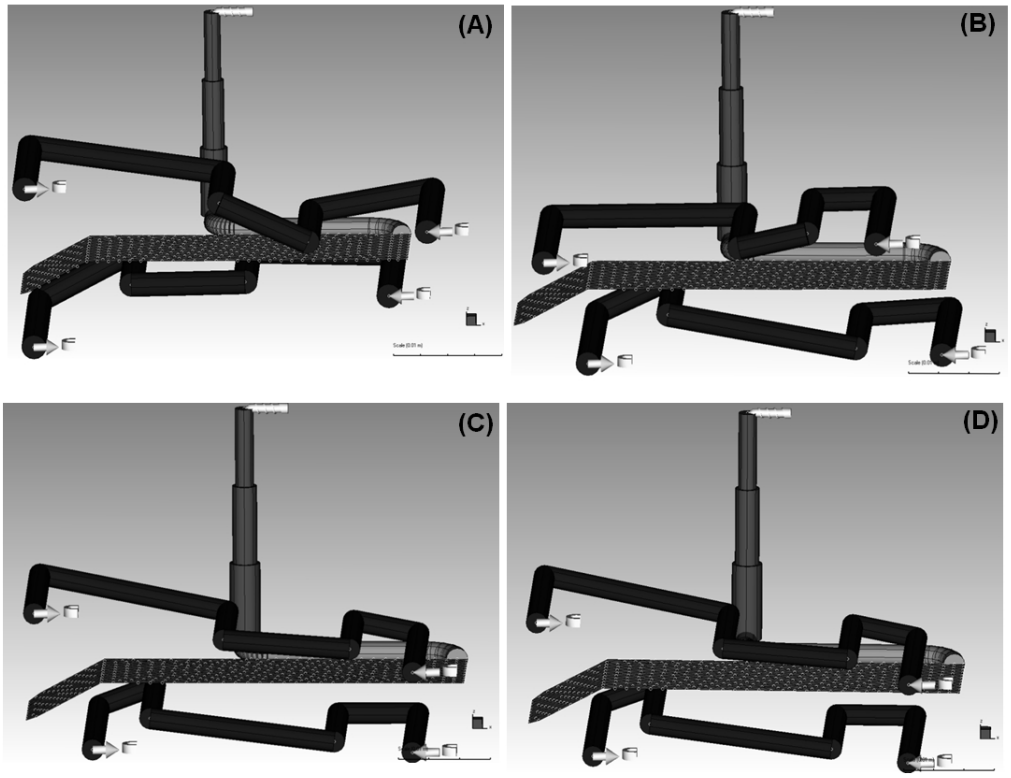

Figure 7.11: Optimal cooling channels designs: solutions corresponding to points P1 to P4 represented in Figure 7.10.

Similar to what have done previously, points P1 and P2 (belonging to initial population) were picked in Figure 7.10 to study their evolution along the optimization process. The cooling channels designs of these points are represented in Figure 7.11. Both points of the final population P3 and P4 have similar cooling channels layouts and the criteria's values determined for these two solutions are very similar too. This means that these two solutions can be considered as only one solution. Therefore, our design cooling channel optimization problem with hot runner system have a unique solution, with a cooling channel diameter of 7 mm.

7.4.4 *Simultaneous processing conditions and cooling channels design optimization results*

Finally, the proposed optimization methodology was used to find simultaneously the best cooling channels design and processing conditions that minimize the deformation angle and the part warpage. In this case only cold runners were used. The results obtained in the criteria's space for the initial and final generations are presented in Figure 7.12.

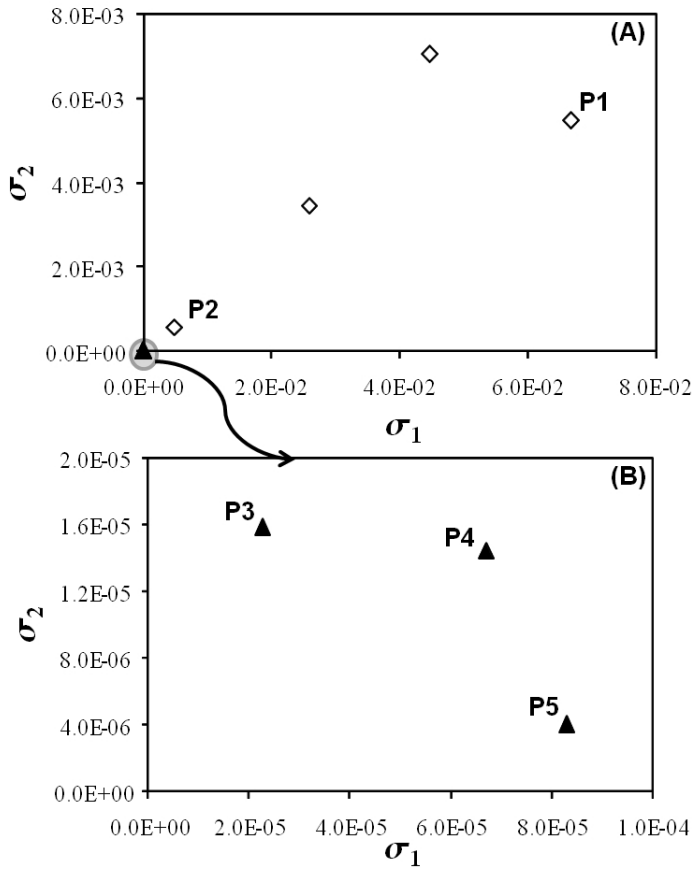

Figure 7.12: Processing conditions and cooling channels design optimization results: (A) Initial population and Pareto frontier at 50th generation; (B) Pareto frontier at 50th generation (σ_1 – dispersion of angular measurements after moulding, σ_2 – dispersion of differences $d\theta_i$, $i = 1, \ldots 4$, relatively to their mean value $\overline{d\theta_i}$).

The cooling channels locations of points P1 to P5 are shown in Figure 7.13 and the correspondent processing conditions are listed in Table 7.8. The final generation solutions (P3, P4 and P5) feature cooling channels designs with identical layout and the optimal processing conditions values are also very similar. Namely, the injection time should be settled at 2.52 s, the melt and mould temperatures at 241 ºC and 32 ºC respectively, and holding pressure at 11.7% of maximum machine injection pressure.

The optimization of cooling channels layout and processing conditions must be done simultaneously.

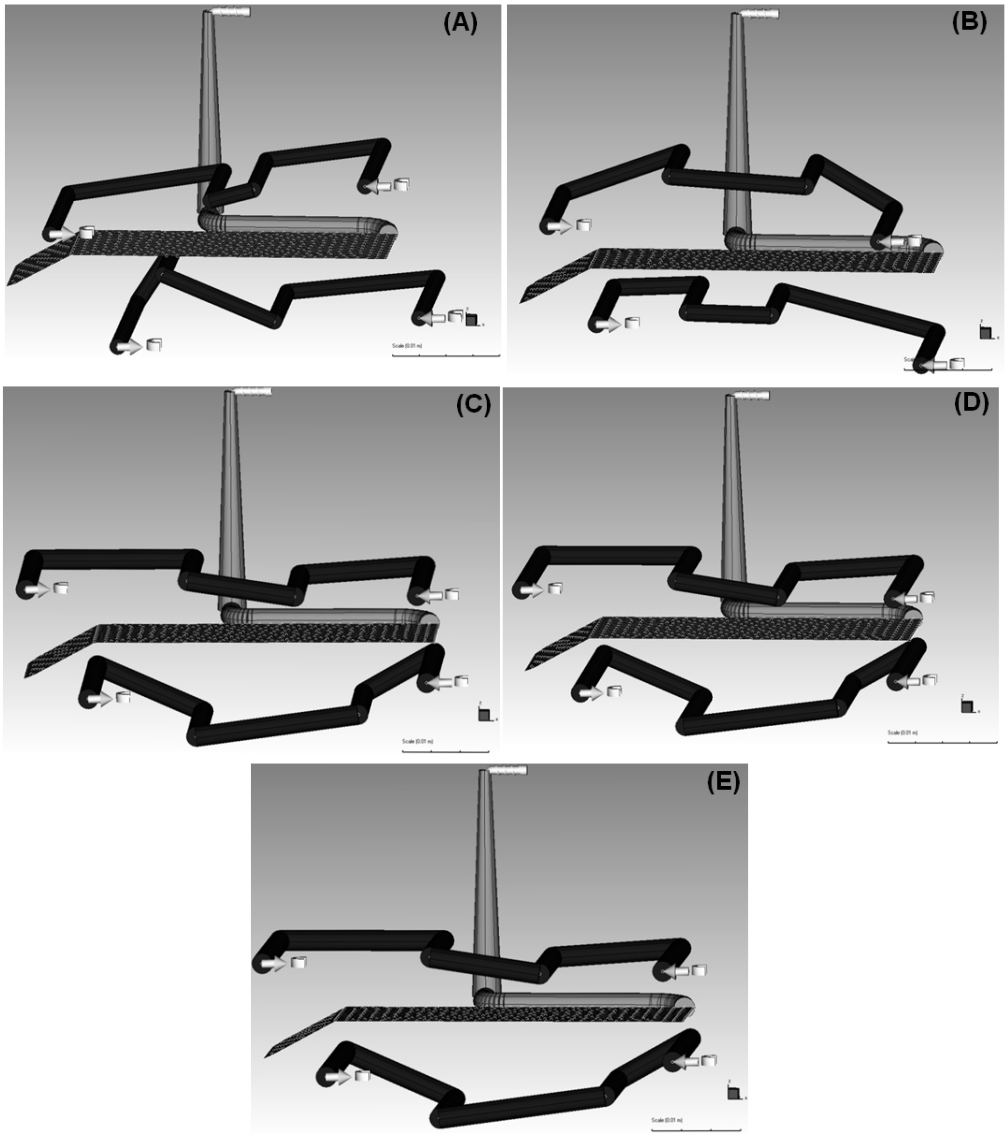

Figure 7.13: Optimal cooling channels designs: solutions corresponding to points P1 to P5 represented in Figure 7.12.

	VARIABLES				OBJECTIVES	
SOLUTIONS	t_{inj} (s)	T_{inj} (ºC)	T_w (ºC)	Ph (%)	σ_1 (º)	σ_2 (º)
P1	0,50	237	53	36,6	0,06668	0,00548
P2	2,59	223	43	25,4	0,00485	0,00056
P3	2,52	241	32	11,6	0,00002	0,00002
P4	2,52	241	32	11,7	0,00007	0,00001
P5	2,52	241	32	11,7	0,00008	0,000004

Table 7.8: Optimal processing conditions to minimize the deformation angle and part warpage.

7.5 CONCLUSIONS

In this work, a multi-objective optimization methodology based on Evolutionary Algorithms (MOEA) was applied to the optimization of processing conditions and cooling channels locations of a L-shaped rectangular moulding in order to minimize the effect of part warpage and deformation angle.

Initially, analysis of variance (ANOVA and MANOVA) are performed allowed to establish the set of iterations between the factors studied (i.e., the iterations between the objectives to be accomplished and the decision variables). As expected, it is not indifferent to consider the objectives separately or simultaneously. This shows the need of an optimization methodology able to take into account both objectives simultaneously such as the one proposed here.

The optimization methodology used was able to produce results with physical meaning for three different studies: first, for individual optimization of processing conditions, then for individual optimization of cooling channels locations and finally simultaneously optimization of processing conditions and cooling channels locations.

The best strategy is to optimize simultaneously the cooling channel layout and processing conditions.

8

OPTIMIZATION OF GATE LOCATION AND PROCESSING CONDITIONS IN INJECTION MOULDING USING A MULTI-OBJECTIVE EVOLUTIONARY ALGORITHM

Abstract[1]

The definition of the gate location in injection moulding is one of the most important factors in achieving dimensionally accuracy of the parts. This paper presents an optimization methodology for addressing this problem based on a MOEA. The algorithm adopted here is called RPSGAe and was used to create a balanced filling pattern using weld line characterization. The aim being to guarantee that the differential shrinkage, at the end of the flow, is close as possible of the pre-defined design value and to, simultaneously, minimize the cycle time necessary to manufacture the part.

The optimization approach proposed in this paper is an integration of evolutionary algorithms with CAE software (Autodesk Moldflow Plastics software). The performance of the proposed optimization methodology was illustrated with an example consisting in the injection of a rectangular part with a non-symmetrical hole.

8.1 INTRODUCTION

Injection moulding is a complex but efficient polymer processing technique for producing a variety of plastics parts. It is especially adequate to produce products with low dimensional tolerances and complex shapes. It consists in reproducing the required geometry previously machined in the mould by injecting molten polymer into the mould cavity. It is a three-phase process, filling the cavity, packing the molten material and cooling the polymer, which were not independent. Therefore, the quality of an injection-moulded part is affected by factors, which are related with this three phases. These steps are dependent of different sets of components, such as, machine control system (e.g., injection cycle times and injection and holdout pressures), cooling system (e.g., cooling channels geometry and cooling liquid

1 C. Fernandes, A.J. Pontes, J.C. Viana and A. Gaspar-Cunha (2012). Optimization of Gate Location and Processing Conditions in Injection Moulding using a Multi-Objective Evolutionary Algorithm, in final phase of preparation.

temperature), gates and runners (e.g., geometry and location) and cavities (e.g., geometry and total flow length). An important factor is the gate location, since it influences the way the polymer flows into the mould cavity, affecting the existence or not of weld lines and its eventual location, the shrinkage, mould filling pattern, dimensional tolerances, degree and direction of orientation, pressure distribution in the cavity, sink marks, gas traps and short shots, warpage and residual stress. Thus, the definition of the number, type and location of the gate(s) is of high importance.

For optimizing gate location it is necessary the integration of tools, such as, simulation software able to take into account the referred three phases present in the process and optimization methodologies. There are in the literature various optimization strategies using different methodologies to optimize gate location in injection moulding. Pandelidis and Zou (1990a) optimized gate location based on the combination of simulated annealing with a hill-climbing method. Three different terms, overpacking, temperature difference and frictional overheating, are used as a measure of part warpage and material degradation. Warpage is influenced by these factors, but in the paper the relationship between the factors is not clear. Therefore, the optimization effect is restricted by the determination of some weighting factors used by the authors.

Young (1994) used a genetic algorithm to optimize gate location for the case of the moulding of a liquid composite based on the minimization of the mould-filling pressure, the uneven-filling pattern and the temperature difference during mould filling.

Lee and Kim (1995a) proposed an automated selection method for gate location, in which a set of initial gate locations were proposed by a designer and, then, the optimal location of the gate was defined using the adjacent node evaluation method. The scheme can be used for complicated parts, but it requires an extensive number of design evaluations to obtain the best gate location.

In their work Douglas et al. (1998) designed a mould by combining process modelling and sensitivity analysis. The gate location and injection pressure profile were optimized through minimizing the filling time while satisfying constraints related with injection pressure, injection flow rate and mould clamp force. The validity of the methodology was demonstrated through the use of a simple geometry. However, the extension of the proposed methodology to more complicated geometries is not obvious.

Lam and Jin (2001) proposed the optimization of gate location based on the flow path concept. Either, standard deviation of flow path length, standard deviation of filling time or

range of variation of filling time were employed as the objective function. The adjacent node evaluation and flow path search schemes were used to determine the location of the gate. The main conclusion is that the range of filling time is a better objective function to represent the uniformity of filling pattern and the flow path search scheme is more efficient. For complicated parts, such as ones including holes, ribs and/or boss, the appropriate boundary is not easy to select automatically by computer being the user input required.

Courbebaisse and Garcia (2002) suggested a shape analysis to estimate the best gate location of injection moulding. Later on the methodology was applied to the optimization of single gate location of an L shape part (Courbebaisse, 2005). This methodology only can be used for simple flat parts with uniform thickness but it is easy to use and is not time-consuming.

Shen et al. (2004) optimized the gate location by minimizing a weighted sum of filling pressure, filling time difference between different flow paths, temperature difference and over-pack percentage. A hill-climbing algorithm was used to search the optimal gate location. The algorithm can be used for complicated parts, without human interaction during the searching process.

Zhai et al. (2005a) developed an efficient search method based on pressure gradient (PGSS) to optimize the location of two gates for a single moulding cavity. The weld lines were subsequently positioned to the desired location by varying runner sizes (Zhai et al., 2006). Zhai et al. (2005b) investigated optimal gate location using as objective the pressure at the end of filling.

Castro et al. (2007) demonstrated the use of a method based on CAE, statistical analysis, ANNs and Data Envelopment Analysis (DEA), in order to find the best compromise between multiple Performance Measures (PMs). The aim being to prescribe the values for the Controllable Process Variables (CPVs) in while considering explicitly their variability. Six PMs (deflection range in the z-direction, time at which the flow front touches hole A, time at which the flow front touches hole B, time at which the flow front touches the outer edge of the part, vertical distance from Edge 1 to the weld line and horizontal distance from Edge 2 to the weld line) and four CPVs (melt temperature, mould temperature, horizontal coordinate of the injection point and vertical coordinate of the injection point) were used in this study. They demonstrate in several stages of the optimization that the methodology proposed is appropriate to determine the dependency of the PMs from the CPVs.

Li et al. (2007) proposed a different objective function to evaluate the warpage of injection moulded parts, used to optimize gate location. The quality of the warpage was defined from the "flow plus warpage" simulation outputs of Moldflow software. The aim is to minimize this objective function in order to achieve the minimum deformation. In this case the optimization method employed was simulated annealing.

Wu et al. (2011) developed a study were the combination of different classes of design variables are considered simultaneously, together with both the length and the position of the weld line as design constraints. This study adopted an enhanced genetic algorithm, called DMPGA, combining a pre-existing optimization algorithm with commercial Moldflow software and a master–slave distributed architecture. The results obtained show that DMPGA can effectively decrease the maximum part warpage without violating the weld line constraint and, also, overcome difficulties attributed to constraint handling and computational demand. However, only runner size, moulding conditions and part geometry are taken into consideration.

The above methodologies proposed to optimize gate location have some important limitations, namely, the capacity to handle with multi-objectives simultaneously, the linkage with the simulation codes and the complexity of the part geometry.

Therefore, in the present work an automatic optimization methodology based on MOEA is used to define the processing conditions and the gate location in injection moulding of a complicated part containing a hole (Gaspar-Cunha and Covas, 2004). For that purpose a MOEA is linked to an injection moulding simulator code (in this case Moldflow). The proposed optimization methodology was applied to a case study where the processing conditions and the gate location are established in order to create a balanced filling pattern, achieved by weld line length minimization, to maximize part quality, guaranteed by difference between the shrinkage at the end of the flow and the pre-defined design value and to minimize the cycle time to provide low costs on part production.

This paper is organized as follows: first is described the optimization methodology used, specifying how the MOEA interacts with the simulation software Moldflow; second, a case study of a rectangular part with a non-symmetrical hole is presented and, finally, gate location optimization results are shown and discussed.

8.2 optimization methodology

A methodology, integrating modelling of the injection moulding process and an optimization strategy based on MOEA, is proposed (Fernandes et al., 2010, 2012). This proposed methodology is used to define the best injection gate location and injection moulding operating conditions in order to minimize the cycle time, the differential shrinkage and the weld line location and length, using as example the production of an injection part with a hole.

EAs are based on the principles of natural selection of survival of the fittest individual by mimicking some of the concepts of this natural process. The selection, crossover and mutation concepts are used by the EA to explore the search space in order to find an optimal solution or a set of optimal solutions. The initial population of chromosomes represents the gate location and/or the set of operative processing variables, which is generated randomly within the feasible search space. Then, these solutions are evaluated using the modelling routine (Autodesk Moldflow 2010 software). The performance of each one of the solutions (chromosomes) proposed by the MOEA is quantified using as objectives the minimization of the cycle time, the differential shrinkage and the length and location of the weld line. In the case of MOEA the different objectives are combined in order to calculate a single fitness function value. The RPSGAe proposed previously by some of the authors was used for that purpose (Gaspar-Cunha and Covas, 2004). After evaluation, the selection operator based on the fitness function is used to select pairs of chromosomes accordingly with the probability of survival. The chromosomes are then subjected to mutation and crossover operators and new population is obtained. The process repeated until a pre-defined number of generations is been reached.

Figure 8.1 shows the interface for integrating Autodesk Moldflow 2010 and the GA-based optimization routine. First, coordinates of the gate are sent to Moldflow Adviser by an AutoIt script which mimics the user interface with computer. Next, geometric Moldflow Adviser file is renamed to geometric Moldflow Synergy file and an AutoIt script is executed to remesh the part and define processing conditions to be used in the simulation. A Fill+Pack+Warp analysis is done through command files provided by Moldflow Synergy software. When the analysis is finished, an AutoIt script is executed in order to obtain differential shrinkage in two different locations and weld line/meld line results files are saved. The optimization

routine will read the results files and calculations are done to measure the cycle time, the dispersion of differential shrinkage and the length of the weld plus meld line.

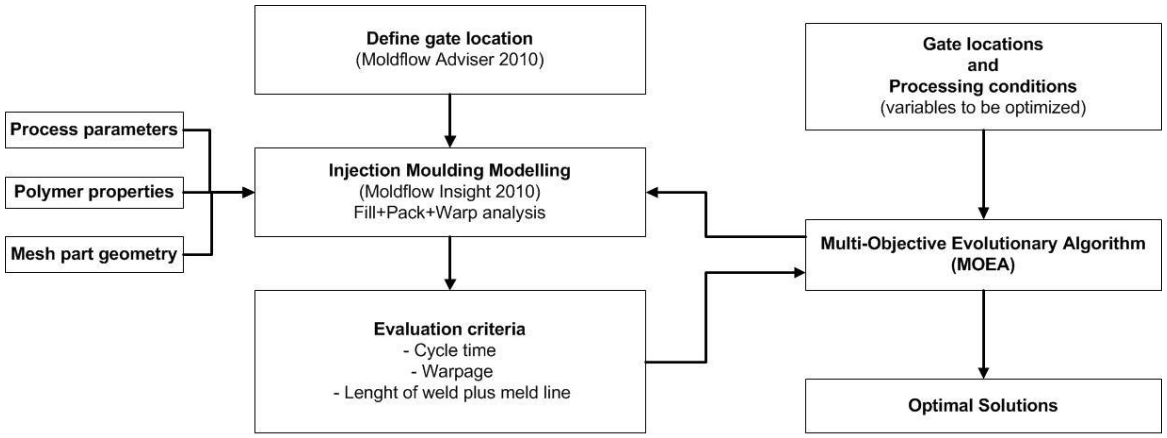

Figure 8.1: Interfacing between optimization routine and Moldflow software.

8.3 CASE STUDY

8.3.1 *Problem description*

To demonstrate the validity of the proposed optimization methodology, the study of the gate location of a rectangular moulding with a hole, as represented in Figure 8.2, was used. The moulding has 1.5mm of thickness, 60 mm of width and 140 mm of length and the finite element mesh used has 940 triangular elements and 525 nodes (see Figure 8.2).

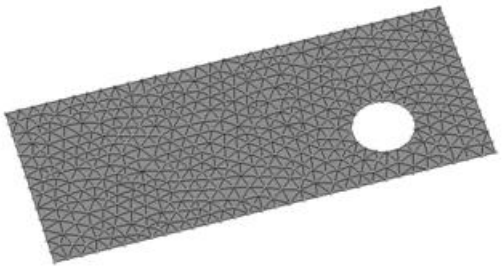

Figure 8.2: Injection moulding part to be used.

The part is moulded in a polypropylene, PPH 5060, from TOTAL Petrochemicals. The polymer properties used in the simulations were obtained from the Moldflow database (Moldflow 2010) and are summarized in Table 8.1.

PROPERTY	VALUE UNIT
Melt density	0.73406 g/cm^3
Solid density	0.90032 g/cm^3
Melting temperature	230 ^oC
Ejection temperature	60 ^oC
Maximum shear stress	0.25 MPa
Maximum shear rate	100000 $(1/s)$
Specific heat	21700 $J/Kg\,^oC$
Thermal conductivity	0.17 $W/m\,^oC$
Elastic module	1400 MPa
Poisson ratio	0.42

Table 8.1: Properties of the PPH 5060.

The material selected for the mould was a P20 steel. Concerning the processing conditions only the mould open time was maintained constant and equal to 5 seconds. The simulations in Moldflow are based on a hybrid finite-element/finite-difference/control-volume numerical solution of the generalized Hele-Shaw flow equation of a compressible viscous fluid under non-isothermal conditions. The polymer rheological and PVT behaviours were modelled by a Cross-WLF and the Tait modified equations, respectively. More details about the software are described in literature (Hieber and Shen, 1980; Chiang et al., 1991a,b; Viana, 1999). The simulations phases considered when using Moldflow are Fill, Pack and Warp analysis, including melt flow, packing, residual stress calculations and structural analysis.

8.3.2 *Decision variables*

Two type of decision variables were considered in this study, design and operating conditions. The design variables are the injection gate location, that are defined by x and y coordinates of the node points in the mesh were they are located. Due to existing experimental restrictions only the left, right and upper boundary nodes were admitted as injection gate location. Six operating conditions were considered, filling time, melt and mould temperatures, holding time, holding pressure and cooling time. Table 8.2 summarizes the design variables selected and the corresponding range of variation.

DESIGN VARIABLE	VALUE RANGE
X coordinate (mm) - x	$[0, 140]$ subject to constraint
Y coordinate (mm) - y	$[0, 60]$ subject to constraint
Fill time (s) - t_f	$[1, 5]$
Melt temperature (ºC) - T_{inj}	$[190, 270]$
Mould temperature (ºC) - T_w	$[10, 50]$
Holding pressure (MPa) - Ph	$[30, 60]$
Packing time (s) - t_p	$[1, 20]$
Cooling time (s) - t_c	$[5, 20]$

Table 8.2: Range of variation of the decision variables.

The RPSGAe uses a real representation of the variables, a simulated binary crossover, a polynomial mutation and a roulette wheel selection strategy (Gaspar-Cunha and Covas, 2004). The following RPSGAe parameters were selected: 10 generations, crossover rate of 0.8, mutation rate of 0.05, internal and external populations with 30 individuals, limits of the clustering algorithm set at 0.2 and NRanks at 30. These values resulted from a carefully analysis made in a previous work (Gaspar-Cunha and Covas, 2004).

The computation time required by the MoldFlow software to evaluate a single candidate solution is approximately 5 minutes. Thus, the time necessary for a complete optimization is circa of 25 hours. The proposed optimization methodology will be used for setting the injection location and to define the selected processing conditions that satisfy the objectives defined.

8.3.3 *Objective function*

The optimization problem consists in defining the values of the decision variables that allow the production of a part with the minimum cycle time, to minimize the production costs, the minimum of warpage due to the anti-symmetric shrinkage and the minimum of weld plus meld line length, so that weakest areas are minimized.

These objectives are defined as follows:

1. Minimize cycle time, CT:

$$\min CT = t_f + t_p + t_c + t_o \tag{8.1}$$

where t_f is the filling time, t_p is the packing time, t_c is the cooling time and t_o is the mould open time.

2. Minimize warpage, $WARP$:

$$\min WARP = \sqrt{\frac{ds_1^2 + ds_2^2}{2}} \tag{8.2}$$

where ds_1 and ds_2 are are the differential shrinkage values measured in longitudinal and transversal directions, respectively.

3. Minimize length of weld plus meld line, $LWML$:

$$\min LWML = \sum_{i,j} \sqrt{(x_i - x_j)^2 + (y_i - y_j)^2 + (z_i - z_j)^2}$$

where (x_*, y_*, z_*) represents the coordinates of the nodes in the finite element mesh were the weld and meld lines are located as calculated by Moldflow. A weld line is formed when separate melt fronts travelling in opposite directions meet. Instead, a meld line occurs if two emerging melt fronts flow parallel to each other and create a bond between them. Thus, the meeting angle is used to differentiate weld lines and meld lines. If the meeting angle is smaller than 135 degrees produces a weld line. If the angle is greater than 135 degrees it will produce a meld line. In the first case, a weld line surface mark will appear in the part, but when the meeting angle reaches 120 - 150 degrees it will disappear. Weld lines are considered to be of lower quality than meld lines, since relatively less molecular diffusion occurs across a weld line after it is formed. Therefore, weld lines are the weakest areas on the part and are the potential failure locations (Moldflow, 2010).

8.4 RESULTS AND DISCUSSION

Figure 8.3 shows the results obtained for an optimization run considering simultaneously the three objectives defined before (minimization of cycle time, length of weld plus meld line and warpage), the aim being to define the best values for the decision variables presented in Table 8.2. The figure represents all solutions of the initial population and the non-dominated

solutions of the final population (10th generation). The operating conditions and objectives of the optimal solutions found are presented in Table 8.3.

	VARIABLES						OBJECTIVES		
SOLUTIONS	T_w (ºC)	T_{inj} (ºC)	t_f (s)	Ph (%)	t_p (s)	t_o (s)	CT (s)	$WARP$ (%)	$LWML$ (m)
P1	46	268	2.20	42	1.16	5.00	13.36	0.815	0.0331
P2	28	268	4.30	56	12.65	10.11	32.06	0.800	0.0216
P3	46	269	2.84	44	6.57	6.39	20.80	0.800	0.0219
P4	38	265	2.61	47	1.49	5.30	14.20	0.820	0.0103
P5	40	265	2.44	46	1.00	5.35	13.79	0.820	0.0216
P6	46	268	2.27	42	1.21	5.40	13.88	0.815	0.0216
P7	44	264	1.37	44	3.02	6.23	15.62	0.815	0.0106

Table 8.3: Solutions for gate location optimization.

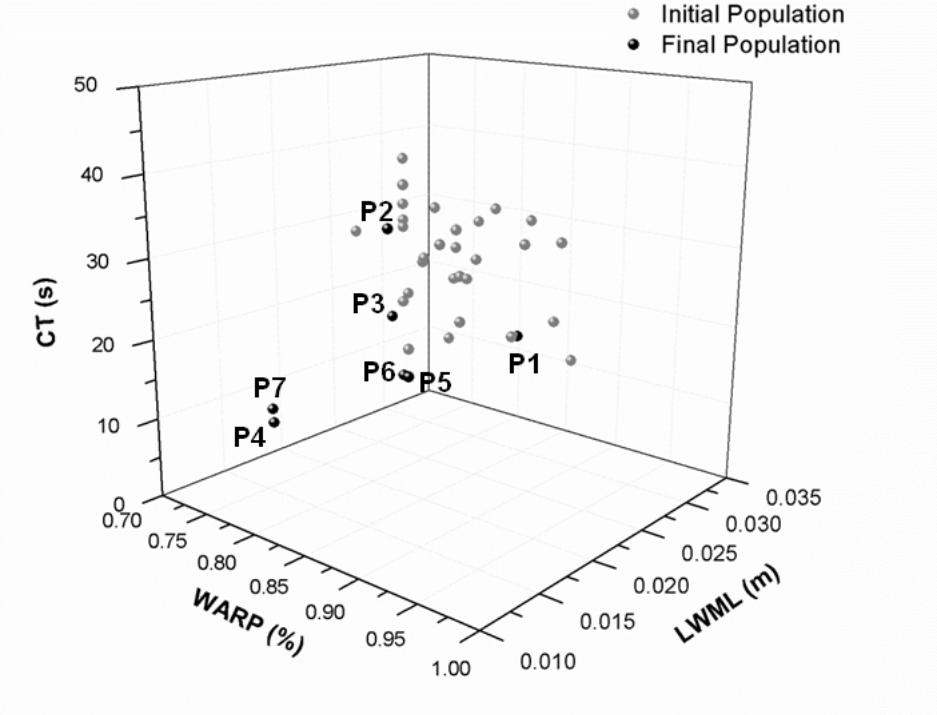

Figure 8.3: Optimization results for three objectives in the objectives domain. Black symbols: Pareto frontier at 10th generation; grey symbols: initial population (CT – cycle time, WARP – warpage, LWML – length of weld plus meld line).

There is a clear improvement from the initial population to the 10th generation, since the optimal points found have better values for the objectives considered. Also, there is not a solution that, simultaneously, provides the better (minimum) values for all three objectives. Therefore, three cases will be analysed considering each one of the objectives as the most important.

If cycle time is considered the most important objective, the point with lower cycle time is P1 in Figure 8.3. In this case CT is equal to 13.36 s, WARP is equal to 0.815 % and LWML is equal to 0.0331 m, that is the highest value found for the length of weld plus meld line. Therefore, this solution is unsatisfactory when the length of weld plus meld line is considered. The injection moulding machine must operate with a fill time of 2.2 s, melt and mould temperatures of 268 ºC and 46 ºC, respectively, holding pressure of 42 MPa, packing time of 1.16 s and cooling time of 5 s.

Figure 8.4 (A) shows the gate location and the filling pattern, while Figure 8.4 (B) shows weld line location for point P1 as calculated by Moldflow. Since gate location is positioned in the top left corner of the part the two melt fronts will meet in the bottom right corner of the hole (were the weld line is plotted in Figure 8.4 (B)). In this case, the flow pattern design does not reach the top, bottom and left cavity boundaries uniformly, as shown by the filling pattern in Figure 8.4 (A). However, no weld lines were formed, since the meeting angles of the flow fronts are kept higher than 135°. The line shown in Figure 8.4 (B) represents both a weld and a meld line, but that does not represent a problem for the moulded part since the weld line does not reach the external boundary of the part. Figure 8.4 (C) shows the warpage distribution for point P1. The value of WARP represents the standard deviation of differential shrinkage values measured on the boundary midpoints in horizontal and vertical directions. For the present case means that the distances between these points after part production only differs of 0.815% when compared with the distances in the mould cavity.

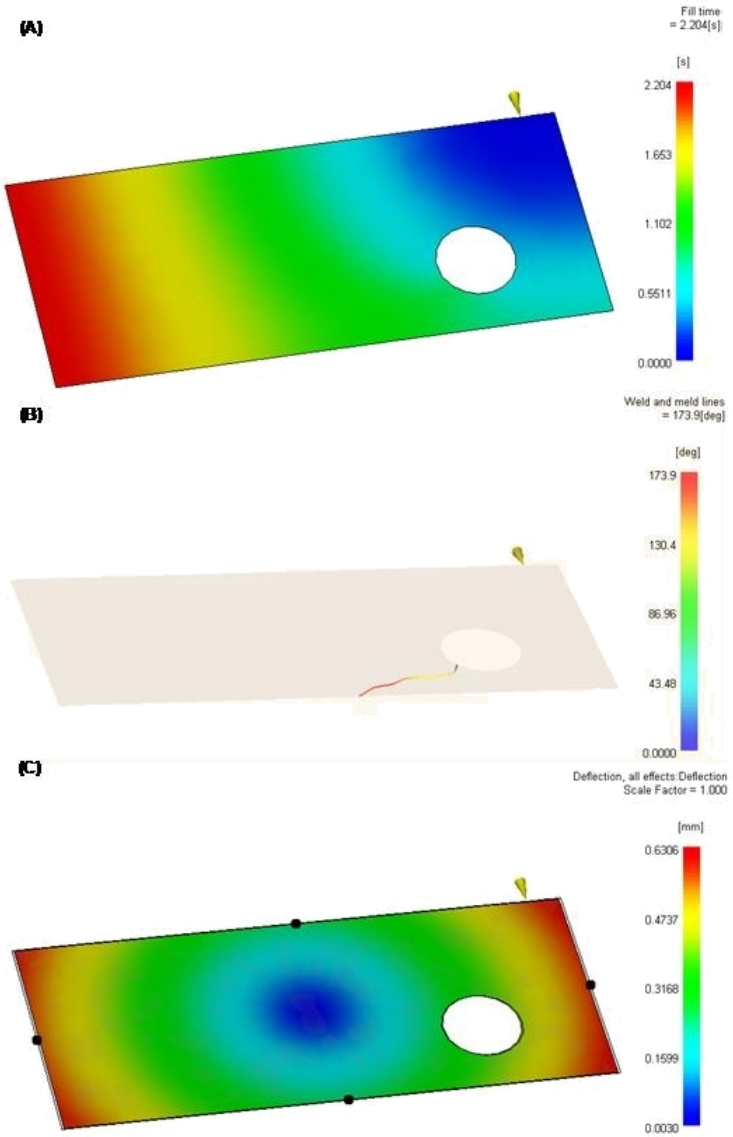

Figure 8.4: Filling pattern (A), weld/meld line position (B) and warpage distribution (C) for point P1.

When warpage is considered the most important objective to satisfy, two points were obtained with lower warpage values, i.e., points P2 and P3.

The main difference between these two points is related with the cycle time, which is 32.06 s for P2 and 20.80 s for P3. Since the values of WARP and LWML are very similar, it is clear that P3 is a much better solution than P2.

Figures 8.5 and 8.6 represents the gate location and the location and length of weld plus meld line, respectively for P2 and P3. In both cases, the gate is located in the top right corner of the part and thus the weld plus meld line appear in the bottom left corner of the hole (see Figures 8.5 (B) and 8.6 (B)). Also, only meld lines are formed for these two solutions in the external boundary of the part. Figure 8.7 presents the modelling results for solution P4, i.e., the solution with lower length of weld plus meld line. In this case only a weld line forms on

the bottom surface of the moulded part (as all the meeting angles of the flow fronts are lower than 135°), which, due to the reasons referred above, makes this a bad solution concerning this aspect. Simultaneously, this solution has the higher value for WARP (0.820 %).

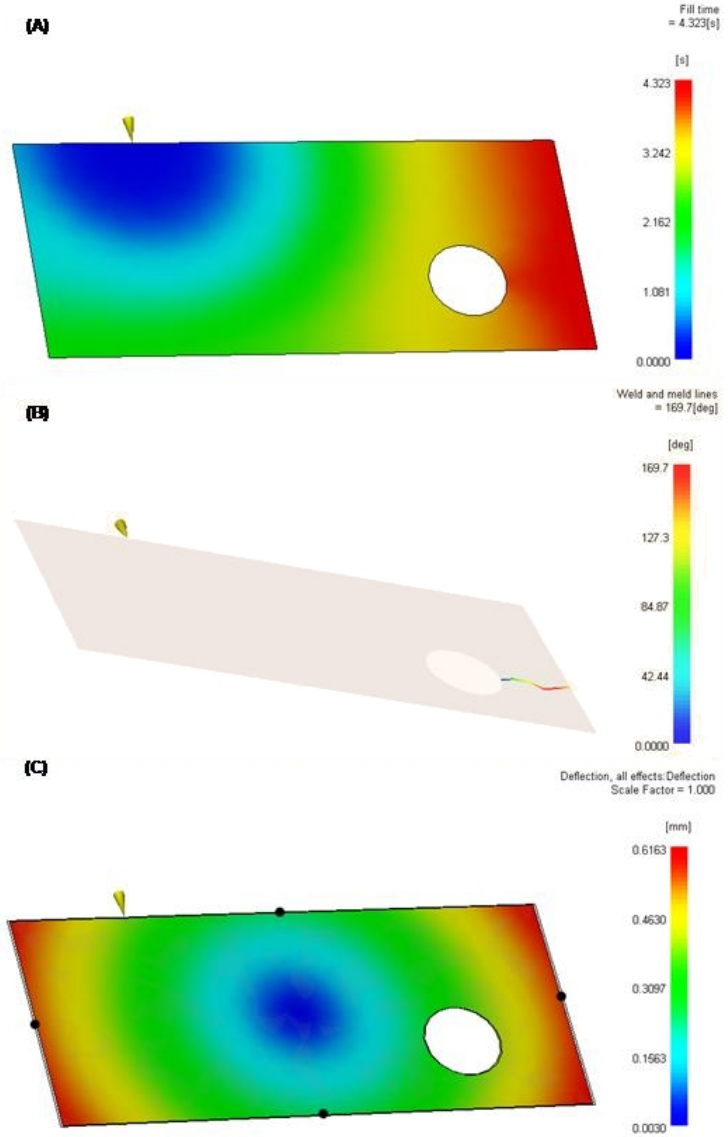

Figure 8.5: Filling pattern (A), weld/meld line position (B) and warpage distribution (C) for point P2.

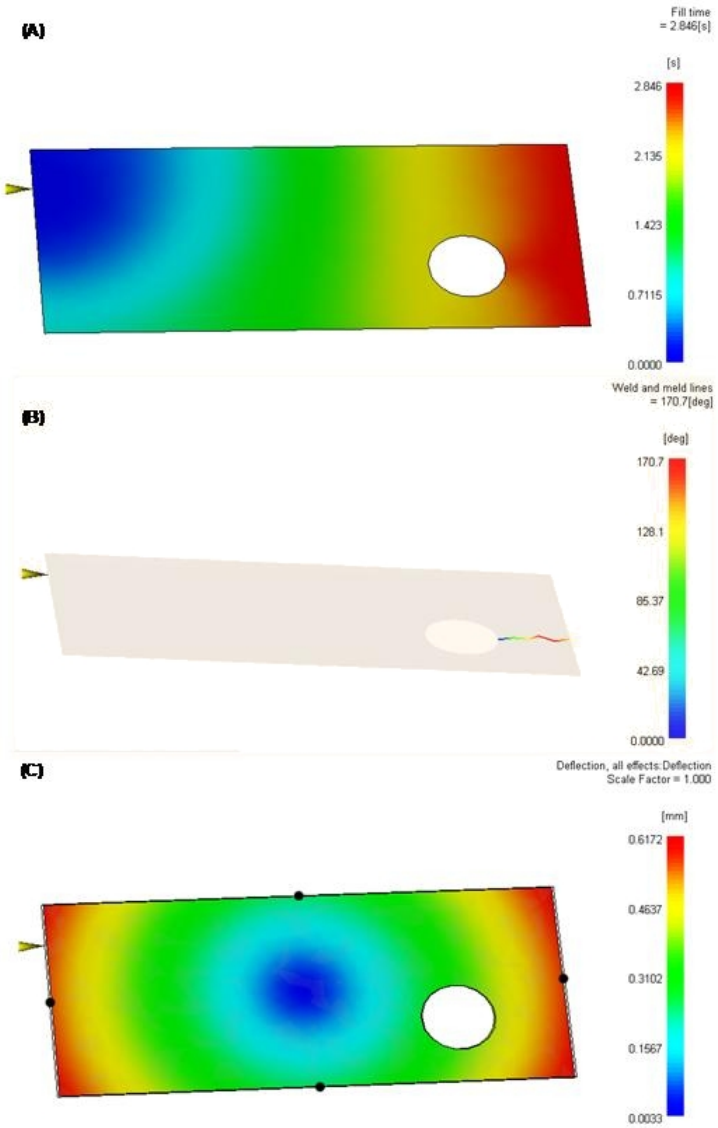

Figure 8.6: Filling pattern (A), weld/meld line position (B) and warpage distribution (C) for point P3.

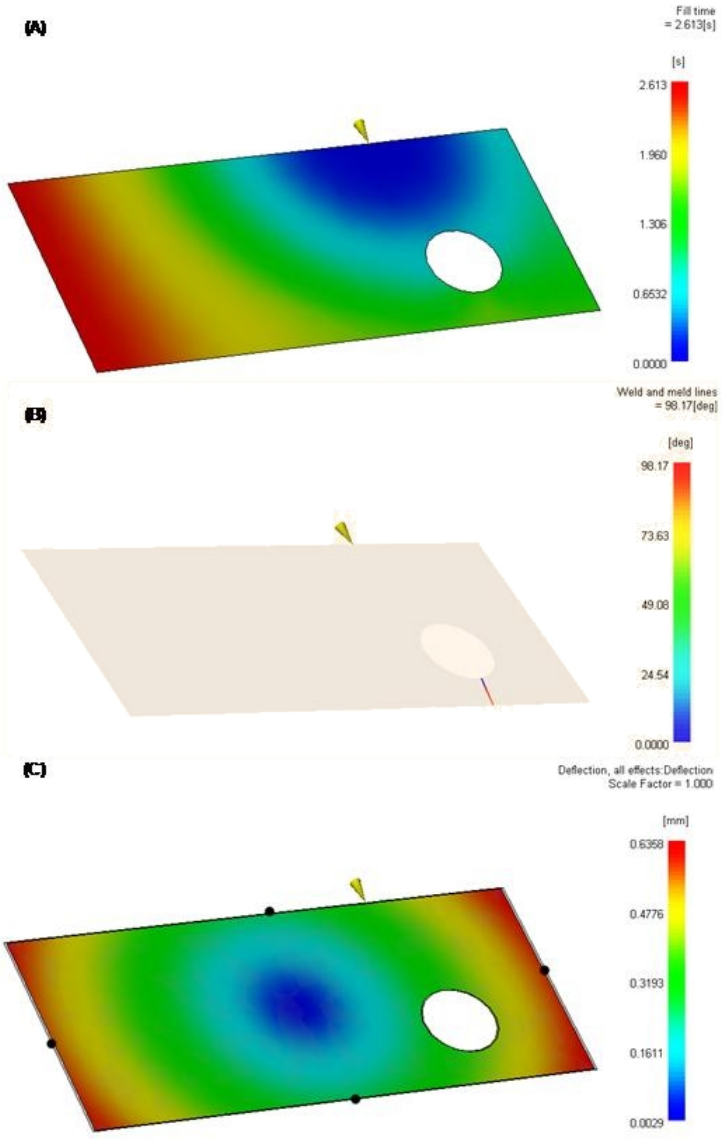

Figure 8.7: Filling pattern (A), weld/meld line position (B) and warpage distribution (C) for point P4.

8.5 CONCLUSIONS

In this work, a multi-objective optimization methodology based on Evolutionary Algorithms (MOEA) was applied to the optimization of processing conditions and gate location of a rectangular moulding with a hole in order to minimize the cycle time, the warpage and the length of weld plus meld line. The methodology proposed was able to produce results with physical meaning. The optimization algorithm is able to minimize simultaneously the three objectives defined through the generation of optimal Pareto frontiers showing the trade-off between the solutions found. This allows the user the comparison between these solutions to select the best that corresponds to their design purposes.

Part V

CONCLUSIONS AND FURTHER WORK

9

CONCLUSIONS

In the present work different studies adressing distinct, but complementary, subjects of injection moulding process were made. These work allowed to contribut to the knowledge about the injection moulding process. The main conclusions of the thesis concerning the objectives defined in Section 1.6 are:

Objective 1

To develop theoretical models able of describing the injection plasticating phase and implementing them in computer.

Conclusion

A modification of the steady-state extrusion model taking into account the backwards movement of the screw, the presence of a non–return valve and the conduction of heat during the idle times was implemented in a computer. During the dynamic phase of the model polymer temperature was computed by using the energy conservation equations for the solids conveying zone, the delay zone, the melting zone and the melt conveying zone using finite difference. During the static phase polymer temperatures are calculated by the 3D transient equation of heat conduction using finite volumes.

The validity of the model was assessed experimentally using two different methods (an IR camera and an IR thermometer) for measuring the average melt temperature that leaves the injection chamber. The effect of some operative variables (e.g., screw speed, backpressure, set barrel temperature profiles and injection chamber length) in the average melt temperature was presented. The experimental measurements made validated the computational results, as the differences obtained for the average melt temperature are below 5% when the IR camera method is used.

Objective 2

To optimize the moulding cycle, simultaneously in terms of the process (no defective parts), dimensional and mechanical performance, based in Evolutionary Algorithms.

Conclusion

A multi-objective optimization methodology based on Evolutionary Algorithms (MOEA) was applied to the optimization of the operating conditions of polymer injection moulding process. For that purpose a MOEA is linked to an injection moulding simulator code (C-Mold). The proposed optimization methodology was used to set the processing conditions of the moulding in polystyrene. The processing variables to optimize were injection time, melt temperature, mould temperature and holding pressure. The objectives used were the temperature difference on the moulding at the end of filling to avoid part distortions and warpage due to different local cooling rates; volumetric shrinkage of the mouldings; maximum cavity pressure to reduce the clamping force; cycle time to increase productivity; and pressure work in order to diminish the residual stress, the energy consumption and to reduce the mechanical efforts supported by the equipment.

Objective 3

To establish relationships between the global processing conditions and the thermomechanical environment.

Conclusion

The optimization results obtained in objective 2 were assessed experimentally. As expected, power work conflicts with volumetric shrinkage of the mouldings, while, cycle time, maximum pressure and temperature difference slightly decrease with power work. Pareto frontiers are a powerful tool enabling the decision maker to select different solutions representing different compromises between the objectives considered. The results obtained showed that the optimization methodology proposed is able to find solutions with physical meaning.

Objectives 4 and 5

To customize the thermomechanical environment for a desired dimensional and mechanical response, defining the processing window and develop a methodology for the full integration of the process, as need in an industrial context.

Conclusion

The optimization methodology was applied to a case study where the layout of the cooling channels and/or the processing conditions are established in order to minimize the part warpage quantified by two conflicting objectives. After moulding, the following two objectives with respect to the angle deformation were defined: minimize dispersion (σ_1) of angular measurements after moulding relatively to the angle of the cavity moulding and minimize dispersion (σ_2) of differences between angular measurements after moulding and angle of the cavity moulding relatively to their mean value. The goal was to minimize the angle warpage and the effect of plane warpage. The geometry used was a rectangular L-shape moulding with a curved end. The proposed optimization methodology was used for setting the diameter and coordinates of the cooling channels and/or to define the selected processing conditions (the same used in objective 2).

A first study was carried out using only processing conditions as optimization variables. In general, σ_1 decreases with injection time while σ_2 increases, except when holding pressure is equal to 7%. σ_1 is lower when melt temperature and holding pressure decreases and mould temperature increases. σ_2 is lower for lower values of all variables.

In a second study, the proposed optimization methodology was applied to find the best cooling channels design variables. In this optimization procedure, the processing conditions were maintained constant. This study was divided in two parts: first, the simulations consider a cold runners system, second, the simulations consider a direct hot runner. Using cold runners cooling channels, three similar cooling channels locations provide a higher minimization of σ_1 and one cooling channel location assure a higher minimization of σ_2. It is also important to note that the cooling channel diameter of solutions who guarantee a higher minimization of σ_1 is of 8 mm and cooling channel diameter of solution that assure a higher minimization of σ_2 is of 7 mm. Design cooling channel optimization problem with hot runner system have a unique solution, with a cooling channel diameter of 7 mm.

Finally, the proposed optimization methodology was used to find simultaneously the best cooling channels design and processing conditions that minimize the deformation angle and the part warpage. In this case only cold runners were used. The final generation solutions feature cooling channels designs with identical layout and the optimal processing conditions values are also very similar. Namely, the injection time should be settled at 2.52 s, the melt and mould temperatures at 241 ºC and 32 ºC, respectively, and holding pressure at 11.7% of maximum machine injection pressure.

Therefore, in order to get better performance, the optimization of cooling channels layout and processing conditions must be done simultaneously.

The same optimization methodology was applied to define processing conditions and position of gate location in injection moulding of a complicated part with a hole. However, in this case the MOEA was linked with Moldlfow instead of C-Mold. The goal was to create a balanced filling pattern which is achieved by weld and meld line length minimization, maximum part quality guaranteed by minimization of warpage and low costs on part production by minimization of cycle time. The injection location is defined by the x and y coordinates of the node points in the mesh and six processing variables were also selected, namely, fill time, melt and mould temperatures, holding time, holding pressure and cooling time. The optimization algorithm is able to minimize simultaneously the three objectives defined through the generation of optimal Pareto frontiers showing the trade-off between the solutions found. This allows the user the comparison between these solutions to select the best that corresponds to their design purposes.

10

FURTHER WORK

For future work it is proposed the following:

- Integrate the commercially available mould filling codes with the plasticating phase models. This integration will allow for a better computation of the thermomechanical environment imposed to the material upon processing. From the modelling of the plasticating phase the temperature distribution of the melt in the injection barrel can be determined. This temperature distribution must be an average temperature as required as input in the commercially available mould filling simulation codes. A representative value of the melt temperature heterogeneity can be proposed, taking into account the computational results obtained in the plasticating phase.

- The multi-objective optimization methodology can be used to optimize the geometry and the processing conditions of the plasticating phase (e.g., screw rotation speed, the back pressure and barrel temperatures). This will allow the optimization of the plasticating phase for improvements on the melt quality (e.g., temperature and additive dispersion homogeneity).

- A fully automatic design optimization considering moulding conditions, runner size, gate location and cooling system can be done, but a distributed architecture of CAE should be used because the ratio of computation time to communication time with Moldflow is large.

Part VI

REFERENCES

REFERENCES

Agazzi, A., Sobotka, V., Goff, R. L., Garcia, D. and Jarny, Y. (2010). A Methodology for the Design of Effective Cooling System in Injection Moulding, *International Journal of Material Forming* **3**: 13–16.

Agur, E. and Vlachopoulos, J. (1982). Numerical Simulation of a Single-Screw Plasticating Extruder, *Polymer Engineering & Science* **22**: 1084–1094.

Alam, K. and Kamal, M. (2003). A Genetic Optimization of Shrinkage by Runner Balancing, *ANTEC 2003 Plastics: Annual Technical Conference, Volume 1: Processing*.

Alam, K. and Kamal, M. (2004). Runner Balancing by a Direct Genetic Optimization of Shrinkage, *Polymer Engineering & Science* **44**: 1949–1959.

Alam, K. and Kamal, M. (2005). A Robust Optimization of Injection Molding Runner Balancing, *Computers and Chemical Engineering* **29**: 1934–1944.

Becker, E., Carey, G. and Oden, T. (1981). *Finite Elements, an Introduction*, Prentice-Hall.

Broyer, E. and Tadmor, Z. (1972). Solids Conveying in Screw Extruders - Part I: A Modified Isothermal Model, *Polymer Engineering & Science* **12**: 12–24.

Cao, W., Shen, C. and Wang, R. (2005). 3d Flow Simulation for Viscous Nonisothermal Incompressible Fluid in Injection Molding, *Polymer-Plastics Technology and Engineering* **44**: 901–917.

Castro, C., Bhagavatula, N., Cabrera-Rios, M., Lilly, B. and Castro, J. (2003). Identifying the Best Compromises Between Multiple Performance Measures in Injection Molding (IM) using Data Envelopment Analysis, *Proceedings SPE technical papers ANTEC'03*.

Castro, C., Cabrera-Rios, M., Lilly, B. and Castro, J. (2007). Multiple Criteria Optimization with Variability Considerations in Injection Molding, *Polymer Engineering & Science* **47**: 400–409.

Chang, R. Y. and Yang, W. H. (2001). Numerical Simulation of Mold Filling in Injection Molding using a Three-dimensional Finite Volume Approach, *International Journal for Numerical Methods in Fluids* **37**: 125–148.

Chang, T. and Faison, E. (2001). Shrinkage Behaviour and Optimization of Injection Molded Parts Studied by the Taguchi Method, *Polymer Engineering & Science* **41**: 703–710.

Changyu, S., Lixia, W. and Qian, L. (2007). Optimization of Injection Molding Process Parameters using Combination of Artificial Neural Network and Genetic Algorithm Method, *Journal of Materials Processing Technology* **183**: 412–418.

Chatfield, C. and Collins, A. (1996). *Introduction to Multivariate Analysis*, Chapman & Hall Publishers.

Chen, B. and Liu, W. (1994). Numerical Simulation of the Post-filling Stage in Injection Molding with a Two Phase Model, *Polymer Engineering & Science* **34**: 835–846.

Chen, W., Fu, G., Tai, P. and W.J., D. (2007). Process Parameter Optimization for MIMO Plastic Injection Molding via soft Computing, *Expert Systems with Applications* **36**: 1114–1122.

Chen, W., Tai, P., Wang, M., Deng, W. and Chen, C. (2008). A Neural Network-based Approach for Dynamic Quality Prediction in a Plastic Injection Molding Process, *Expert Systems with Applications* **35**: 843–849.

Chen, X., Gao, F. and Chen, G. (2004). A Soft-sensor Development for Melt-flow-length Measurement During Injection Mold Filling, *Materials Science and Engineering* **384**: 245–254.

Chiang, H., Hieber, C. and Wang, K. (1991a). A Unified Simulation of the Filling and Postfilling Stages in Injection Molding. Part I: Formulation, *Polymer Engineering & Science* **31**: 116–124.

Chiang, H., Hieber, C. and Wang, K. (1991b). A Unified Simulation of the Filling and Postfilling Stages in Injection Molding. Part II: Experimental Verification, *Polymer Engineering & Science* **31**: 125–139.

Chiang, H., Himasekhar, K., Santhanam, N. and Wang, K. (1993). Integrated Simulation of Fluid Flow and Heat Transfer in Injection Molding for the Prediction of Shrinkage and Warpage, *Journal of Engineering Materials and Technology* **115**: 37–47.

Chung, C. I. (1971). Plasticating Single-Screw Extrusion Theory, *Polymer Engineering & Science* **11**: 93–98.

Chung, S. T. and Kwon, T. H. (1996). Coupled Analysis of Injection Molding Filling and Fiber Orientation, Including In-plane Velocity Gradient Effect, *Polymer Composites* **17**: 859–872.

Cmold (1999). *Cmold User's Manual*.

Coello, C., Veldhuizen, V. and Lamont, G. (2002). *Evolutionary Algorithms for Solving Multi-Objective Problems*, Kluwer.

Courbebaisse, G. (2005). Numerical Simulation of Injection Molding Process and the Pre-molding Concept, *Computational Materials Science* **34**: 397–405.

Courbebaisse, G. and Garcia, D. (2002). Shape Analysis and Injection Molding Optimization, *Computational Materials Science* **25**: 547–553.

Cunha, A. (2003). *Manual do Projetista para Moldes de Injeção de Plástico*, Centimfe.

Deb, K. (2001). *Multi-Objective Optimization using Evolutionary Algorithms*, Wiley.

Dong, S., Jong, S. and Young, B. (2008). Experimental Characterization of Transcription Properties of Microchannel Geometry Fabricated by Injection Molding Based on Taguchi Method, *Microsystem Technology* **14**: 1581–1588.

Donovan, R. (1971). A Theoretical Melting Model for a Reciprocating-screw Injection Molding Machine, *Polymer Engineering & Science* **11**: 361–368.

Donovan, R. (1974). The Plasticating Process in Injection Molding, *Polymer Engineering & Science* **14**: 101–111.

Donovan, R., Thomas, D. and Leversen, L. (1971). An Experimental Study of Plasticating in a Reciprocating Screw Injection Molding Machine, *Polymer Engineering & Science* **11**: 353–360.

Douglas, E., Daniel, A. and Charles, L. I. (1998). Analysis and Sensitivity Analysis for Polymer Injection and Compression Molding, *Computer Methods in Applied Mechanics and Engineering* **167**: 325–344.

Douglas, M. (1996). *Plastic Injection Molding: Manufacturing Process Fundamentals*, Society of Manufacturing Engineers.

Duff, A. (2000). Increased Speed to Market using CAE Simulation for Injection Molded Plastics Parts, *Proceedings of 58th annual meeting of the Society of Plastics Engineers*.

Elbirli, B., Lindt, J., Gottgetreu, S. and Baba, S. (1984). Mathematical Modelling of Melting of Polymers in a Single-Screw Extruder, *Polymer Engineering & Science* **24**: 988–999.

Feng, C., Jeffrey, K. and Su, K. (2006). Optimization of Multiple Quality Characteristics for Polyether Ether Ketone Injection Molding Process, *Fibers and Polymers* **7**: 404–413.

Fenner, R. (1977). Developments in the Analysis of Steady Screw Extrusion of Polymers, *Polymer* **18**: 617–635.

Fenner, R. (1979). *Principles of Polymer Processing*, McMillan.

Fernandes, C., Pontes, A., Viana, J. and Gaspar-Cunha, A. (2010). Using Multi-Objective Evolutionary Algorithms in the Optimization of Operating Conditions of Polymer Injection Molding, *Polymer Engineering & Science* **50**: 1667–1678.

Fernandes, C., Pontes, A., Viana, J. and Gaspar-Cunha, A. (2012). Using Multi-Objective Evolutionary Algorithms for Optimization of the Cooling System in Polymer Injection Molding, *International Polymer Processing* **2**: 213–223.

Fogel, L., Owens, A. and Walsh, M. (1966). *Artificial Intelligence through Simulated Evolution*, John Wiley.

Gaspar-Cunha, A. (2000). *Modelling and Optimisation of Single Screw Extrusion*, PhD thesis, University of Minho.

Gaspar-Cunha, A. (2009). *Modelling and Optimisation of Single Screw Extrusion - Using Multi-Objective Evolutionary Algorithms*, Lambert Academic Publishing.

Gaspar-Cunha, A. and Covas, J. (2004). *Lecture Notes in Economics and Mathematical Systems*, Springer-Verlag, chapter RPSGAe – Reduced Pareto Set Genetic Algorithm: Application to Polymer Extrusion, pp. 221–255.

Gaspar-Cunha, A. and Viana, J. (2005). Using Multi-objective Evolutionary Algorithms to Optimize Mechanical Properties of Injection Molded Parts, *International Polymer Processing* **3**: 274–285.

Goldberg, D. (1989). *Genetic Algorithms in Search, Optimization and Machine Learning*, Addison-Wesley.

Han, C., Lee, K. and Wheeler, N. (1996). Plasticating Single-Screw Extrusion of Amorphous Polymers: Development of a Mathematical Model and Comparison with Experiment, *Polymer Engineering & Science* **36**: 1360–1376.

Han, K. H. and Im, Y. T. (1997). Compressible Flow Analysis of Filling and Postfilling in Injection Molding with Phase-change Effect, *Composite Structures* **38**: 179–190.

Harry, D. and Parrott, R. (1970). Numerical Simulation of Injection Mold Filling, *Polymer Engineering & Science* **10**: 209–214.

Herbert, F. (n.d.).
URL: *http://www.quotationspage.com/quote/26173.html*

Hieber, C. and Shen, S. (1980). A Finite Element/finite Difference Simulation of the Injection-molding Filling-process, *Journal of Non-Newtonian Fluid Mechanics* **7**: 1–32.

Himasekhar, K., Lottey, L. and Wang, K. (1992). CAE of Mold Cooling in Injection Molding using a Three-dimensional Numerical Simulation, *Journal of Engineering for Industry* **114**: 213–221.

Holland, J. H. (1975). *Adaptation in Natural and Artificial Systems*, University of Michigan Press.

Holm, E. J. and Langtangen, H. P. (1999). A Unified Finite Element Model for the Injection Molding Process, *Computer Methods in Applied Mechanics and Engineering* **178**: 413–429.

Hétu, J., Gao, D. M., Garcia-Rejon, A. and Salloum, G. (1998). 3D Finite Element Method for the Simulation of the Filling Stage in Injection Molding, *Polymer Engineering & Science* **38**: 223–236.

Huang, H. and Peng, Y. (1993). Theoretical Modelling of Dispersive Melting Mechanism of Polymers in an Extruder, *Advances in Polymer Technology* **12**: 343–352.

Huang, J. and Fadel, G. (2001). Bi-objective Optimization Design of Heterogeneous Injection Mold Cooling Systems, *Journal of Mechanical Design* **123**: 226–239.

Huang, M. and Tai, C. (2001). The Effective Factors in the Warpage Problem of an Injection-molded Part with a Thin Shell Feature, *Journal of Materials Processing Technology* **110**: 1–9.

Huang, S. and Lee, T. (2003). Application of Neural Networks in Injection Moulding Process Control, *The International Journal of Advanced Manufacturing Technology* **21**: 956–964.

Ilinca, F. and Hétu, J. (2000). 3D Simulation of the Packing-cooling Stage in Polymer Injection Molding, *SPE ANTEC Tech Papers*.

Jensen, R. (1981). *The Mould Filling Process: Technical Requirements and Findings*, D. Rheinfeld.

Jong, W. and Wang, K. (1990). Automatic and Optimal Design of Runner Systems in Injection Molding based on Flow Simulation, *SPE ANTEC Tech Papers*.

Kacir, L. and Tadmor, Z. (1972). Solids Conveying in Screw Extruders - Part III: The Delay Zone, *Polymer Engineering & Science* **12**: 387–395.

Kamal, M., Isayev, A. and Liu, S. (2009). *Injection Molding Technology and Fundamentals*, Hanser Publications.

Kamal, M. and Kenig, S. (1972). The Injection Molding of Thermoplastics Part I: Theoretical Model, *Polymer Engineering & Science* **12**: 294–301.

Khayat, R., Plaskos, C. and Genouvrier, D. (2001). An Adaptive Boundary-element Approach for 3D Transient Free Surface Cavity Flow, as Applied to Polymer Processing, *International Journal for Numerical Methods in Engineering* **50**: 1347–1368.

Kim, B., Nam, G., Ryu, H. and Lee, J. (2000). Optimization of Filling Process in RTM using Genetic Algorithm, *Korea-Australia Rheology Journal* **12**: 83–92.

Kim, S., Lee, K. and Kim, Y. (1996). Optimization of Injection-molding Conditions using Genetic Algorithm, *Proceedings of SPIE – the 4th Int. Conf. on Computer-Aided Design and Computer Graphics*.

Koza, J. (1992). *Genetic Programming: On the Programming of Computers by Means of Natural Selection*, MIT Press.

Krose, B. and Smagt, P. (1996). An Introduction to Neural Networks, *Technical report*, University of Amsterdam.

Kumar, A., Ghoshdastidar, P. and Muju, M. (2002). Computer Simulation of Transport Processes during Injection Mold-filling and Optimization of the Molding Conditions, *Journal of Materials Processing Technology* **120**: 438–449.

Kurtaran, H., Ozcelik, B. and Erzurumlu, T. (2005). Warpage Optimization of a Bus Ceiling Lamp Base using Neural Network Model and Genetic Algorithm, *Journal of Materials Processing Technology* **169**: 314–319.

Lam, Y., Deng, Y. and Au, C. (2006). A GA/gradient Hybrid Approach for Injection Moulding Conditions Optimisation, *Engineering with Computers* **21**: 193–202.

Lam, Y. and Jin, S. (2001). Optimization of Gate Location for Plastic Injection Molding, *Journal of Injection Molding Technology* **5**: 180–192.

Lam, Y. and Seow, L. (2000). Cavity Balance for Plastic Injection Molding, *Polymer Engineering & Science* **40**: 1273–1280.

Lam, Y., Zhai, L., Tai, K. and Fok, S. (2004). An Evolutionary Approach for Cooling System Optimization in Plastic Injection Moulding, *International Journal of Production Research* **42**: 2047–2061.

Lee, B. and Kim, B. (1995a). Automated Selection of Gate Location based on Desired Quality of Injection Molded Part, *SPE Annual Technical Conference*.

Lee, B. and Kim, B. (1995b). Optimization of Part Wall Thickness to Reduce Warpage of Injection-molded Parts based on the Modified Complex Method, *Polymer-Plastics Technology and Engineering* **34**: 793–811.

Lee, K. and Han, C. (1990). Analysis of the Performance of Plasticating Single-Screw Extruders with a New Concept of Solid-Bed Deformation, *Polymer Engineering & Science* **30**: 665–676.

Lee, K. S., Low, C. Y., Rahman, M. and Zhang, Y. F. (2001). A Genetic Algorithm based Process Planning System for Mould Base, *International Journal of Computer Applications in Technology* **14**: 190–203.

Li, J., Li, D., Guo, Z. and LV, H. (2007). Single Gate Optimization for Plastic Injection Mold, *Journal of Zhejiang University Science A* **8**: 1077–1083.

Liao, X., Xiew, H., Zhou, Y. and Xia, W. (2007). Adaptive Adjustment of Plastic Injection Processes based on Neural Network, *Journal of Materials Processing Technology* **187–188**: 676–679.

Lindt, J. and Elbirli, B. (1985). Effect of the Cross-Channel Flow on the Melting Performance of a Single-Screw Extruder, *Polymer Engineering & Science* **25**: 412–418.

Lipshitz, S., Lavie, R. and Tadmor, Z. (1974). A Melting Model for Reciprocating Screw Injection-molding Machines, *Polymer Engineering & Science* **14**: 553–559.

Lord, H. and Williams, G. (1975). Mold-filling Studies for the Injection Molding of Thermoplastic Materials. Part II: The Transient Flow of Plastic Materials in the Cavities of Injection-molding Dies, *Polymer Engineering & Science* **15**: 569–582.

Lotti, C. and Bretas, R. E. S. (2003). The Influence of Morphological Features on Mechanical Properties of Injection Molded PPS and Sits Prediction Using Neural Networks, *Europe-Africa Meeting of The Polymer Processing Society*.

Maddock, B. (1959). A Visual Analysis of Flow and Mixing in Extruder Screws, *SPE Journal* **15**: 383–389.

Mathey, E., Penazzi, L., Schmidt, F. and Rondé-Oustau, F. (2004). Automatic Optimization of the Cooling of Injection Mold based on the Boundary Element Method, *Materials Processing and Design: Modeling, Simulation and Applications* **712**: 222–227.

Menges, G. and Mohren, P. (1986). *How to make injection molds*, Hanser.

Mok, S., Kwong, C. and Lau, W. (2001). A Hybrid Neural Network and Genetic Algorithm Approach to the Determination of Initial Process Parameters for Injection Moulding, *The International Journal of Advanced Manufacturing Technology* **18**: 404–409.

Moldflow (2010). *Moldflow User's Manual*.

Nóbrega, J., Pinho, F., Oliveira, P. and Carneiro, O. (2004). Accounting for Temperature-Dependent Properties in Viscoelastic Duct Flows, *International Journal of Heat and Mass Transfer* **47**: 1141–1158.

Newton, I. (n.d.).
URL: *http://www.goodreads.com/author/quotes/135106.Isaac_Newton*

Nunn, R. and Fenner, R. (1977). Flow and Heat Transfer in the Nozzle of an Injection Molding Machine, *Polymer Engineering & Science* **17**: 811–818.

Osswald, T., Turng, L. and Gramann, P. (2008). *Injection Molding of Plastics - Handbooks*, Carl Hanser Verlag.

Ozcelik, B. and Erzurumlu, T. (2005). Determination of Effecting Dimensional Parameters on Warpage of Thin Shell Plastic Parts using Integrated Response Surface Method and Genetic Algorithm, *International Communications in Heat and Mass Transfer* **32**: 1085–1094.

Ozcelik, B. and Erzurumlu, T. (2006). Comparison of the Warpage Optimization in the Plastic Injection Molding using ANOVA, Neural Network Model and Genetic Algorithm, *Journal of Materials Processing Technology* **171**: 437–445.

Pandelidis, I. and Zou, Q. (1990a). Optimization of Injection Molding Design. Part I: Gate Location Optimization, *Polymer Engineering & Science* **30**: 873–882.

Pandelidis, I. and Zou, Q. (1990b). Optimization of Injection Molding Design. Part II: Molding Conditions Optimization, *Polymer Engineering & Science* **30**: 883–892.

Park, S. and Kwon, T. (1998a). Optimal Cooling System Design for the Injection Molding Process, *Polymer Engineering & Science* **38**: 1450–1462.

Park, S. and Kwon, T. (1998b). Thermal and Design Sensitivity Analyses for Cooling System of Injection Mold, Part I: Thermal Analysis, *Journal of Manufacturing Science and Engineering* **120**: 287–295.

Park, S. and Kwon, T. (1998c). Thermal and Design Sensitivity Analyses for Cooling System of Injection Mold, Part II: Design Sensitivity Analysis, *Journal of Manufacturing Science and Engineering* **120**: 296–305.

Pichelin, E. and Coupez, T. (1998). Finite Element Solution of the 3D Mold Filling Problem for Viscous Incompressible Fluid, *Computer Methods in Applied Mechanics and Engineering* **163**: 359–371.

Pichelin, E. and Coupez, T. (1999). A Taylor Discontinuous Galerkin Method for the Thermal Solution in 3D Mold Filling, *Computer Methods in Applied Mechanics and Engineering* **178**: 153–169.

Pirc, N., Bugarin, F., Schmidt, F. and Mongeau, M. (2008). 3D BEM-based Cooling-channel Shape Optimization for Injection Moulding Processes, *International Journal for Simulation and Multidisciplinary Design Optimization* **2**: 245–252.

Pirc, N., Schmidt, F., Mongeau, M., Bugarin, F. and Chinesta, F. (2007). Optimization of BEM-based Cooling Channels Injection Moulding using Model Reduction, *International Journal of Material Forming* **1**: 1043–1046.

Pontes, A. (2002). *Shrinkage and Ejection Forces in Injection Moulded Products*, PhD thesis, University of Minho.

Potente, H., Schulte, H. and Effen, N. (1993). Simulation of Injection Molding and Comparison with Experimental Values, *International Polymer Processing* **3**: 224–235.

Qiao, H. (2006). A Systematic Computer-aided Approach to Cooling System Optimal Design in Plastic Injection Molding, *International Journal of Mechanical Sciences* **48**: 430–439.

Rajupalem, V., Talwar, K. and Friedl, C. (1997). Three-dimensional Simulation of the Injection Molding Process, *SPE ANTEC Papers*.

Rao, N. (1986). *Computer Aided Design of Plasticating Screws*, Hanser.

Rauwendaal, C. (1992). Conveying and Melting in Screw Extruders with Axial Screw Movement, *International Polymer Processing* **1**: 26–31.

Rauwendaal, C., Osswald, T., Tellez, G. and Gramann, P. (1998). Flow Analysis in Screw Extruders-Effect of Kinematic Conditions, *International Polymer Processing* **13**: 327–333.

Rechenberg, I. (1973). *Evolutionsstrategie - Optimierung technischer Systeme nach Prinzipien der biologischen Evolution*, Frommann-Holzboog.

Reznikoff, C. (n.d.).
URL: *http://www.brainyquote.com/quotes/quotes/c/charlesrez311900.html*

Rosato, D., Rosato, D. and Rosato, M. (2000). *Injection Molding Handbook*, Kluwer Academic Publishers.

Rosenman, M. (1997). The Generation of Form using an Evolutionary Approach, *Technical report*, Department of Architectural and Design Science University of Sydney.

Sadeghi, B. (2000). A BP-neural Network Predictor Model for Plastic Injection Molding Process, *Journal of Materials Processing Technology* **103**: 411–416.

Schlichting, H. (1979). *Boundary Layer Theory*, McGraw-Hill.

Seaman, C., Desrochers, A. and List, G. (1993). A Multiobjective Optimization Approach to Quality Control with Application to Plastic Injection Molding, *IEEE Transactions on systems, man and cybernetics* **23**: 414–426.

Seaman, C., Desrochers, A. and List, G. (1994). Multiobjective Optimization of a Plastic Injection Molding Process, *IEEE Transactions on control systems technology* **2**: 157–168.

Seow, L. and Lam, Y. (1997). Optimising Flow in Plastic Injection Moulding, *Journal of Materials Processing Technology* **72**: 333–341.

Shen, C., Yu, X., Li, Q. and Li, H. (2004). Gate Location Optimization in Injection Molding by using Modified Hill-climbing Algorithm, *Polymer-Plastics Technology and Engineering* **43**: 649–659.

Shi, F., Lou, Z., Lu, J. and Zhang, Y. (2003). Optimisation of Plastic Injection Moulding Process with Soft Computing, *The International Journal of Advanced Manufacturing Technology* **21**: 656–661.

Shie, J. (2008). Optimization of Injection-molding Process for Mechanical Properties of Polypropylene Components Via a Generalized Regression Neural Network, *Polymers for Advanced Technologies* **19**: 73–83.

Steller, R. and Iwko, J. (2008). Polymer Plastication During Injection Molding, *International Polymer Processing* **23**: 252–262.

Stevens, M. and Covas, J. (1995). *Extruder Principles and Operation*, Chapman & Hall.

Stevenson, J. and Chuck, W. (1979). A Simplified Method for Analyzing Mold Filling Dynamics. Part II: Extensions and Comparisons with Experiment, *Polymer Engineering & Science* **19**: 849–857.

Stevenson, J. F. (1978). A Simplified Method for Analyzing Mold Filling Dynamics Part I: Theory, *Polymer Engineering & Science* **18**: 577–582.

Tadmor, Z. (1974). Dynamic Model of a Plasticating Extruder, *Polymer Engineering & Science* **14**: 112–119.

Tadmor, Z., Broyer, E. and Gutfinger, C. (1974). Flow Analysis Network (FAN) A Method for Solving Flow Problems in Polymer Processing, *Polymer Engineering & Science* **14**: 660–665.

Tadmor, Z. and Gogos, C. (1979). *Principles of Polymer Processing*, John Willey & Sons.

Tadmor, Z. and Klein, I. (1968). *Computer Programs for Plastic Engineers*, Reinhold Book Corporation.

Tadmor, Z. and Klein, I. (1970). *Engineering Principles of Plasticating Extrusion*, Van Nostrand Reinhold.

Talwar, K., Costa, F., Rajupalem, V., Antanovski, L. and Friedl, C. (1998). Three-dimensional Simulation of Plastic Injection Molding, *SPE ANTEC Papers*.

Tan and Yuen (1996). Computer-aided System for the Initial Setting of Injection-molding Machine.

Tang, L., Chassapis, C. and Manoochehri, S. (1997). Optimal Cooling System Design for Multi-cavity Injection Molding, *Finite Elements Analysis and Design* **26**: 229–251.

Tang, L., Pochiraju, K., Chassapis, C. and Manoochehri, S. (1998). A Computer-aided Optimization Approach for the Design of Injection Mold Cooling Systems, *Journal of Mechanical Design* **120**: 165–174.

Tang, S., Tan, Y., Sapuan, S., Sulaiman, S., Ismail, N. and Samin, R. (2007). The Use of Taguchi Method in the Design of Plastic Injection Mould for Reducing Warpage, *Journal of Materials Processing Technology* **182**: 418–426.

The Encyclopedia Britannica (2000).

Thyregod, P. (2001). *Modelling and Monitoring in Injection Molding*, PhD thesis, Technical University of Denmark.

Torner, R. (1977). *Principles of Polymer Processing*, Chimija Publishers.

Turng, L. and Peic, M. (2002). Computer Aided Process and Design Optimization for Injection Moulding, *Journal of Engineering Manufacture* **216**: 1523–1532.

Twain, M. (n.d.).
URL: *http://www.quotedb.com/quotes/138*

Viana, J. (1999). *Mechanical Characterisation of Injection Moulded Plates*, PhD thesis, University of Minho.

Viana, J. (2004). Development of the Skin Layer in Injection Moulding: Phenomenological Model, *Polymer* **45**(3): 993 – 1005.

Viana, J., Billon, N. and Cunha, A. (2004). The Thermomechanical Environment and the Mechanical Properties of Injection Moldings, *Polymer Engineering & Science* **44**(8): 1522–1533.

Viana, J., Cunha, A. and Billon, N. (2002). The Thermomechanical Environment and the Microstructure of an Injection Moulded Polypropylene Copolymer, *Polymer* **43**(15): 4185 – 4196.

Wang, V., Hieber, C. and Wang, K. (1986). Dynamic Simulation and Graphics for the Injection Molding of Three-dimensional Thin Parts, *Journal of Polymer Engineering* **7**: 21–45.

White, F. (1991). *Viscous Fluid Flow*, McGraw-Hill.

White, F. (2007). *Fluid Mechanics*, McGraw-Hill.

Wilde, F. (2004). Neural Networks, *Technical report*, King's College London.

Williams, G. and Lord, H. (1975). Mold-filling Studies for the Injection Molding of Thermoplastic Materials. Part I: The Flow of Plastic Materials in Hot and Cold-walled Circular Channels, *Polymer Engineering & Science* **15**: 553–568.

Winterthur (1998). *Plastics Processing. Injection Molding, Extrusion, Die Casting.*

Wu, C., Ku, C. and Pai, H. (2011). Injection Molding Optimization with Weld Line Design Constraint using Distributed Multi-population Genetic Algorithm, *The International Journal of Advanced Manufacturing Technology* **52**: 131–141.

Wu, C. and Liang, W. (2005). Effects of Geometry and Injection-molding Parameters on Weld-line Strength, *Polymer Engineering & Science* **45**: 1021–1030.

Wu, P., Huang, C. and Gogos, C. (1974). Simulation of the Mold-filling Process, *Polymer Engineering & Science* **14**: 223–230.

Xue, S. C., Tanner, R. I. and Phan-Thien, N. (1999). Three-dimensional Numerical Simulations of Viscoelastic Flows - Predictability and Accuracy, *Computer Methods in Applied Mechanics and Engineering* **180**: 305–331.

Yarlagadda, P. (2002). Development of an Integrated Neural Network System for Prediction of Process Parameters in Metal Injection Moulding, *Journal of Materials Processing Technology* **130–131**: 315–320.

Yarlagadda, P. and Khong, C. (2001). Development of a Hybrid Neural Network System for Prediction of Process Parameters in Injection Moulding, *Journal of Materials Processing Technology* **118**: 110–116.

Ye (1999). Optimization of Injection-molding Process with Genetic Algorithms.

Young, W. (1994). Gate Location Optimization in Liquid Composite Molding using Genetic Algorithm, *Journal of Composite Materials* **12**: 1098–1113.

Yung, K. and Xu, Y. (2001). Analysis of a Melting Model for an Extruder with Reciprocation, *Journal of Materials Processing Technology* **117**: 21–27.

Yung, K., Xu, Y. and Lau, K. (2003). Transient Melting Models for the Three Stages of Reciprocating Extrusion, *Journal of Materials Processing Technology* **139**: 170–177.

Zavaliangos, A. (2001). Injection Molding, *Technical report*, Department of Materials Engineering Drexel University.

Zawadzky, E. and Karnis, J. (1985). Mathematical Model of a Single-Screw Plasticating Extruder, *Rheological Acta* **24**: 556–565.

Zhai, M., Lam, L. and Au, C. (2005a). Algorithms for Two Gate Optimization in Injection Molding, *International Polymer Processing* **20**: 14–18.

Zhai, M., Lam, L., Au, C. and Liu, D. (2005b). Automated Selection of Gate Location for Plastic Injection Molding Processing, *Polymer-Plastics Technology and Engineering* **44**: 229–242.

Zhai, M., Lam, L. C. and Au, C. K. (2006). Runner Sizing and Weld Line Positioning for Plastics Injection Moulding with Multiple Gates, *Engineering with Computers* **21**: 218–224.

Zhao, C. and Gao, F. (1999). Melt Temperature Profile Prediction for Thermoplastic Injection Molding, *Polymer Engineering & Science* **39**: 1787–1801.